NIST-GCR-97-731

# EVALUATION OF THE HDR FIRE TEST DATA AND ACCOMPANYING COMPUTATIONAL ACTIVITIES WITH CONCLUSION FROM PRESENT CODE CAPABILITIES. VOLUME 2: CFAST VALIDATION FOR T51 GAS FIRE TEST SERIES

**Jason Floyd, Lothar Wolf**
**and John Krawiec**

**Nuclear Engineering Program**
**Department of Materials and Nuclear Engineering**
**University of Maryland**
**College Park, MD 20742**

**United States Department of Commerce**
**Technology Administration**
National Institute of Standards and Technology

NIST-GCR-97-731

# EVALUATION OF THE HDR FIRE TEST DATA AND ACCOMPANYING COMPUTATIONAL ACTIVITIES WITH CONCLUSION FROM PRESENT CODE CAPABILITIES. VOLUME 2: CFAST VALIDATION FOR T51 GAS FIRE TEST SERIES

Prepared for
U.S. Department of Commerce
Building and Fire Research Laboratory
National Institute of Standards and Technology
Gaithersburg, MD 20899

By
Jason Floyd, Lothar Wolf
and John Krawiec
Nuclear Engineering Program
Department of Materials and Nuclear Engineering
University of Maryland
College Park, MD 20742

November 1997

## Notice

This report was prepared for the Building and Fire Research Laboratory of the National Institute of Standards and Technology under grant number 60NANB6D0127. The statement and conclusions contained in this report are those of the authors and do not necessarily reflect the views of the National Institute of Standards and Technology or the Building and Fire Research Laboratory.

# Evaluation of the HDR Fire Test Data and Accompanying Computational Activities with Conclusions from Present Code Capabilities

NIST CONTRACT 60NANB6D0127

## **Volume 2**:
## CFAST Validation for
## T51 Gas Fire Test Series

November 1997

Jason Floyd
Lothar Wolf
John Krawiec


Nuclear Engineering Program
Department of Materials and Nuclear Engineering
University of Maryland at College Park

## EXECUTIVE SUMMARY

Between 1984 and 1992 four major fire test series were performed in the HDR containment encompassing various fuels and three different axial positions in the high-rise, multi-level, multi-compartment facility. At that time each HDR fire test series was accompanied by extensive efforts to evaluate the predictive capabilities of a variety of fire models and codes developed in different countries by both blind pre-test and open post-test computations. A quite large number of open issues remained in the area of fire computer code predictive qualities upon completion of the HDR program.

In the meantime, large progress has been made in improving and consolidating fire models and computer codes of all levels of simulations. This progress merits revisiting both experimental results and fire computer code validations. The results of the research efforts for this grant during FY 1996/97 are documented in two separate volumes:

Volume 1: Test Series Description Report for T51 Gas Fire Test Series [1]
Volume 2: CFAST Validation for HDR T51 Gas Fire Test Series [2,3]

Volume 2 focuses on the validation of the zone model fire computer code CFAST, which has been developed by NIST, on the basis of a selected set of T51 gas burner tests described in Volume 1 [1].

The present report addresses the following aspects of CFAST validation:

- Section 1 briefly describes the rationale for selecting the four different experiments from the total of 11 HDR gas burner experiments in the HDR containment. Three of the four tests were chosen to cover the total span of fire powers applied: T51.11 (229 kW), T51.21 (716 kW), and T51.23 (1011 kW). The fourth experiment, T51.25, was selected to test CFAST's capability to simulate time-dependent fire room ventilation.
- Section 2 documents in great detail the individual aspects of input data addressing: environment and runtime control, combustion model, and surface properties which are generic to different CFAST models developed for comparison with the 4 HDR experiments. The model-specific specifications of the compartments and their interconnections are provided in subsection 2.4 for the 3 different CFAST models compared with the HDR data.
- Section 3 provides detailed comparisons between data and CFAST model predictions for the CFAST models described in Section 2. This section also includes the results of a parametric study in comparison with major T51.11 data.
- Section 4 addresses all of the accomplishments achieved with CFAST during this project phase, as well as various findings and issues regarding the model setup and application of CFAST and relate to topics such as: documentation, pre- and post-processing, code execution, and physical models. It also provides suggestions for further validation efforts.
- Complete input files for all CFAST computations documented in this report are presented in the Appendix A., while Appendix B documents the input data for CFAST and GOTHIC 3.4e for studying the effect of unphysical vertical flows in a simple model setup.

## ACKNOWLEDGMENTS

The research achieved for this grant during FY 1997 was performed under the auspices of the Building and Fire Research Laboratory at the National Institute of Standards and Technology, Gaithersburg, MD. It was funded by the U.S. Department of Commerce.

This project was monitored at NIST by Dr. Kevin McGrattan whose continued interest in and support of this research is greatly appreciated.

Also, we would like to thank Dr. Walter Jones, Dr. Richard Peacock, and Dr. Glenn Forney in supporting the validation efforts documented in this present Volume 2.

# TABLE OF CONTENTS

## LIST OF FIGURES

## LIST OF FIGURES (CONTINUED)

# LIST OF TABLES

# 1 INTRODUCTION

Traditionally zone model fire codes have been applied to single level structures with comparatively small numbers of interconnected rooms. Currently, there is an increased interest from within the fire safety community to move from prescriptive to performance based fire codes which will require well qualified "best estimate" computational tools. To do this for realistic structures requires making computations for multiple-level buildings with many rooms. To date CFAST, a zone model fire code, has not been rigorously tested under these conditions. The research efforts documented in this volume provides a first step in this direction for a single test series from the HDR test facility in Karlstein, Germany.

This report documents efforts undertaken to model the HDR T51 Gas Fire Test Series [1] using CFAST v3, a zone model fire code developed by the National Institute of Standards and Technology's Building and Fire Research Lab. It is assumed that the reader is familiar with both Volume 1 of this report series, which documents the HDR T51 Gas Fire Test Series [1], and with the CFAST computer code, [2,3].

Four of the eleven gas fire tests were chosen for the modeling efforts reported in the following sections. Three tests; T51.11 (229 kW), T51.21 (716 kW), and T51.23 (1011 kW); were selected as they spanned the range of fire powers used in the T51 series. An additional test, 51.25, which examined the effects of changing the fire room ventilation during the test was also included. For each selected test, three different models of increasing geometric complexity were developed, run, and compared with the respective data.

One test, T51.11, was selected for examining the effects of input data uncertainties on CFAST results. Perturbations of both fire related and geometric related input parameters of the T51.11 model were executed with CFAST to examine the impact on the computed results.

The remainder of this report will describe in detail the models developed, the results of executing those models, the results of sensitivity testing, and also presents overall conclusions of the CFAST computer code applications documented herein.

Accounting for the 10% excess air results in

$$C_3H_8 + 5.5(O_2 + 3.76N_2) \rightarrow 3CO_2 + 4H_2O + 0.5O_2 + 20.68N_2 + 2044\ kJ \qquad (2\text{-}2)$$

Complete combustion of the propane does not truly occur however. From [4] it is obvious that combustion of propane with 10% excess air does not completely burn, but rather results in the formation of the combustion products shown in Table 2.2. These results which were interpolated from the plotted, experimental data in [4] have been read off a chart, Thus, they may not total to one mole of propane due to rounding and chart reading error.

**Table 2.2: Combustion Products for One Mole of Propane with 10% Excess Air**

| Product | Moles |
|---|---|
| $CO_2$ | 2.26 |
| CO | 0.15 |
| $H_2O$ | 3.57 |
| $H_2$ | 0.05 |
| Hydrocarbon | 0.13 |
| Soot | 0.18 |

With the combustion product information and the basic fuel information, the CFAST input cards relating to combustion can now be specified. The applicable cards and their values are shown in Table 2.3 for test T51.21 which was a 716 kW test. For the other tests modeled, modified cards include FAREA (changed to reflect the number of burners used), FMASS (to reflect the propane supplied to reach the test's fire power), and FQDOT (to reflect the current tests fire power). These fire power related changes can be seen in the input decks presented in the Appendix. The remaining combustion parameters did not differ between the tests modeled.

# 2 T51 CFAST MODEL

Three different geometric models were developed for the T51 gas fire tests. The models incorporated an increasing level of geometric complexity. The purpose of this progression was to examine the effects of modeling assumptions on the computations made by CFAST. Compartment surface descriptions, environmental parameters, execution parameters, and combustion parameters remained unchanged for each of the three geometric models. Furthermore, each geometric model has associated with it a related model to allow for the additional ventilation duct used for the T51.2 tests [1]. The remainder of this section will discuss the runtime and environmental parameters, the combustion properties for the fire, the room surface properties, and the different geometric models developed for the CFAST computations.

## 2.1 Environment and Runtime Control

The T51 tests consisted of a one hour fire with a half hour cooldown period with about ten minutes of pre-fire data collection to establish a baseline. No preconditioning of the containment building was performed before the start of any tests, i.e. the containment was at ambient conditions at the start of each test in the series. The CFAST models reproduced these conditions with a 100 s pretest period with no fire to generate a baseline followed by a one hour fire with a half hour cooldown. Table 2.1 below shows the CFAST input cards for environment and runtime control.

**Table 2.1: Environment and Runtime Control Input Cards for CFAST**

| Card | Variable | Value | Reason |
|---|---|---|---|
| TIMES | Simulation Time (s) | 5500 | 100 s +3600 s+1800 s |
| | Print Interval (s) | 100 | |
| | History Interval (s) | 50 | |
| | Display Interval (s) | 0 | No graphics |
| | Copy Count | 0 | No graphics to copy |
| STPMAX | Maximum Time Step (s) | 1 | Advice of code developers |
| TAMB/ EAMB | Ambient Temperature (K) | 288 | 15° C |
| | Ambient Pressure (Pa) | 101300 | 1 atm. |
| | Station Elevation (m) | 0 | Set hallway floor as 0 elevation |

## 2.2 Combustion Model

Each of the tests in the T51 series used propane gas premixed with 10% excess air and fed into one or more burners mounted along the back wall of the fire room at an elevation of 0.375 m above the fire room floor, see Figure 2.2 on page 2-5. This forms the basis for the combustion parameters used for the CFAST models. Complete combustion of propane occurs according to the following stoichiometric relation:

$$C_3H_8 + 5(O_2 + 3.76N_2) \rightarrow 3CO_2 + 4H_2O + 18.8N_2 + 2044\ kJ \qquad (2\text{-}1)$$

**Table 2.3: Combustion Related Input Cards for CFAST**

| Card | Variable | Value | Reason |
|---|---|---|---|
| LFBO | Fire Origin | 1 | Fire is in compartment 1 |
| LFBT | Fire Type | 2 | Constrained fire |
| CHEMI | Molar Weight (GMW)<br>Relative Humidity (%)<br>Lower Oxygen Limit (%)<br>Heat of Combustion (J/kg)<br>Initial Fuel Temp. (K)<br>Gas Ignition Temp. (K)<br>Radiative Fraction (%) | 44<br>0<br>0<br>4.65E+07<br>300.<br>388.<br>0.10 | Molar weight of propane<br>No comparisons being made to water vapor<br>Fuel is premixed with air<br>Heat of combustion for propane<br>Assume propane starts at room temperature<br>Left unchanged from template file<br>Default value |
| CJET | Ceiling Jet | Off | No data in fire room about wall temperature profiles; therefore, there is no need for the additional precision of the ceiling jet routine. |
| FAREA | Fuel Area ($m^2$) | 0.0 0.0 0.28 0.28 0.0 0.0 | 4 burners assumed to be 30 cm in diameter |
| FHIGH | Fuel Height (m) | 0.0 0.0 0.375 0.375 0.0 0.0 | Burners are 0.375 m above the floor |
| FMASS | Mass Loss Rate (kg/s) | 0.0 0.0 0.0154 0.0154 0.0 0.0 | $\frac{716\ kW}{4.65\times10^7 J/kg} = 0.0154$ kg/s |
| FPOS | Depth (m)<br>Breadth (m)<br>Height (m) | 0.000<br>1.475<br>0.000 | Locate fire along center of back wall of fire room. Height is set to zero as FHIGH has been set to 0.375. |
| FQDOT | Heat Release Rate (W) | 0.0 0.0 716000. 716000. 0.0 0.0 | One hour fire at 716 kW |
| FTIME | Time Points (s) | 100.0 101.0 3700.0 3701.0 5500.0 | 100 s with no fire followed by a one hour fire with a 1 s ramp up and ramp down followed by a half hour cooldown period. |
| HCR | H to C Mass Ratio | 0.0 0.0 0.222 0.222 0.222 0.222 | $\frac{8\times1}{3\times12} = 0.222$ |
| OD | C to $CO_2$ Ratio | 0.0 0.0 0.022 0.022 0.022 0.022 | $\frac{0.18\times12}{2.26\times(12+2\times16)} = 0.022$ |
| CO | CO to $CO_2$ Ratio | 0.0 0.0 0.042 0.042 0.042 0.042 | $\frac{0.15\times(12+16)}{2.26\times(12+2\times16)} = 0.042$ |

## 2.3 Surface Properties

To model the HDR with CFAST requires generating material properties for the HDR's construction materials. For the T51 gas fire tests there are three materials which must be defined which are the HDR structural concrete, Ytong fire brick, and Alsiflex fireproof, glass fiber matting. A CFAST material library was created for these materials and the surfaces which were constructed from them. Table 2.4 gives the thermophysical material properties which were obtained from [14].

**Table 2.4: Thermophysical Properties for HDR Construction Materials**

| Material | Density ($kg/m^3$) | Conductivity (W/m·K) | Heat Capacity J/(kg·K) | Emissivity |
|---|---|---|---|---|
| Concrete | 2,225 | 2.10 | 879 | 0.8[1] |
| Ytong Firebrick | 340 | 0.24 | 950 | 0.8[1] |
| Alsiflex Mats | 130 | 0.17 | 1,000 | 0.9[2] |

[1] Taken as firebrick from default CFAST material library
[2] Taken from Alsiflex properties in [15]

The above thermophysical properties were used to create a seven material library for use with CFAST. The seven materials included five single layer materials and two, two layer materials. The materials in the order listed below are 3 cm thick Alsiflex matting, 100 cm of concrete, 50 cm of concrete, 10 cm of Ytong firebrick, 25 cm of Ytong firebrick, the Alsiflex matting and Ytong firebrick ceiling for the fire room, and the Ytong firebrick and concrete floor of the fire room. The material library is shown below. For single layer materials the format is material name, conductivity, density, heat capacity, thickness, emissivity, and seven parameters for HCl production. For multiple layer materials the format is the same with a '/' denoting values for each layer.

```
ALSIFLEX  0.17 1000 130 0.03 0.9 0 0 0 0 0 0 0
CONCR100  2.1 879 2225 1 0.8 0 0 0 0 0 0 0
CONCR050  2.1 879 2225 0.5 0.8 0 0 0 0 0 0 0
YTONG100  0.24 950 340 0.1 0.8 0 0 0 0 0 0 0  0
YTONG250  0.24 950 340 0.25 0.8 0 0 0 0 0 0 0  0
FIRECEIL  0.17/0.24 1000/950 130/340 0.03/0.25 0.9 0 0 0 0 0 0 0
FIRE_FLR  0.24/2.1 950/879 340/2225 0.25/1 0.8 0 0 0 0 0 0 0
```

## 2.4 Compartments and Compartment Interconnections

The final portion of the CFAST model is of course the compartments and the compartment interconnections. As the HDR facility contains 9 levels and over 60 compartments with complex interconnections, it could not be modeled explicitly with CFAST. Therefore, simplifications were needed to model the HDR facility with CFAST. To this end, three different geometric models of the HDR facility were created with an increasing level of complexity. This was done,

in part, to see how different modeling assumptions affected the predictions made by CFAST. The following subsection will document the three geometric models in detail.

### 2.4.1 A Model

The A model was the simplest of the three models. It only encompasses the significant compartments on Level 1.400. This model best complies with traditional simulations of single level, horizontal fires and fire product spreading. The A model assumed that since the HDR was such a large facility with large flow areas between compartments, it was reasonable to consider rooms far from the fire room being part of the outside. That is, once hot gasses leave Level 1.400 through the maintenance hatch that they were considered to have departed the facility. While this assumption will not yield information on the behavior of floors above the fire room, it should suffice for obtaining reasonable predictions of the fire floor itself.

Figure 2.1 shows Level 1.400. From this figure it is obvious that the important compartments were the fire room and its doorway, the hallway, and the curtained area as these compartments defined the location of the fire and the flowpath taken by the combustion products. The curtained area had a 0.5 m gap at the floor for the return of cold air. This air could come from either room 1.402 or the main staircase, which in itself was connected to room 1.402. Room 1.402 had a fairly narrow connection to the rest of the containment building, so this restriction should be accounted for to create a flowpath resistance for returning cold air. Therefore, the A model, shown in Figure 2.5, page 2-8, consisted of five compartments which were the fire room and its doorway, the hallway, the curtained area, the main staircase, and room 1.402.

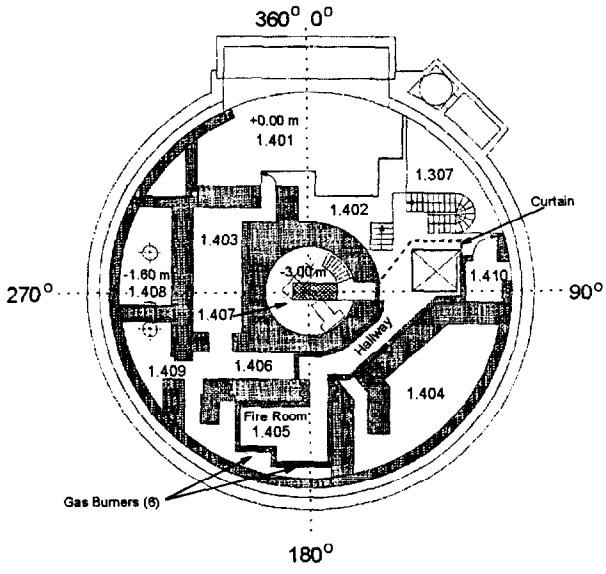


**Figure 2.1: Level 1.400**

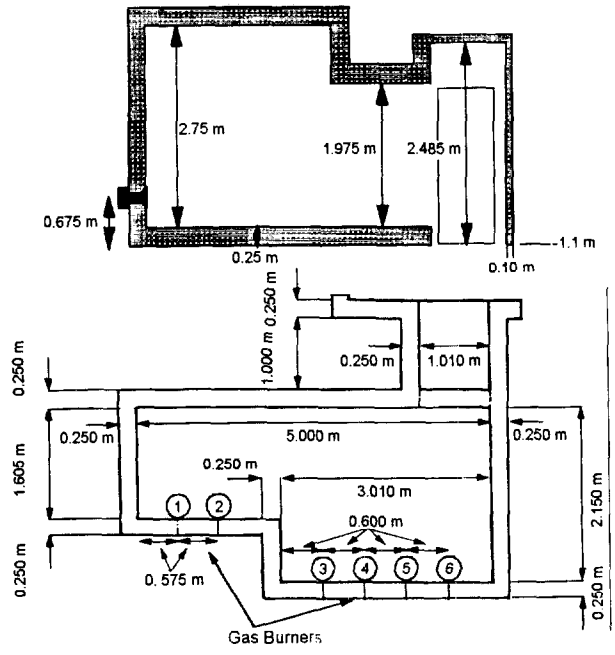


**Figure 2.2: Fire Room and Doorway**

From the dimensions given in Figure 2.2, the volume of the fire room and doorway was calculated to be 29.6 $m^3$ with the doorway having 3 $m^3$ of that volume. Since the doorway was

such a small volume in comparison to the fire room and the hallway, it was assumed to be part of the fire room. Therefore, as the fire room was 2.75 m in height, the floor area of the fire room is 10.77 $m^2$. If the linear distance from the fire room's back wall, the location of the burners, to the doorway opening into the hallway was preserved, the floor dimensions of the fire room became 3.65 m x 2.95 m. The surfaces of the fire room consisted of a ceiling lined with 0.25 m of Ytong firebrick covered by 0.03 m of Alsiflex mats, the walls of the fire room lined with 0.25 m of Ytong firebrick, and the fire room floor which was 0.25 m of Ytong firebrick on top of a 1 m thick concrete floor. The fire room was connected to the hallway by a 1.01 m x 1.975 m doorway.

Figure 2.3 shows the hallway that connected the fire room to the maintenance hatch. Reference [12] gives the volume of the hallway as 22.15 $m^3$ with a ceiling height of 2.485 m. The hallway had a variable width and a curved length which did not readily translate into a rectangular parallelepiped for modeling purposes with CFAST. The dimensions of significance for the hallway were the height and the width of the hallway were it connected to the maintenance hatch; this was also the widest cross section of the hallway. This resulted in the hallway having floor dimensions of 1.8 m x 4.95 m. The hallway surfaces were 0.10 m of Ytong firebrick for the walls and ceiling and 0.50 m of concrete for the floor. The hallway was connected to the curtained area by a 1.8 m x 2.75 m opening.

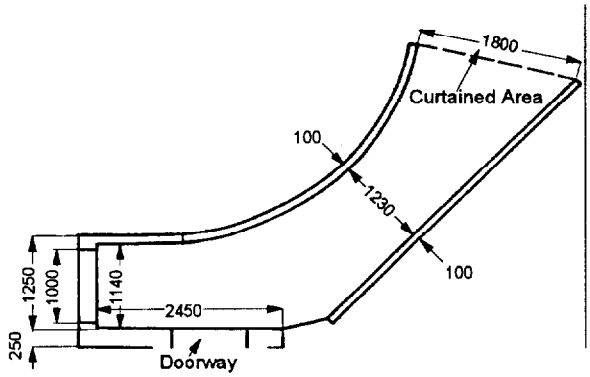


**Figure 2.3: Hallway**

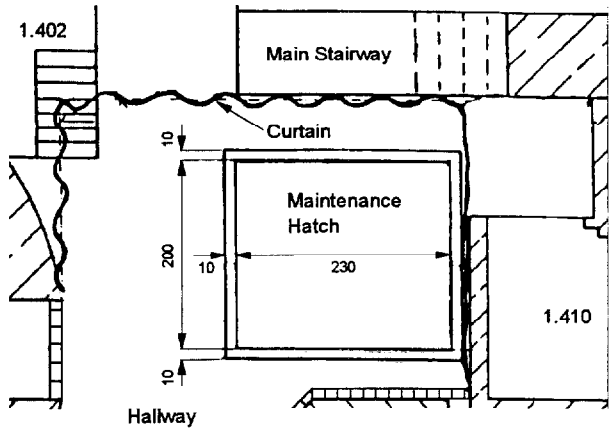


**Figure 2.4: Maintenance Hatch and Curtain**

Figure 2.4 shows the curtained area beneath the maintenance hatch. The hatch itself was a rectangular opening 4.54 $m^2$ in area. Using the hatch dimensions shown in the figure and assuming the figure was to scale, the curtained area floor dimensions were found to be 4.30 m x 2.75 m. The height of this region was 4.60 m. All surfaces were assumed to be 0.50 m thick concrete. The hatch was connected to the outside by a 4.54 $m^2$ rectangular opening. From Figure 2.4, the flow path underneath the curtain to room 1.402 and the main staircase was estimated to be 2.0 m x 0.5 m and 4.3 m x 0.5 m, respectively.

The main staircase had the same floor and ceiling elevations as the hatch area, 4.60 m in height. The floor area of the main staircase was estimated to be 11.78 $m^2$, 4.33 m x 2.72 m, by using Figure 2.1 and the HDR steel shell diameter of 20 m. All surfaces were again assumed to be

0.50 m thick concrete. The vertical flow path up the main staircase was 5.75 $m^2$. The connection to room 1.402 was estimated from Figure 2.1 to be 2.7 m x 3.1 m.

Room 1.402 also had its floor area dimensions estimated from Figure 2.1. The floor dimensions were estimated to be 1.80 m x 6.50 m with a height of 3.50 m. All surfaces were 0.50 m thick concrete. The connection from room 1.402 to the outside is given in [5] as 0.8 m x 1.5 m.

The final portion of the A model was the fresh air supply for the gas burners. In reality this connected room 1.603 to the fire room; however, Level 1.600 was not included in the A model. This ventilation system was assumed to be an 0.30 m ID duct. Since this ventilation system operates at a constant flow rate, the duct diameter is not a significant parameter. The duct goes from the burner location at -0.475 m absolute elevation, 0.375 m relative to the fire room floor, and was assumed to end 0.5 m above the floor of room 1.603 at 10.50 m absolute elevation, 11.60 m relative to the fire room floor. This was a vertical run of 11 m, and if a 7 m horizontal pipe run was assumed, the total duct length became 18 m. This duct was created as two separate portions connected by a constant speed fan. As the T51 tests used a constant flow rate air supply, it was not necessary to model the pipe resistances as these were accounted for in the real experiment when supplying the air for the burners. The inlet area of the duct was based on an assumed diameter of 0.30m. The outlet area of the duct was set to be the assumed area of the gas burners used in the tests as described in Section 2.1.

The CFAST geometric input cards for the A model are shown below:

```
HI/F   0.250  0.000  0.000  0.000  0.000
WIDTH  2.950  4.950  4.300  4.330  1.800
DEPTH  3.650  1.800  2.750  2.720  6.350
HEIGH  2.750  2.485  4.600  4.600  3.500
CEILI FIRECEIL YTONG100 CONCR050 CONCR050 CONCR050
WALLS YTONG250 YTONG100 CONCR050 CONCR050 CONCR050
FLOOR FIRE_FLR CONCR100 CONCR050 CONCR050 CONCR050
HVENT  1  2  1  1.010  1.975  0.000
CVENT  1  2  1  1.000  1.000  1.000  1.000  1.000  1.000
HVENT  2  3  1  1.800  2.485  0.000
CVENT  2  3  1  1.000  1.000  1.000  1.000  1.000  1.000
HVENT  3  4  1  4.300  0.500  0.000
CVENT  3  4  1  1.000  1.000  1.000  1.000  1.000  1.000
HVENT  3  5  1  2.000  0.500  0.000
CVENT  3  5  1  1.000  1.000  1.000  1.000  1.000  1.000
HVENT  4  5  1  2.700  3.100  0.000
CVENT  4  5  1  1.000  1.000  1.000  1.000  1.000  1.000
HVENT  5  6  1  0.800  1.500  0.000
CVENT  5  6  1  1.000  1.000  1.000  1.000  1.000  1.000
VVENT  6  3  4.54000  2
VVENT  6  4  5.75000  2
MVDCT  1  2   1.000  0.300  1.00E-004  0.000  1.000  0.000  1.000  0  0
MVDCT  3  4  18.000  0.300  1.00E-004  0.000  1.000  0.000  1.000  0  0
MVFAN  3  2   0.000 900.00  0.0730     0.000  0.000  0.000  0.000  0  0
MVOPN  1  1 H  0.375  0.143  0  0  0  0
MVOPN  6  4 V 11.600  0.070  0  0  0  0
INELV  2  0.625  0  0
INELV  3  0.625  0  0
```

Figure 2.5 shows a block diagram of this model geometry including ventilation systems, vent connections between compartments, and vent connections to the outside.

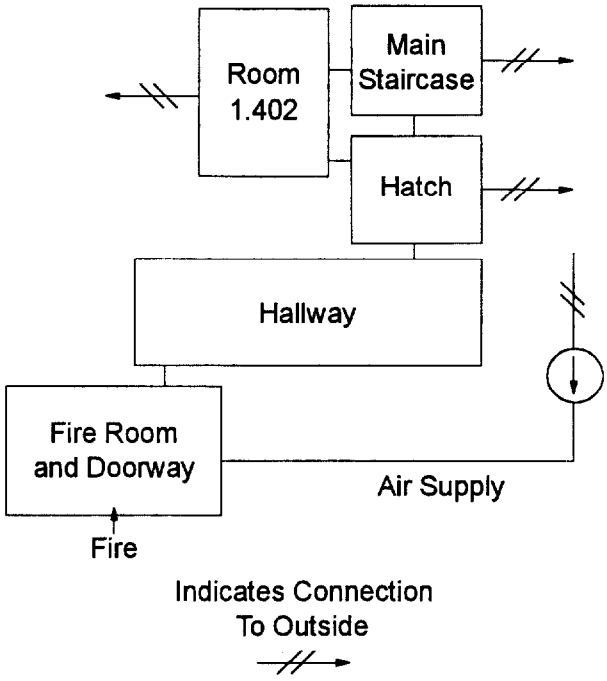


**Figure 2.5: A Model Block Diagram**

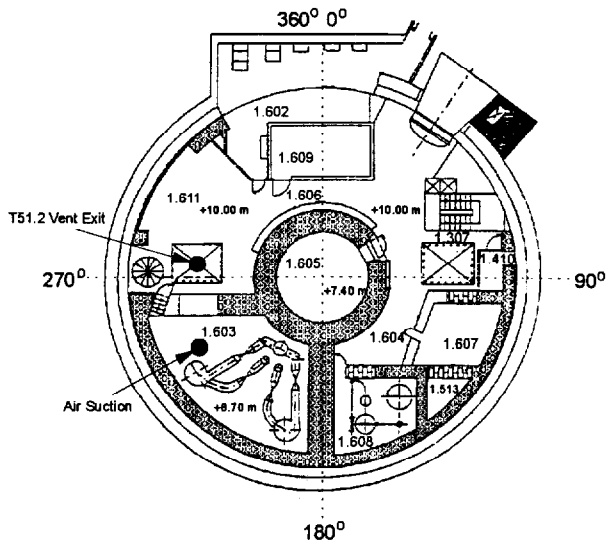


**Figure 2.6: Level 1.600**

2.4.2 B Model

The B model took the A model one step further by including Level 1.600 of the HDR. Since the fire room fresh air supply and the additional ventilation duct exit were located on Level 1.600, it would be appropriate to incorporate these into the CFAST model. As with the A model, since the volume of the containment above Level 1.600 is very large it was considered to be part of the outside. Also, since the post-test analysis indicated that Level 1.500 played a minor role in the building circulation due to the spiral staircase hatches being closed, it was excluded from the B model.

If the B model was to include Level 1.600, a coupling between Level 1.400 and Level 1.600 was required. This was done by extending the height of the curtained area and main staircase compartments of the A model so that they ended at the floor elevation of Level 1.600.

On Level 1.600, there were four significant regions, a shown in Figure 2.6. The vertical flow paths created by Level 1.400 main staircase and maintenance hatch must be continued. The fresh air supply located in room 1.603 needed to be included. Finally, the spiral staircase and its maintenance hatch also needed to be included. Room 1.603 was an isolated compartment connected to the spiral staircase by a large doorway, so the two could be considered as one lumped compartment. Since the spiral and main staircase regions were on opposite sides of the containment, the remainder of Level 1.600 must be included to join the two sections together. Therefore, the B model contained four additional compartments: the curtained area on Level 1.600, the main staircase on Level 1.600, the spiral staircase and room 1.603, and the remainder of Level 1.600 as depicted in Figure 2.7, see page 2-10.

The main staircase and hatch compartments were given the same floor dimensions on Level 1.600 as they were on Level 1.400. The height of these compartments was set to 5.05 m which places the ceiling of these compartments at the elevation of Level 1.700's floor. All surfaces were set to 0.50 m thick concrete. The maintenance hatch area leading to the outside remained unchanged from the A model, but the main staircase vent was set to a 6.97 $m^2$ rectangle.

The volume of the room 1.603 and spiral staircase compartment was set to equal the sum of the compartment volumes for 1.603 and 1.611 which is 472 $m^3$. A height of 5.05 m was also used for this compartment. The dimensions of the floor were set to a square as there was no dominant linear dimension of interest for this compartment. The floor area was therefore set to 9.67 m x 9.67 m and all room surfaces were 0.50 m thick concrete. The hatch and spiral staircase vent to the outside was set to a 5.28 $m^2$ rectangle.

The remainder of Level 1.600 included all of this level except for rooms 1.602 and 1.609 which were closed off and the portions of the level already incorporated into the B model. This resulted in a compartment volume of 288 $m^3$. The resulting compartment dimensions using a square floor were 7.92 m x 7.92 m x 4.60 m. All room surfaces were set to 0.50 m thick concrete. Vent connections were established between this compartment and the other three compartments on the level as well as between the main staircase and hatch. The fresh air ventilation system was also modified to connect to room 1.603 rather than to the outside as it did in the A model. The final B Model layout is shown in Figure 2.7. The geometric input cards for CFAST are shown below:

```
HI/F   0.250  0.000  0.000  0.000  0.000 11.100 11.100 11.100 11.100
WIDTH  2.950  4.950  4.300  4.330  1.800  7.920  4.300  4.330  9.760
DEPTH  3.650  1.800  2.750  2.720  6.350  7.920  2.750  2.720  9.760
HEIGH  2.750  2.485 11.100 11.100  3.500  4.600  5.050  5.050  5.050
CEILI FIRECEIL FIRECEIL YTONG100 CONCR050 CONCR050 CONCR050 CONCR050 CONCR050 CONCR050 CONCR050
WALLS YTONG250 YTONG250 YTONG100 CONCR050 CONCR050 CONCR050 CONCR050 CONCR050 CONCR050 CONCR050
FLOOR FIRE_FLR FIRE_FLR CONCR100 CONCR050 CONCR050 CONCR050 CONCR050 CONCR050 CONCR050 CONCR050
HVENT  1  2  1  1.010  1.975  0.000
CVENT  1  2  1  1.000  1.000  1.000  1.000  1.000  1.000
HVENT  2  3  1  1.800  2.485  0.000
CVENT  2  3  1  1.000  1.000  1.000  1.000  1.000  1.000
HVENT  3  4  1  4.300  0.500  0.000
CVENT  3  4  1  1.000  1.000  1.000  1.000  1.000  1.000
HVENT  3  5  1  2.000  0.500  0.000
CVENT  3  5  1  1.000  1.000  1.000  1.000  1.000  1.000
HVENT  4  5  1  2.700  3.100  1.100
CVENT  4  5  1  1.000  1.000  1.000  1.000  1.000  1.000
HVENT  5 10  1  0.800  3.500  0.000
CVENT  5 10  1  1.000  1.000  1.000  1.000  1.000  1.000
HVENT  6  7  1  3.000  4.250  0.000
CVENT  6  7  1  1.000  1.000  1.000  1.000  1.000  1.000
HVENT  6  8  1  3.000  4.250  0.000
CVENT  6  8  1  1.000  1.000  1.000  1.000  1.000  1.000
HVENT  6  9  1  3.000  4.250  0.000
CVENT  6  9  1  1.000  1.000  1.000  1.000  1.000  1.000
HVENT  7  8  1  3.000  4.250  0.000
CVENT  7  8  1  1.000  1.000  1.000  1.000  1.000  1.000
VVENT  7  3  4.54000  2
VVENT  8  4  5.75000  2
VVENT 10  7  4.54000  2
VVENT 10  8  6.97000  2
VVENT 10  9  5.28000  2
MVDCT  1  2   1.000  0.300  1.00E-004  0.000  1.000  0.000  1.000  0  0
MVDCT  3  4  18.000  0.300  1.00E-004  0.000  1.000  0.000  1.000  0  0
```

```
MVFAN  3  2   0.000 900.00  0.073       0.000  0.000  0.000  0.000  0  0
MVOPN  1  1 H  0.375  0.143  0  0  0  0
MVOPN  9  4 V  0.500  0.070  0  0  0  0
INELV  2  0.625  0  0
```

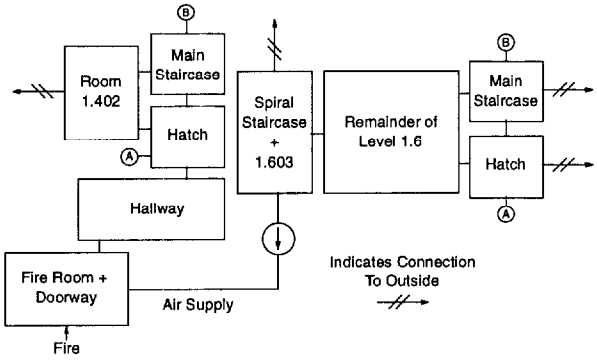


**Figure 2.7: B Model Block Diagram**

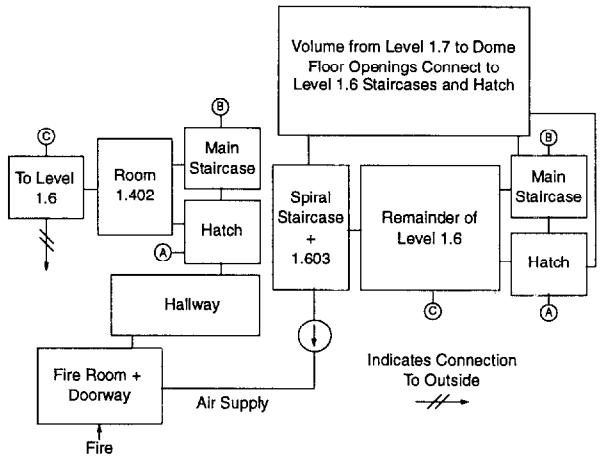


**Figure 2.8: C Model Block Diagram**

### 2.4.3 C Model

The final and most complex model was the C model. To model the HDR facility in a manner that captures all the basic flow phenomena observed in the gas fire tests would require that the model be completely enclosed and contain the dome region. This would force any combustion products traveling up the main staircase side of the facility to return to the fire floor by descending the shafts formed by the spiral staircase and neighboring hatches. Therefore, Level 1.600 as modeled in the B model must be vented to an enclosed compartment rather than the outside. Therefore, the C model added a compartment to represent the volume of the HDR above Level 1.600. Just adding this volume, however, would not necessarily result in return flow from the upper levels. A flowpath must be provided to lower containment elevations for this to happen. Even though the spiral staircase hatch to Level 1.500 was closed, there did exist numerous floor penetration in the form of pipe channels, cable trays, and other conduits that connected Level 1.600 to Level 1.500 and Level 1.400. These connections must also be included in the model. The C model, therefore, resulted from adding two additional compartments to the B model.

The portion of the HDR facility above Level 1.600 was modeled as a single compartment. The volume of this compartment was obtained by summing up the volume of all compartments above Level 1.600 excluding rooms 1.702 and 1.706. This yielded a total volume of 7215 $m^3$ and preserving the full HDR height resulted in a compartment with dimensions of 14.37 m x 14.37 m x 39.95 m. All wall surfaces for this compartment were set to 0.5 m thick concrete which is not a true representation for the steel shell dome. The B model hatch and staircase openings to the outside were considered as openings into this compartment for the C model.

The second compartment added for the C model was a connecting compartment from Level 1.600 to room 1.402. This was done to provide a flow path from the upper levels to the lower level in order to avoid unrealistic pressure gradients that would ultimately prevent recirculation

flow. The room connection list [1] was consulted and the area of available connections from Level 1.400 to Level 1.600 (excluding hatches and staircases) was totaled. This yielded a flow area of 9 $m^2$. Initially, this room was modeled to span the elevation from the floor of room 1.402 to the ceiling of Level 1.600. CFAST would not run, however, with a completely enclosed geometry. A vent to the outside was needed. This vent was added to this second compartment as it is the furthest removed from the flow regions of interest, namely the vertical shafts and the fire room and hallway. This configuration would run for a short period of time until the layer height in the connection room decreased to near zero which then propagated throughout the remainder of Level 1.400. A series of permutations was made to this compartment changing the elevations, vent connections, and internal flow area until a combination was determined that would allow CFAST to execute for both the duration of the fire and the cooldown period. The resultant compartment started at an elevation of 0.3 m and extended vertically for 13.2 m, 2.4 m above the floor of Level 1.600. The Level 1.600 compartment connected with a 3.0 m x 2.4 m doorway, room 1.402 connected with a 1.8 m x 3.2 m doorway, and there was a connection to the outside that was 0.05 m wide that extended from the ceiling of room 1.402 to the floor of Level 1.600. While it would clearly be preferable not to have manipulated the vent connections to ensure CFAST's operation, the end result coupled Level 1.600 cold layer to Level 1.400 hot later which is, in reality, what the flow actually does. However, the true vent area was not totally preserved. All surfaces of this room were 0.5 m thick concrete. The difficulties with this particular compartment demonstrate the need for more user guidance from the code manual.

A block diagram of the C model is shown in Figure 2.8 on page 2-10. Shown below are the CFAST input cards for this model.

```
HI/F   0.250  0.000  0.000  0.000  0.000 11.100 11.100 11.100 11.100 16.150  0.300
WIDTH  2.950  4.950  4.300  4.330  1.800  7.920  4.300  4.330  9.670 14.370  3.000
DEPTH  3.650  1.800  2.750  2.720  6.350  7.920  2.750  2.720  9.670 14.370  3.000
HEIGH  2.750  2.485 11.100 11.100  3.500  4.600  5.050  5.050  5.050 34.950 13.200
CEILI FIRECEIL YTONG100 CONCR050 CONCR050 CONCR050 CONCR050 CONCR050 CONCR050 CONCR050 CONCR050 CONCR050
WALLS YTONG250 YTONG100 CONCR050 CONCR050 CONCR050 CONCR050 CONCR050 CONCR050 CONCR050 CONCR050 CONCR050
FLOOR FIRE_FLR CONCR100 CONCR050 CONCR050 CONCR050 CONCR050 CONCR050 CONCR050 CONCR050 CONCR050 CONCR050
HVENT  1  2  1  1.010  1.975  0.000
CVENT  1  2  1  1.000  1.000  1.000  1.000  1.000  1.000
HVENT  2  3  1  1.800  2.485  0.000
CVENT  2  3  1  1.000  1.000  1.000  1.000  1.000  1.000
HVENT  3  4  1  4.300  0.500  0.000
CVENT  3  4  1  1.000  1.000  1.000  1.000  1.000  1.000
HVENT  3  5  1  2.000  0.500  0.000
CVENT  3  5  1  1.000  1.000  1.000  1.000  1.000  1.000
HVENT  4  5  1  2.700  3.100  1.100
CVENT  4  5  1  1.000  1.000  1.000  1.000  1.000  1.000
HVENT  5 11  1  1.800  3.500  0.300
CVENT  5 11  1  1.000  1.000  1.000  1.000  1.000  1.000
HVENT  6  7  1  3.000  4.250  0.000
CVENT  6  7  1  1.000  1.000  1.000  1.000  1.000  1.000
HVENT  6  8  1  3.000  4.250  0.000
CVENT  6  8  1  1.000  1.000  1.000  1.000  1.000  1.000
HVENT  6  9  1  3.000  4.250  0.000
CVENT  6  9  1  1.000  1.000  1.000  1.000  1.000  1.000
HVENT  7  8  1  3.000  4.250  0.000
CVENT  7  8  1  1.000  1.000  1.000  1.000  1.000  1.000
HVENT 11 12  1  0.050  9.800  3.300
CVENT 11 12  1  1.000  1.000  1.000  1.000  1.000  1.000
HVENT  6 11  1  3.000  2.400  0.000
CVENT  6 11  1  1.000  1.000  1.000  1.000  1.000  1.000
VVENT  7  3  4.54000  2
VVENT  8  4  5.75000  2
VVENT 10  7  4.54000  2
VVENT 10  8  6.97000  2
```

```
VVENT 10  9  5.28000  2
MVDCT  1  2   1.000  0.300  1.00E-004  0.000  1.000  0.000  1.000  0  0
MVDCT  3  4  18.000  0.300  1.00E-004  0.000  1.000  0.000  1.000  0  0
MVFAN  3  2   0.000 900.00  0.0073     0.000  0.000  0.000  0.000  0  0
MVOPN  1  1 H  0.375  0.143  0  0  0  0
MVOPN  9  4 V  0.500  0.070  0  0  0  0
INELV  2  0.625  0  0
INELV  3  0.625  0  0
```

### 2.4.4 Additional Ventilation

The T51.25 test incorporated a ventilation duct in the fire room. This duct was a naturally ventilated, 0.4 m diameter duct that connected the fire room with the 1.600 level. The duct started near the ceiling of the wall adjacent to burner #1, extended approximately 2 m into Level 1.600, and had its exit centered beneath the spiral staircase maintenance hatch. There was a damper inside the duct that was adjusted during the fire tests to change the room ventilation. Since the duct flow area changed during the fire test, it could not be modeled in CFAST as a ventilation system as CFAST does not allow for time-dependent ventilation systems. Therefore, this duct had to be modeled as a compartment. The initial attempt at including this duct was for a horizontal connection to the fire room and a vertical connection to the spiral staircase compartment using the actual elevations of the pipe openings. CFAST would not execute properly with this configuration. As with the connecting volume developed for the C model, a number of permutations were required to determined a configuration which would execute. The final configuration for this duct was a 0.7 m x 0.7 m x 13.5 m compartment starting at an elevation of 2.65 m with a 0.7 m x 0.18 m connection to the fire room and a 0.35 m x 0.35 m connection to the spiral staircase compartment This configuration preserved the true flow areas at the vent connections. Ideally, since the duct was insulated in the test, the wall heat transfer should be turned off as the presence of insulation makes the duct walls nearly adiabatic. CFAST would not execute properly with the wall heat transfer turned off for this compartment. It would run however using the 0.5 m thick concrete walls as used for other compartments in the model. The vent connection cards for this compartment are shown below:

```
HVENT  1 12  1  0.700  2.750  2.570
CVENT  1 12  1  1.000  1.000  1.000  1.000  0.000  0.000  0.000  0.000
HVENT  9 12  1  0.350  5.050  4.700
CVENT  9 12  1  1.000  1.000  1.000  1.000  1.000  1.000  1.000  1.000
```

# 3 RESULTS

This section compares the CFAST predictions from the various models to measured data from the actual tests. Instrument descriptions and locations can be found in the companion volume to this report [1]. The subsections that follow will examine the effects of modeling assumptions and geometry on the quality of CFAST predictions for test T51.21, compare predictions made for varying test powers with CFAST predictions to examine the effects of fire power on CFAST's predictive capabilities, assess how well CFAST can capture time dependent ventilation conditions, and examine CFAST's sensitivity to input changes. In each of the figures that follow, the HDR instrumentation is identified by its instrument number and its position in terms of the HDR building elevation. Section 3 of Volume 1 [1] of this report shows the locations of the HDR sensors.

As this section discusses model comaprisons with data, it is important to define what the authors consider a good versus a poor comparison. CFAST is designed to be a quickly executed engineering tool with a relatively small learning curve. Therefore, CFAST can not be expected to make exact or near exact predictions to the data especially given the complexity of the HDR facility. However, it can be expected that CFAST should reproduce the same trends as seen in the data, predict with reasonable accuracy the significant phenomena of the experiments, and not introduce signifcant non-existing phenomena.

## 3.1 Model Comparison (T51.21)

This subsection compares the CFAST predictions to measured data for test T51.21 for each of the three models described in section 2. Test T51.21 was chosen as the fire power was large enough to cause a noticeable temperature change throughout the HDR facility while remaining small enough that a cold layer remained in the fire room throughout the test.

Figure 3.1 on the next page shows the layer heights calculated in the fire room for each of the three models. For the first ten minutes of the fire the three models all predict that the fire room layer quickly approaches an absolute elevation of +0.07 m. After ten minutes, the C model layer height drops to -0.23 m and slowly increase back to -0.10 m; whereas, the A shows a slight change in layer height to +0.06 m and the B model remains essentially unchanged. It is unclear why the C model predicts a sudden drop in layer height at 10 minutes since there is no physical reason for it..

The next two figures, Figures 3.2 and 3.3, show the CFAST predictions for the fire room layer temperatures.

The three models initially predict the same layer temperatures with the hot layer being overpredicted and the cold layer being underpredicted. After the first ten minutes the C model predicts both a higher cold layer and a higher hot layer temperature. This results in a much worse prediction for the hot layer temperature, but a more reasonable temperature for the cold layer. The reason for the cold layer temperature increase is the drop in layer height shown in Figure 3.1.

The hot layer temperature increase appears to result from a large drop in the mass flow rate out of the fire room shown in Figure 3.4.

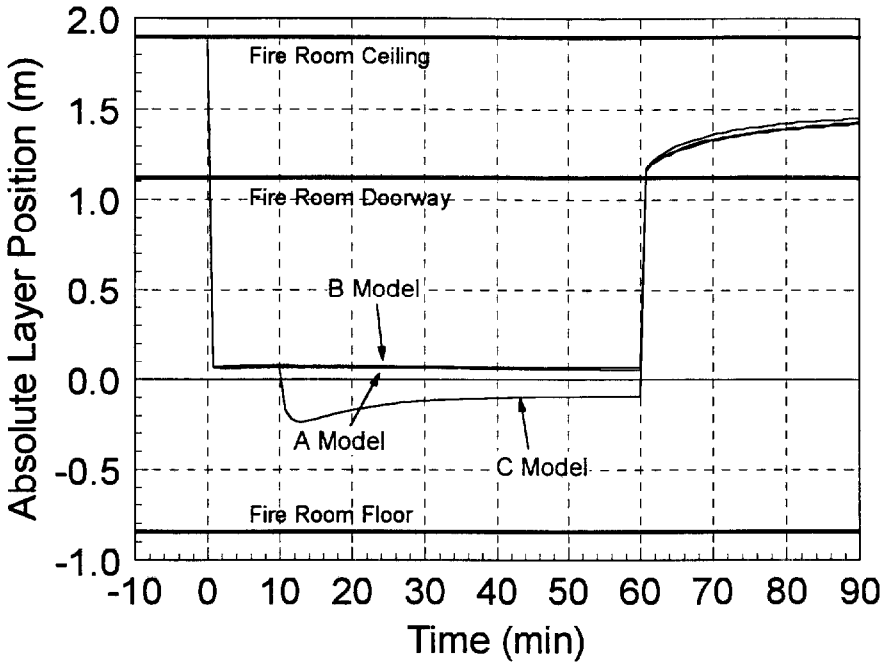


**Figure 3.1: T51.21 Fire Room Layer Height**

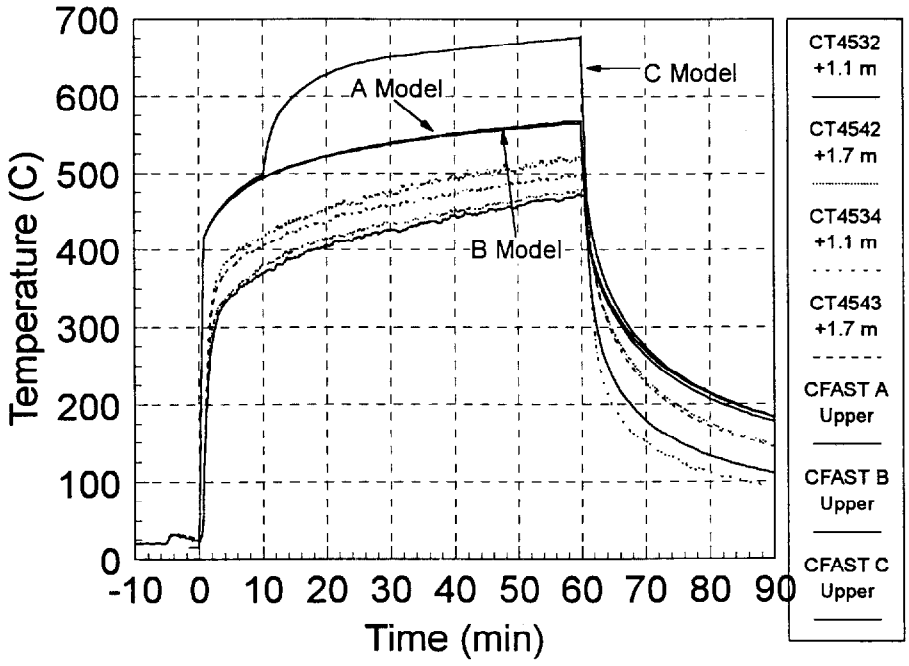


**Figure 3.2: T51.21 Fire Room Upper Layer Temperature**

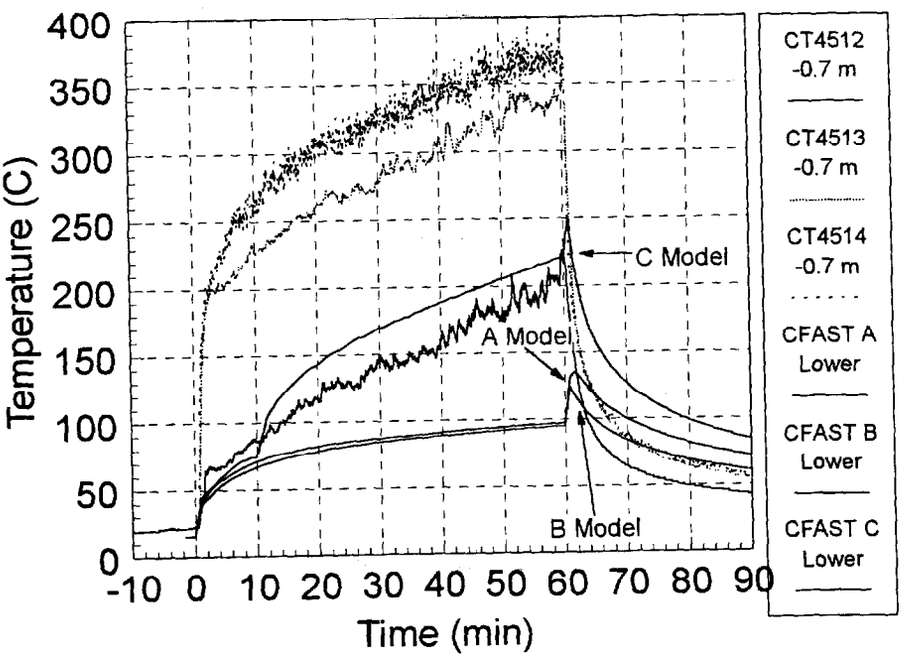


**Figure 3.3: T51.21 Fire Room Lower Layer Temperature**

Figures 3.4 and 3.5 on the next page show predicted versus measured velocities at the fire room doorway. Again, all three models agree until ten minutes into the fire when the C model diverges. Since the CFAST prediction represents an average velocity in the layer and the measurement is a fixed local position, a direct comparison between the two can only yield qualitative. Though given the magnitude of the difference between the predicted and measured data, CFAST appears to underpredict the lower layer velocities for all three models and overpredict the hot layer velocity for the A and B models. However, if this is the case then the temperature predictions for the fire room are less accurate than initially indicated. If the hot layer velocity is overpredicted, this should act to decrease the fire room's upper layer temperature, yet the code is overpredicting this temperature. Similarly, if the cold layer velocity is being underpredicted, then this should act to increase the lower layer temperature; however, the code is underpredicting the temperature. Together, the velocity and temperature predictions indicate that CFAST is biasing the energy balance in the fire compartment to the upper layer.

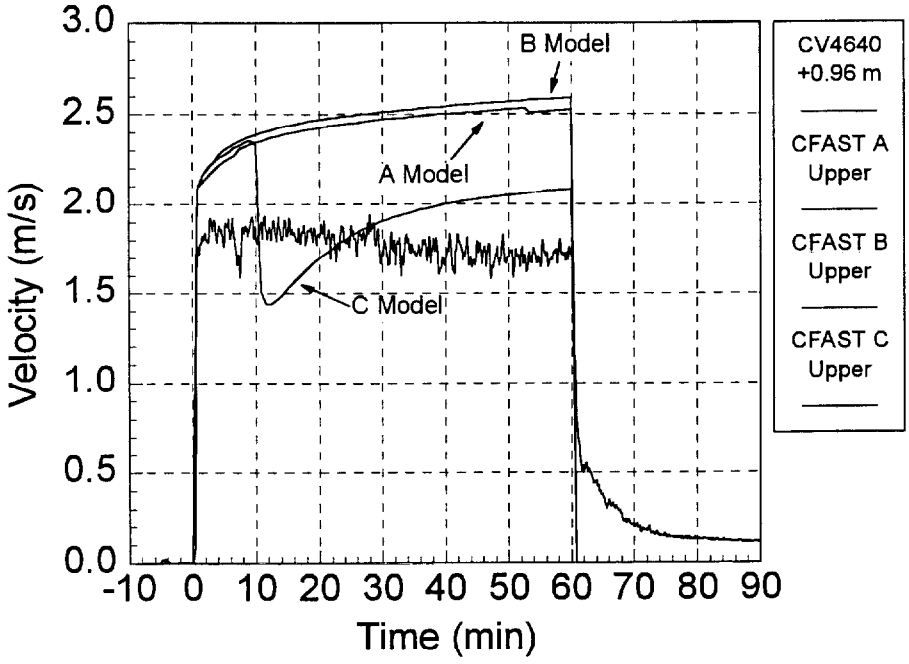


**Figure 3.4: T51.21 Fire Room Doorway Upper Layer Velocity**

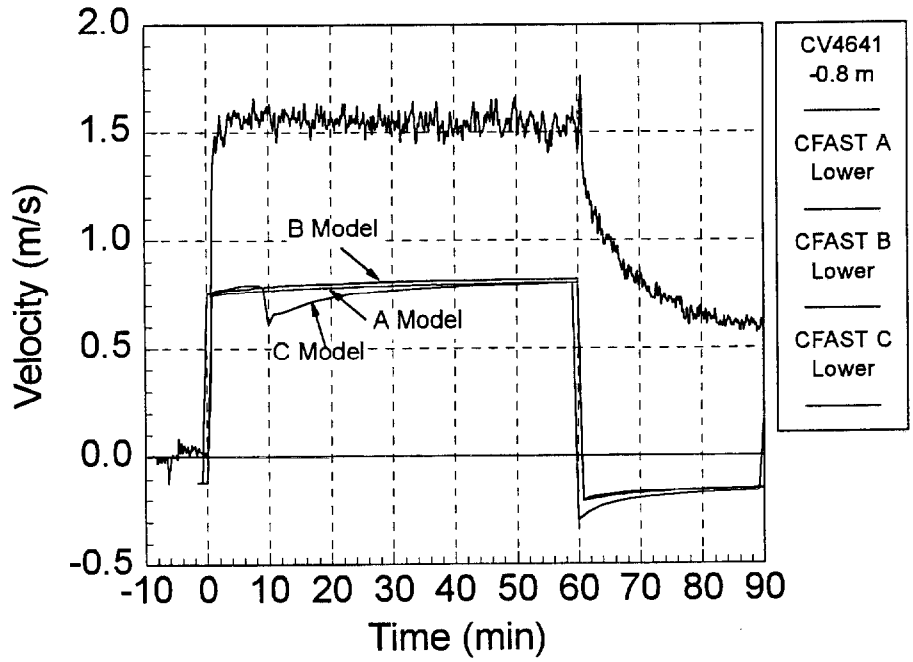


**Figure 3.5: T51.21 Fire Room Doorway Lower Layer Velocity**

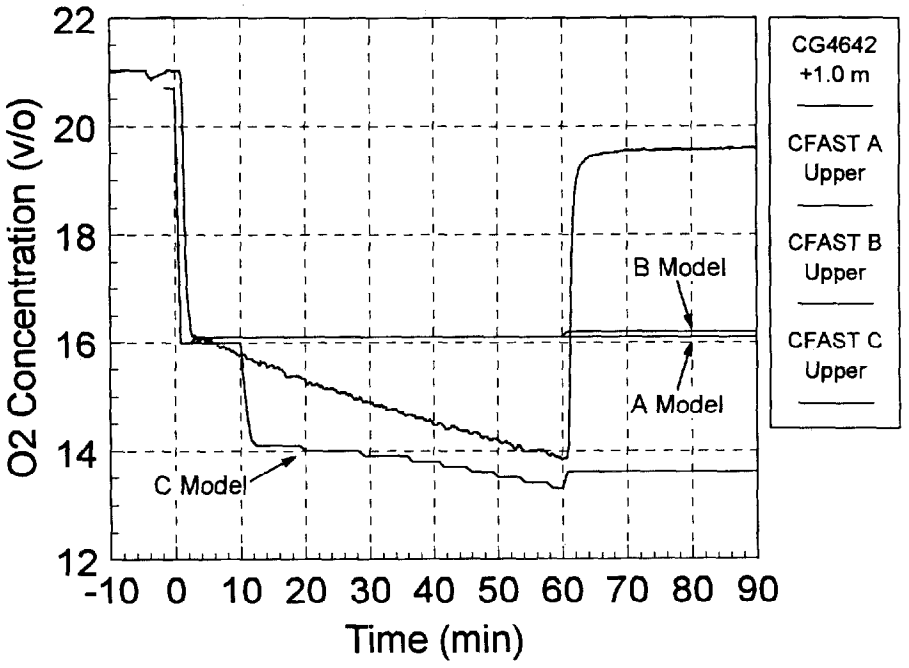


**Figure 3.6: T51.21 Fire Room Upper Layer $O_2$ Concentration**

Figure 3.6 shows that while the A and B models reasonably predict the magnitude of the oxygen concentration in the doorway, they do not do a reasonably follow the general trend of the data. The data show a continuous decrease in the oxygen concentration; whereas, the A and B models predict a constant value which does not increase after the end of the fire. The C model performs well for this parameter. It closely matches both the magnitude and trend shown in the data; however, as with the A and B models it does not predict the recovery of the oxygen concentration close to its pre-fire level. Furthermore, the C model displays a distinct stairstep behavior which may be a result of poorly defined branching conditions within the species tracking algorithms.

In Figure 3.7, similar behavior is observed for the $CO_2$ concentration as was seen for the oxygen concentration. This indicates that the difficulties that CFAST is having with species concentration is generic to the transport algorithm and not specific to a given species. As with the $O_2$ concentration, the A and B models predict a steady-state concentration that is not impacted by the cessation of the fire. The C model correlates well with the data for the duration of the fire, but does not calculate the reduction in the $CO_2$ concentration observed after the fire ends. The root cause of this latter difficulty, predicting the post fire species concentration, appears to be that CFAST predicts the upper layer velocity to be zero immediately after the fire ends rather than allowing it to decay to zero as shown in the data. The velocity is predicted to be zero because CFAST calculates that the upper layer collapses immediately after the end of the fire.

Figure 3.8 indicates large deficiencies are present in the species transport algorithms. The A and B models predict that no $CO_2$ is convected into the lower layer of the doorway; however, the C model correctly predicts the measured $CO_2$ concentration. While differences in layer heights and mass flow rates between the models exist, those differences are not large; hence, the poor

performance of the A and B models is puzzling and indicates that the transport model is seemingly not properly mixing gases at interfaces.

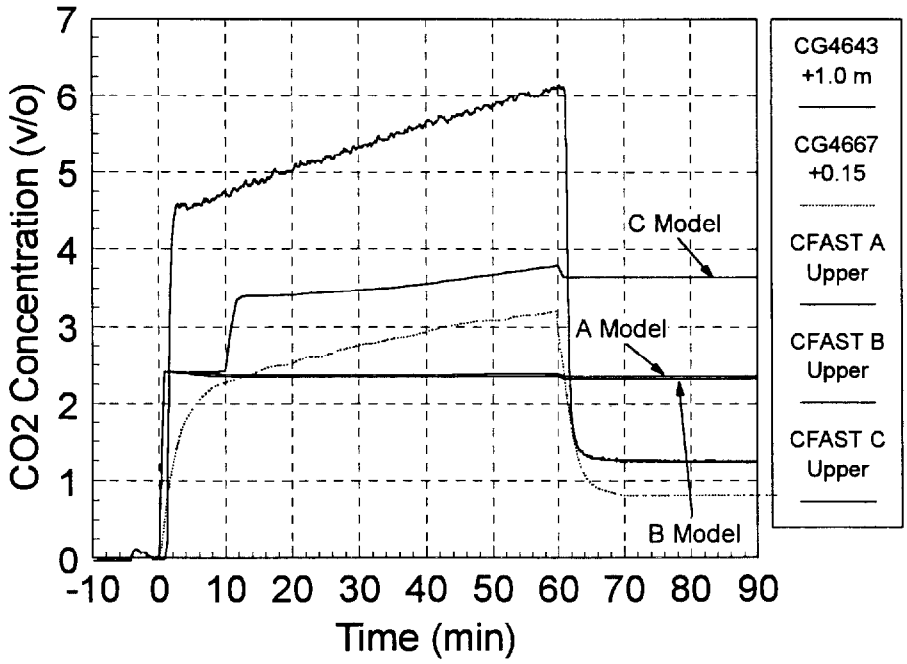


**Figure 3.7: T51.21 Fire Room Upper Layer $CO_2$ Concentration**

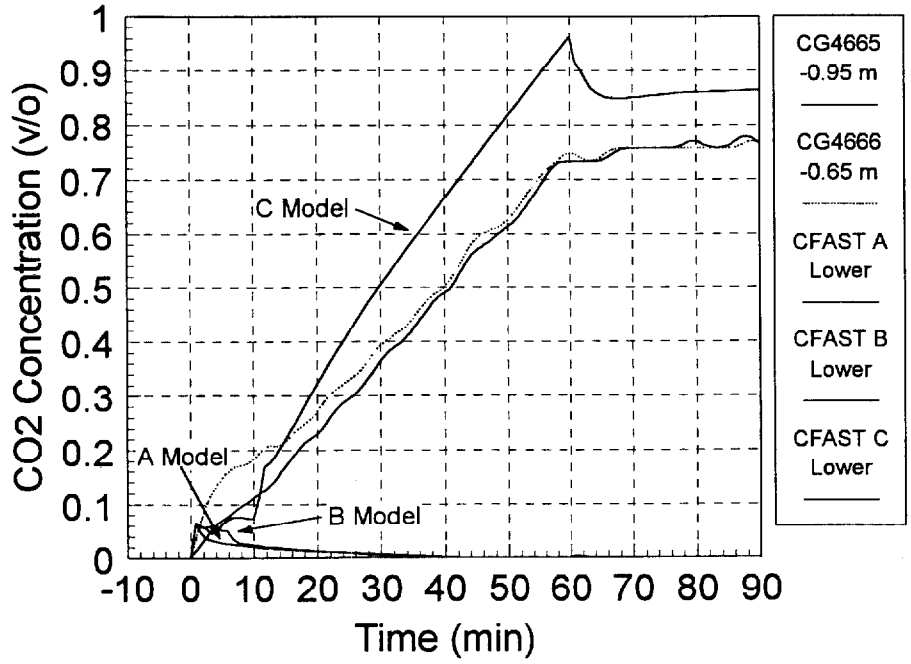


**Figure 3.8: T51.21 Fire Room Lower Layer $CO_2$ Concentration**

Figures 3.9 and 3.10 show the comparison of the CFAST predicted layer temperatures for the hallway and the measured data. The sensors for which the data are shown in the plots lie at different distances from the doorway of the fire room, and, thus, form a sort of average temperature for the hallway. For the A and B models, similar results can be seen as with the fire room temperatures. That is the hot layer is overpredicted and the cold layer is underpredicted. For the C model, the quality of prediction has been altered. In the fire room the C model greatly overpredicted the upper layer temperature but is in agreement with measured temperatures in the lower layer. For the hallway, the C model results in fair agreement with the temperatures of both layers once the shift in predicted values at ten minutes occursas the predicted temperatures lies within the range of measured tempertures. As discussed earlier in reference to the predicted layer heights, it is unclear as to why this shift in predicted values occurs at ten minutes.

Figures 3.11 and 3.12 show the CFAST predicted temperature and velocity compared with the data in the maintenance hatch leading from Level 1.600 to Level 1.700. Only the B and C models are shown on these plots as the A model did not include Level 1.600. In Figure 3.11 the measured data are for locations about 2 m above the floors of Level 1.600 and Level 1.700. The CFAST results represents the average temperature for Level 1.600. Thus, one would expect the CFAST prediction to lie close to the Level 1.600 thermocouple. The figure shows that the B model prediction lies slightly above the measured data for Level 1.600, and the C model lies significantly above this temperature. The B model appears to be correctly predicting the temperature and hence the vertical entrainment. The C model results indicate that the predicted entrainment rate is too low. Figure 3.12 confirms these observations. The B model velocity is close to that measured in the hatch which indicates that the correct entrainment is being predicted. The C model velocity is significantly lower than the measured velocity which indicates that the entrainment is being underpredicted. However, a closer look at the results indicates there is more to these results. At negative times, before the fire starts, the B model is already predicting a large velocity without any driving force present. Since there is no temperature difference with the ambient conditions, nor any wind there is no physical reason why such a flow should exist. A further examination of this is made in the appendix.

Comparing the code predictions to the data for each of the three models leads to the conclusion that the C model overall provides the best predictions of the HDR's response to the gas fires under consideration. The C model reasonably predicts the major phenomena observed in the fire tests including layer temperatures, gas concentrations, and vertical flows. This is likely due to the attempt to include additional regions of the facility to capture the predominate flow pattern observed in the building, specifically the large global circulation up the main staircase and down the spiral staircase. However, the intermediate model, the B model, which included more of the building's complexity than the A model, did not perform better than the A model. Both models had difficulties predicting lower layer gas concentrations and the B model predicted a large, unphysical flow prior to the start of the fire.

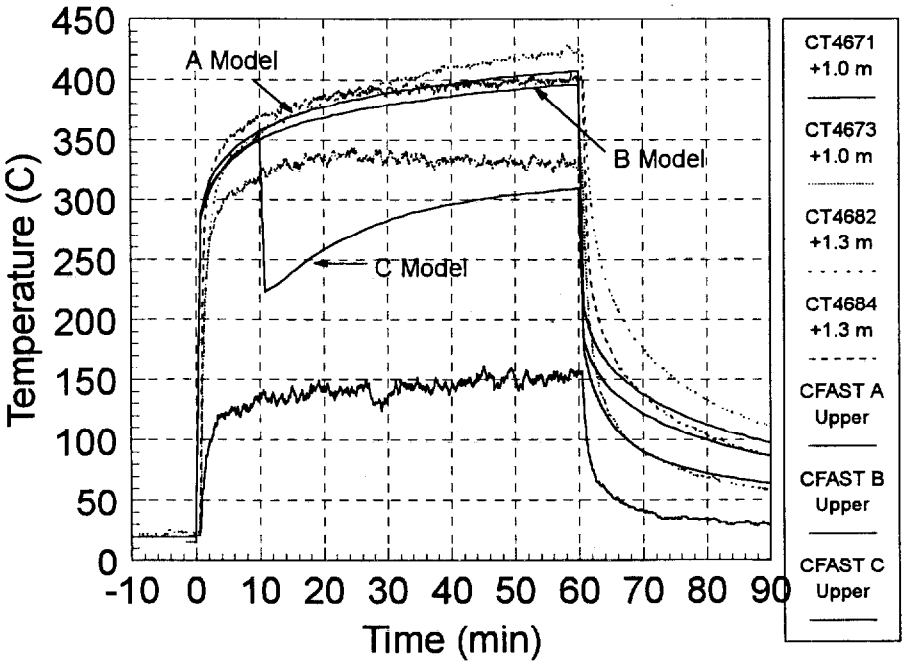


**Figure 3.9: T51.21 Hallway Upper Layer Temperature**

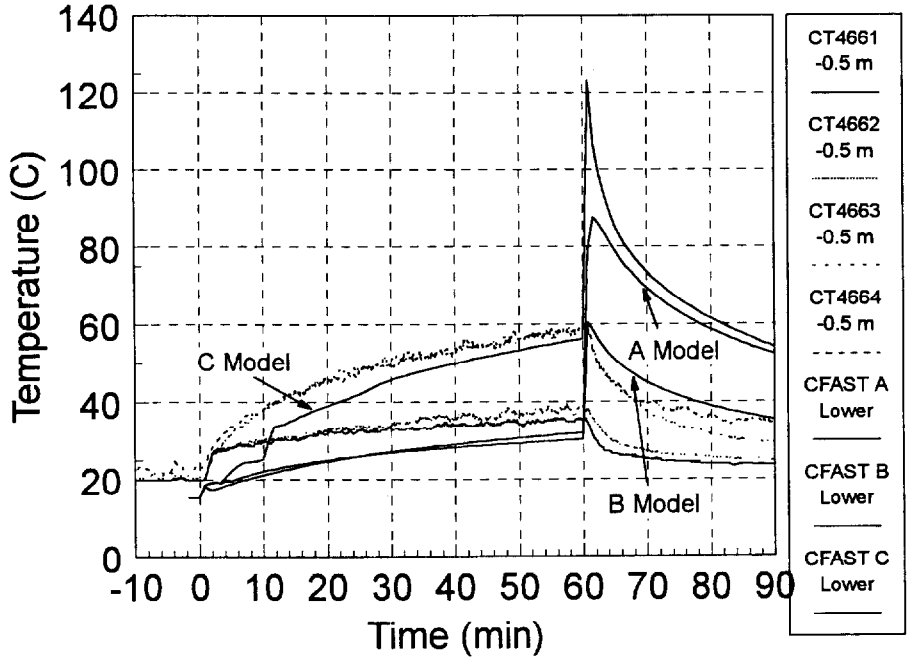


**Figure 3.10: T51.21 Hallway Lower Layer Temperature**

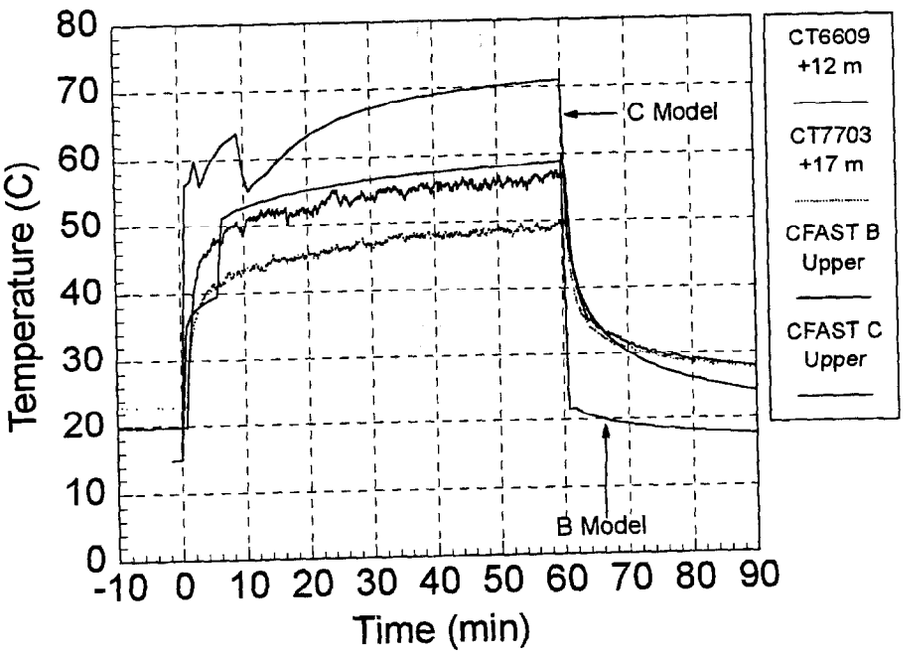


**Figure 3.11: T51.21 Main Staircase Hatch Temperature at Level 1.600**

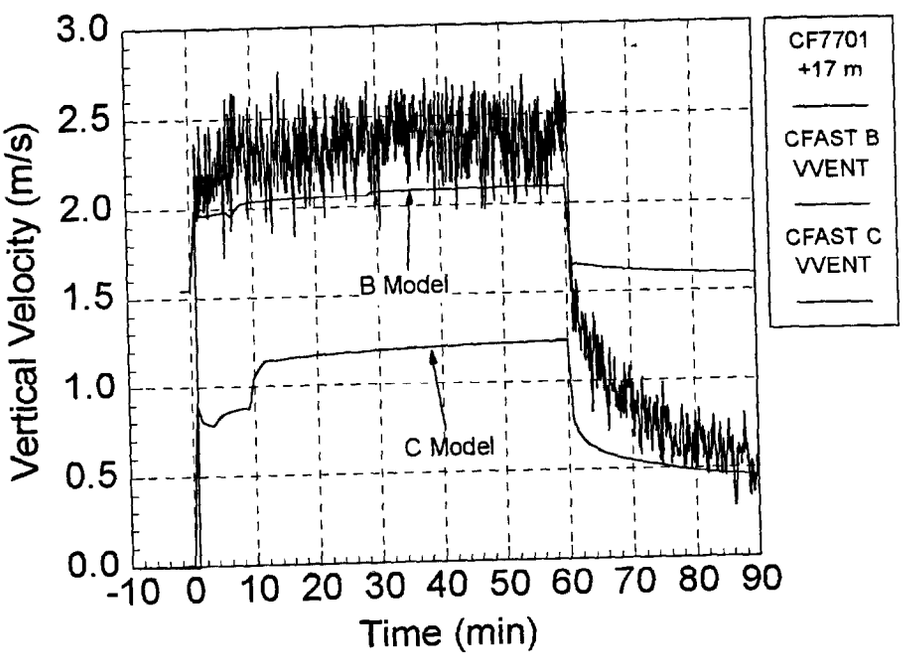


**Figure 3.12: T51.21 Main Staircase Hatch Velocity at Level 1.600**

## 3.2 Constant Ventilation (T51.11,T51.21, and T51.23)

This subsection will compare the CFAST predictions to measured data for tests T51.11, T51.21, and T51.23 for the C models described in Section 2.4.3. These three tests span the range of fire powers used in the T51 test series, and thus, constitute a comprehensive challenge for CFAST.

Figures 3.13 and 3.14 on the next page along with Figure 3.2 on page 3-2 plot the CFAST predicted upper layer temperatures in the fire room. For test T51.11, CFAST overpredicts the layer temperature by 50 °C. For test T51.21, CFAST overpredicts the temperature by 180 °C. However, for test T51.23, the CFAST predicted temperature matches the measured temperatures in the fire room. The CFAST hot layer predictions do not appear to be consistent as the deviation appears to have little correlation to the fire power. It is also interesting to note that the CFAST predicted fire room temperatures for T51.11 has a spike near +15 minutes. Considering that the remainder of the temperature prediction and the data both show a smooth variation in temperature, this spike must be considered a numerical artifact. Lastly, it is worth noting that the data for test T51.11 shows that the upper layer temperatures in the fire room reached a steady-state value approximately 35 minutes into the fire. CFAST does not reach a steady-state value at any point in its predictions, and thus, misses completely this new equilibrium state.

The predicted vs. measured lower layer, fire room temperatures are shown Figures 3.15, 3.16 and 3.3 on page 3-3. For the lower layer temperatures, CFAST overpredicts slightly for T51.11, predicts the temperature well for T51.21, and underpredicts for T51.23. For the lower fire powers, CFAST calculates well the fire room lower layer temperature indicating that heat transfer to the lower layer is being modeled reasonably well. Though the lower layer temperature for T51.23 is being underpredicted, this does not indicate a failing on the part of CFAST. During T51.23 the fire room reached flashover conditions indicated by the high temperatures measured in the lower layer. This means that there was no distinct lower layer in the room, and zone model codes which are based on the assumption of the existence of two layers should not be expected to handle flashover conditions well.

Upper layer velocities in the doorway are shown in Figures 3.17, 3.18, and 3.4 on page 3-4. Both the T51.11 and the T51.23 predictions are a factor of two less than the measured velocities in the doorway. Even though the measured velocities represents a point velocity and the CFAST velocities represent averaged quantities, a factor of two difference indicates that the velocities are being underpredicted. The T51.21 velocities, however, are very well predicted. Again, as with the upper layer temperatures, the deviations from the measured data do not correlate with the fire power. All the models show a discontinuity in the predicted velocity at +10 minutes which echoes the change in layer height shown in Figure 3-1. However, as was previously mentioned it is unclear as to why this jump occurs.

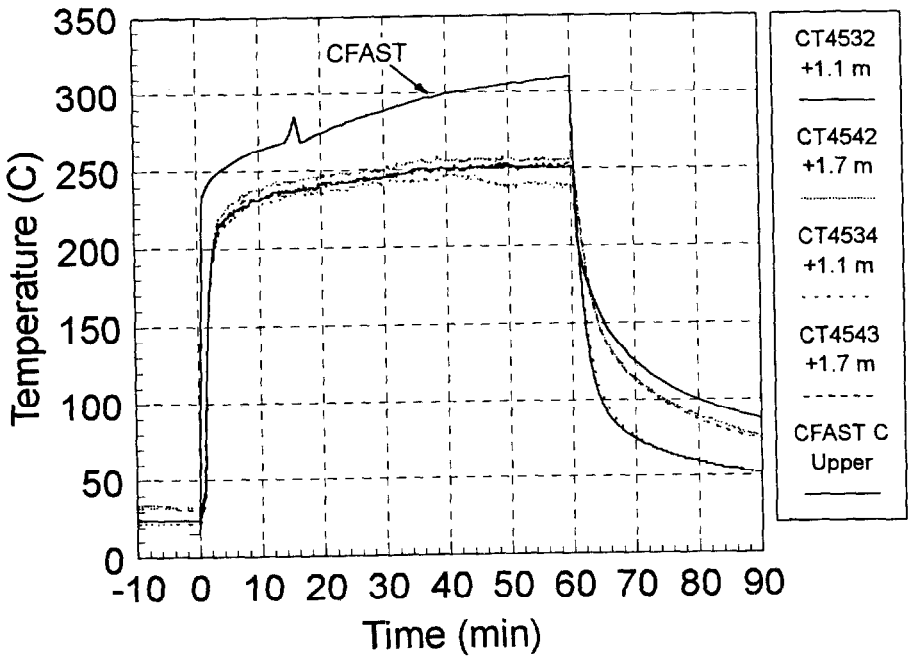


**Figure 3.13: T51.11 Fire Room Upper Layer Temperature**

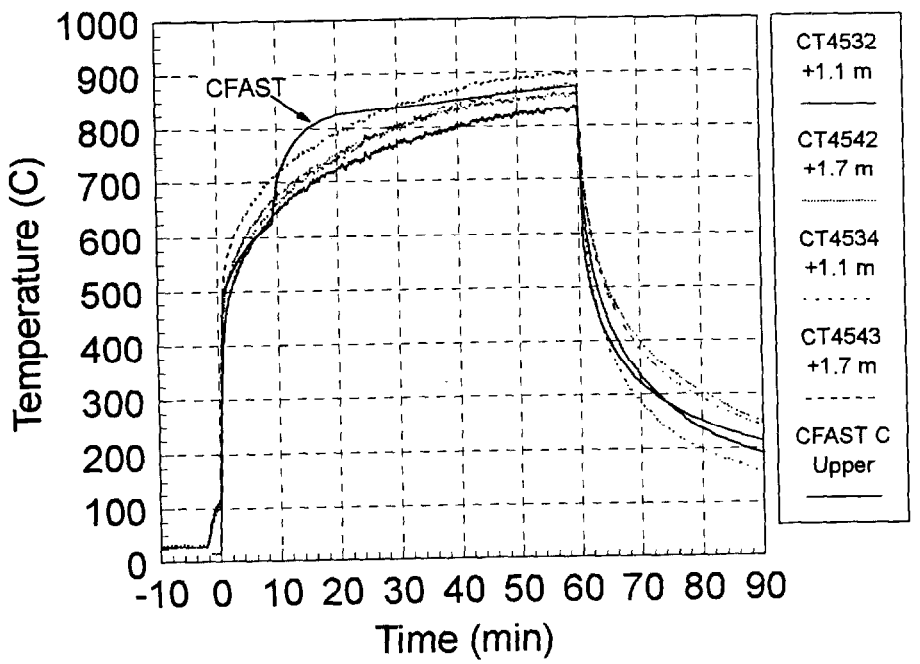


**Figure 3.14: T51.23 Fire Room Upper Layer Temperature**

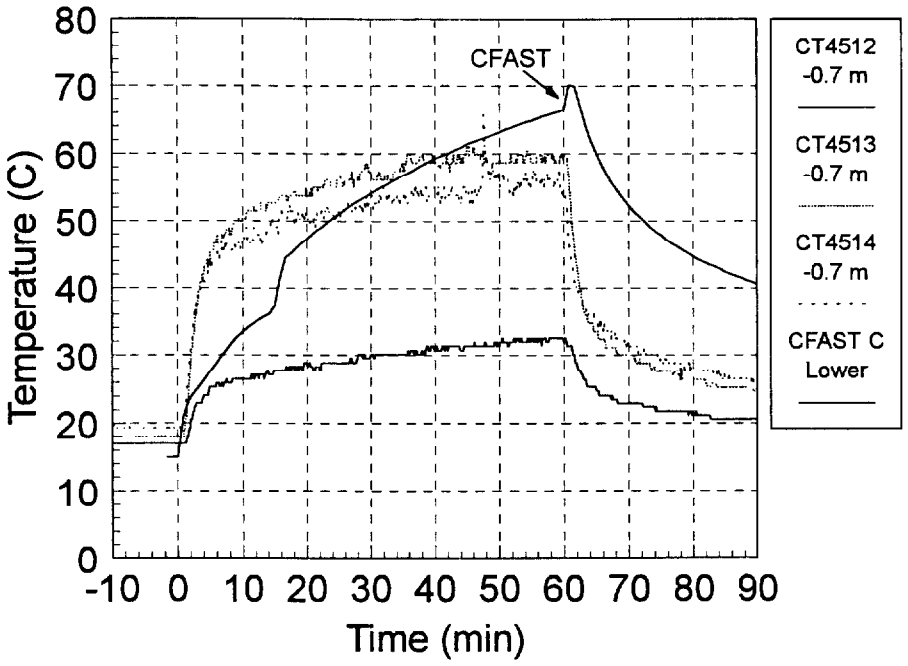


**Figure 3.15: T51.11 Fire Room Lower Layer Temperature**

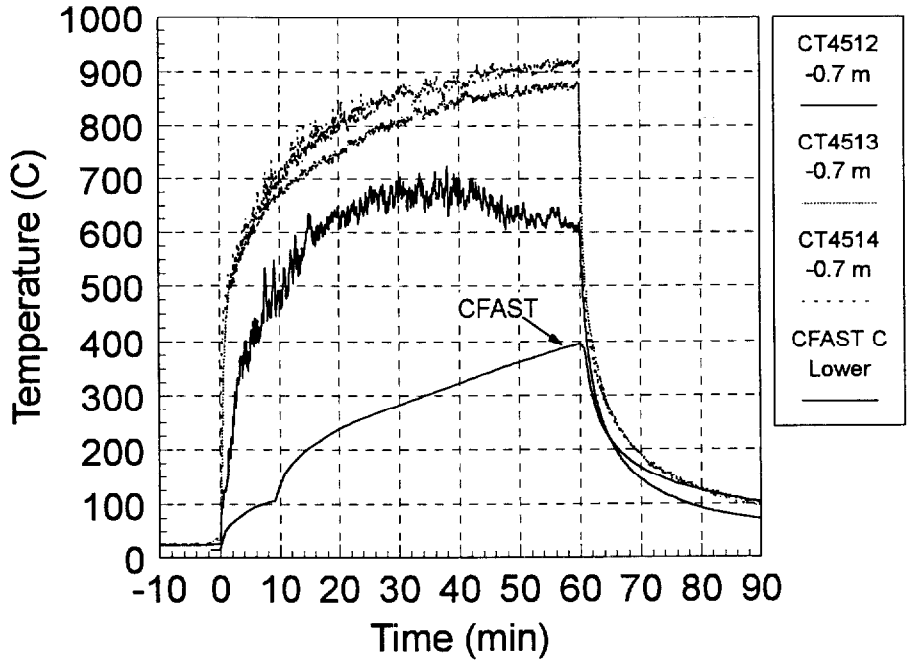


**Figure 3.16: T51.23 Fire Room Lower Layer Temperature**

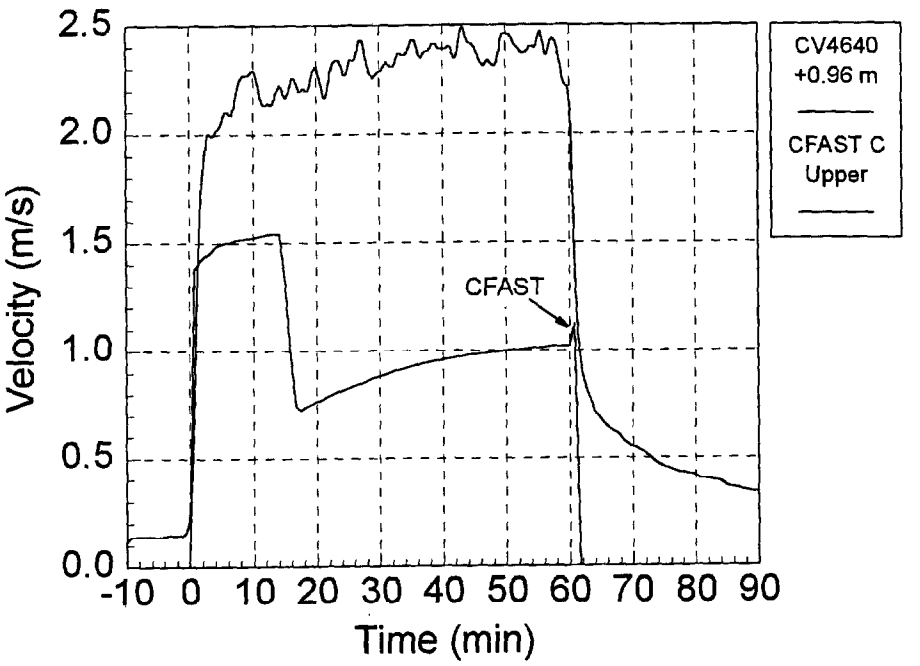


**Figure 3.17: T51.11 Fire Room Doorway Upper Layer Velocity**

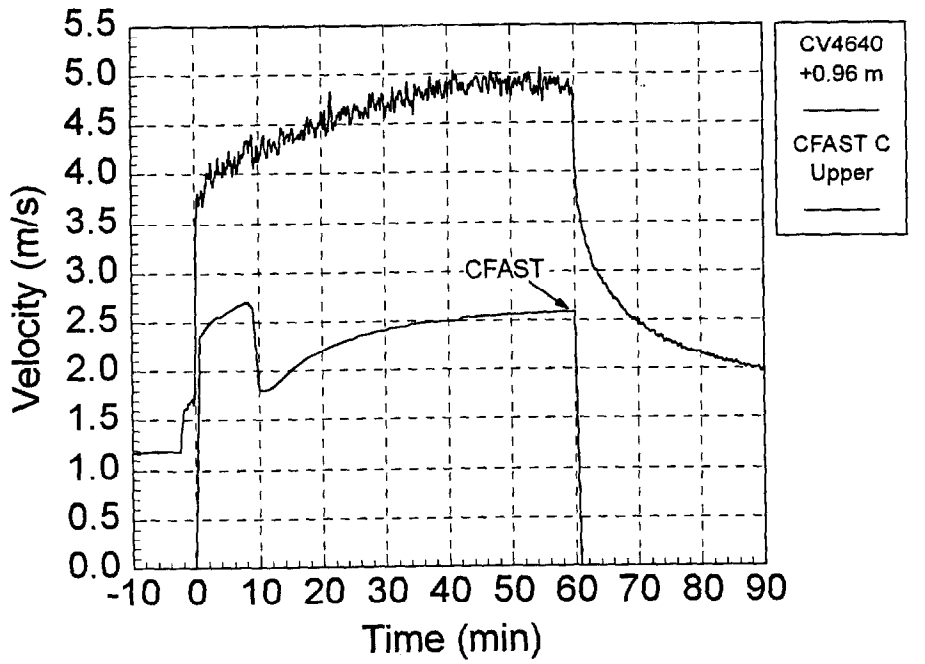


**Figure 3.18: T51.23 Fire Room Doorway Upper Layer Velocity**

Figure 3.19 shows the lower layer velocity for T51.23 and Figure 3.5 shows the lower layer velocity for T51.21. No velocity probe existed in the lower layer for T51.11, so no comparison can be made for that test. For both tests CFAST is predict velocities significantly lower than the measured velocities, again indicating that even accounting for point vs. average measurements that the velocities are being underpredicted. Lower overall velocities in and out of the fire room would cause higher fire temperatures which could account for the discrepancies seen in the upper layer temperatures for tests T51.11 and T51.23, but since T51.21's upper layer temperature was well predicted, there are other errors present in the CFAST solution that wind up compensating the flow error for T51.21.

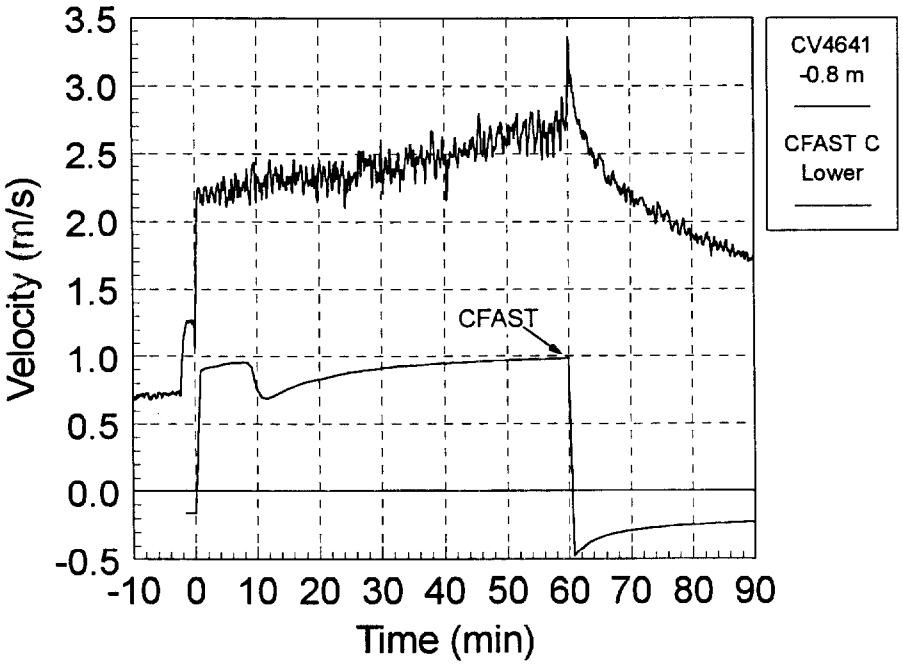


**Figure 3.19: T51.23 Fire Room Lower Layer Velocity**

Figures 3.20 and 3.21 on the following page show the upper and lower $CO_2$ concentrations for test T51.23. Figures 3.7 and 3.8 show this for test T51.21. Test T51.11 had no sensors for $CO_2$ concentration in the lower layer, and the upper layer sensor was nonfunctional for test T51.11. For both the upper and the lower layer, CFAST performs well in predicting the $CO_2$ concentration. In the lower layer the $CO_2$ concentration is overpredicted slightly by CFAST, but not by a significant amount. CFAST performs well for this parameter.

Figures 3.22 through 3.25 along show the upper and lower layer temperatures in the hallway for tests T51.11 and T51.23. Figures 3.9 and 3.10 show these temperatures for test T51.21. In all cases the CFAST code correctly predicts the temperatures measured in the hallway. Since CFAST did not correctly predict the fire room temperatures, there exists some compensating error or errors in the code that allows CFAST to correctly predict the hallway temperatures.

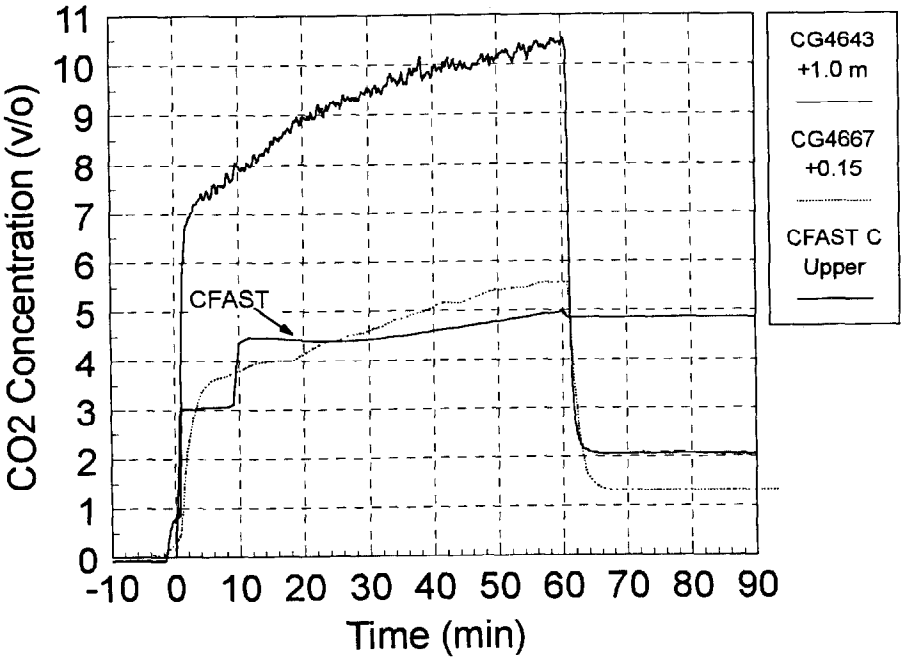


**Figure 3.20: T51.23 Fire Room Upper Layer $CO_2$ Concentration**

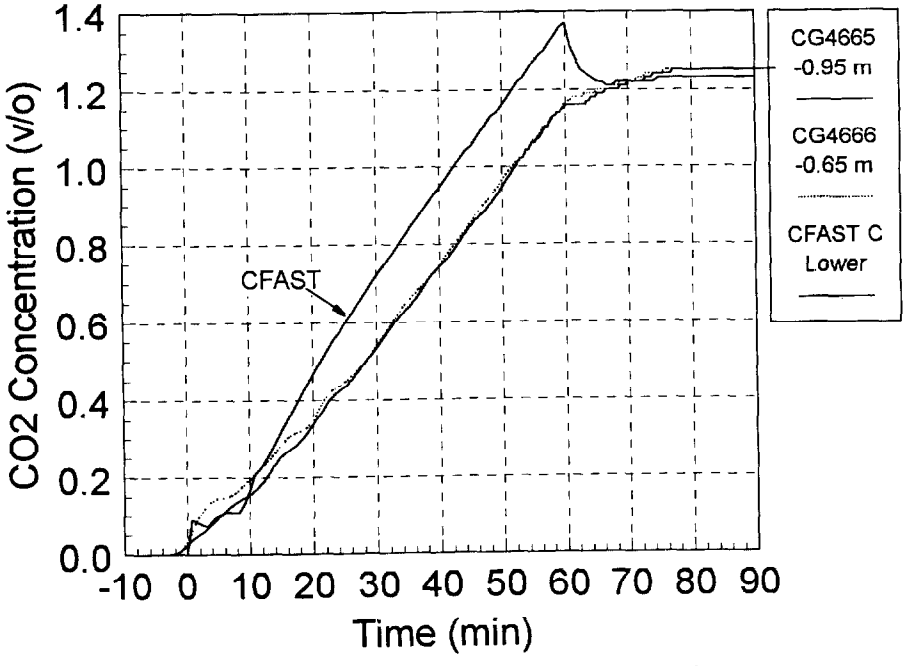


**Figure 3.21: T51.23 Fire Room Lower $CO_2$ Concentration**

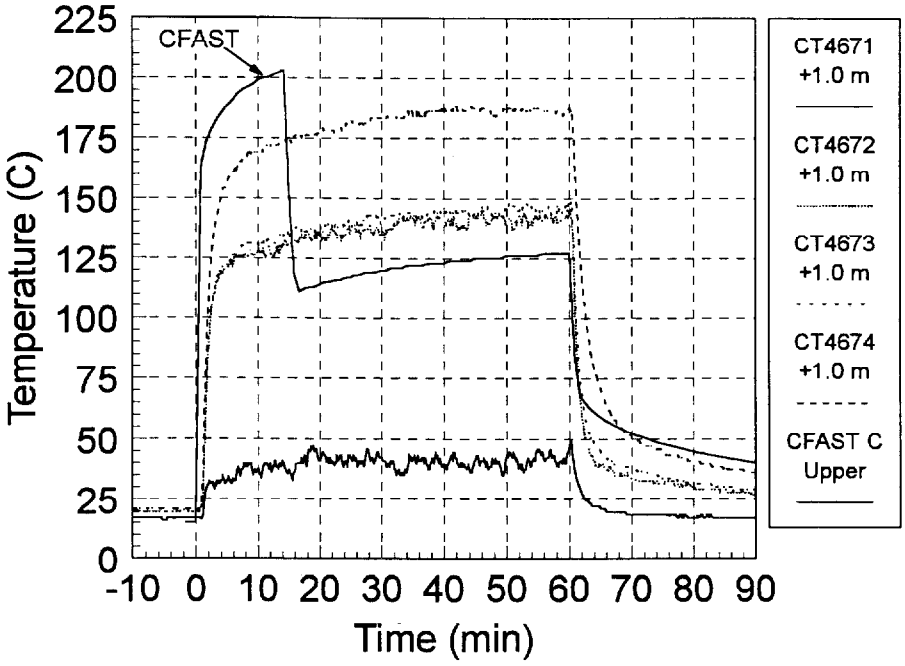


**Figure 3.22: T51.11 Hallway Upper Layer Temperature**

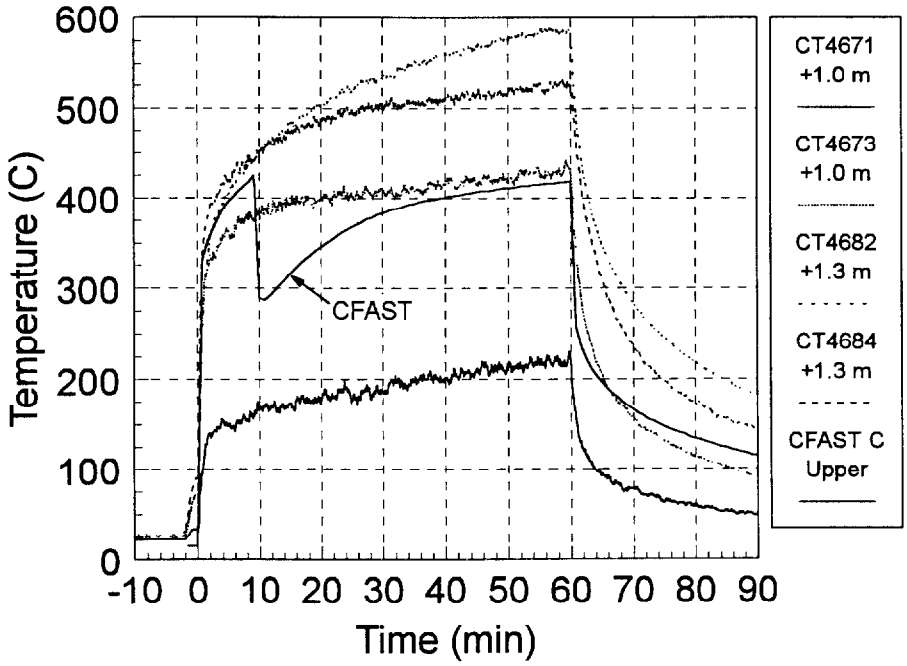


**Figure 3.23: T51.23 Hallway Upper Layer Temperature**

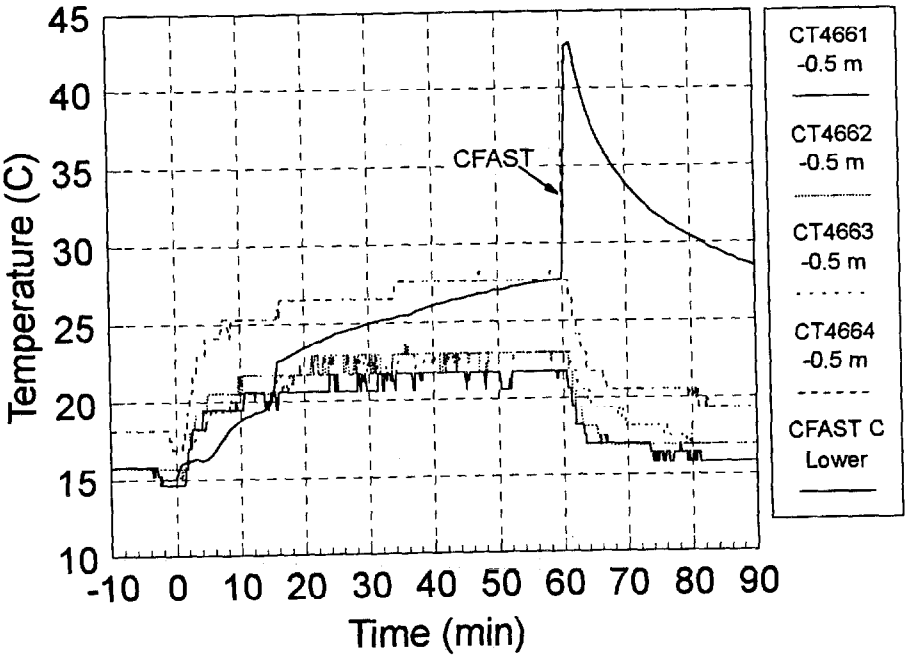


**Figure 3.24: T51.11 Hallway Lower Layer Temperature**

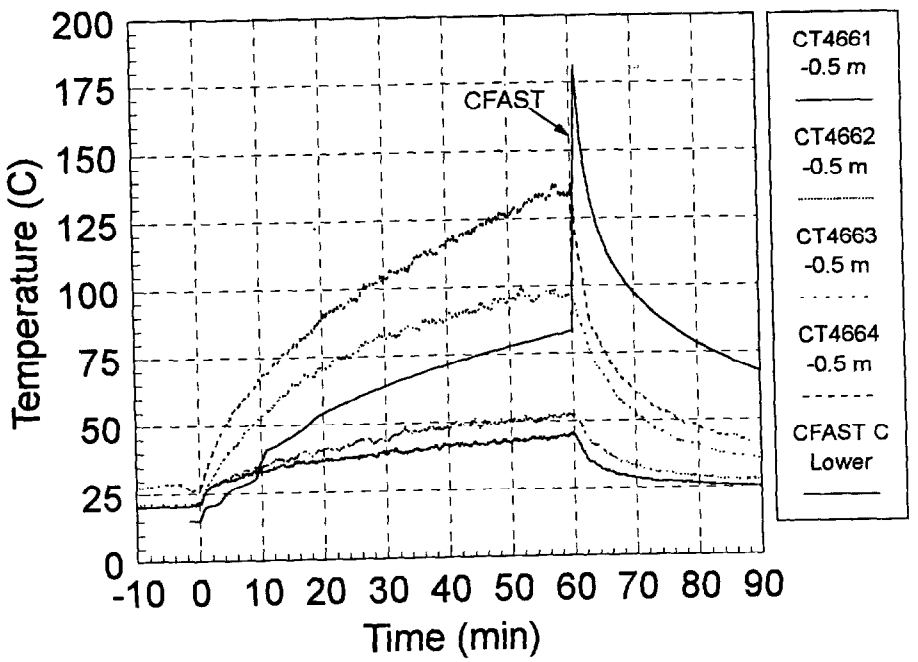


**Figure 3.25: T51.11 Hallway Lower Layer Temperature**

The next few sets of figures cover phenomena occurring on levels above Level 1.400. Thus, they represent the real test of CFAST's capabilities. The first set consisting of Figures 3.26, 3.27, and 3.11, page 3-9, show the measured vs. predicted temperatures in the main staircase hatch between Level 1.600 and Level 1.700. The measured temperatures that are depicted are from thermocouple locations located at the midpoint of the levels above and below the hatch between Level 1.600 and Level 1.700. Since the CFAST temperature represents the average temperature seen in the compartment at Level 1.600, the prediction should lie near the Level 1.600 thermocouple's measurement. In all cases the CFAST prediction is significantly higher. This indicates that CFAST is not entraining enough air into the rising plume. However, in Figures 3.28, 3.29 and 3.12 which show the measured vs. predicted velocities at the hatch, CFAST underpredicts the velocities by a factor of two for all the tests. This indicates that CFAST is overpredicting the energy removal from the plume and thus calculating the velocity too low. This conflicts with the overpredicted temperatures, however.

The final three figures, Figures 3.30, 3.31, and 3.32, show the predicted vs. measured temperatures for the remainder of the HDR facility above Level 1.600. For each of the experiments modeled, CFAST predicts reasonable temperatures for this portion of the HDR facility. However. since this region of the HDR experienced much smaller temperature increases than the remainder of the facility, it's impact on heat removal for these tests was small and as such it should be expected that the code should also consider this impact as small.

Overall, the CFAST comparisons have shown mixed results. Gas concentrations are well predicted by CFAST. Velocities are in general not well predicted by CFAST. Layer temperatures are predicted with some success, but the types of errors seen are not consistent between different experiments.

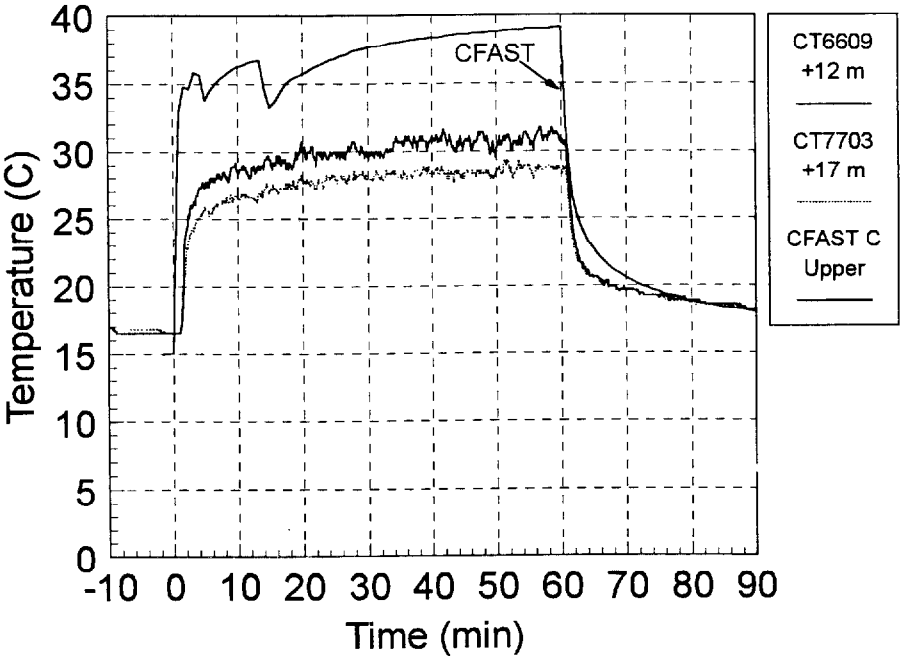


**Figure 3.26: T51.11 Main Staircase Hatch Temperature at Level 1.600**

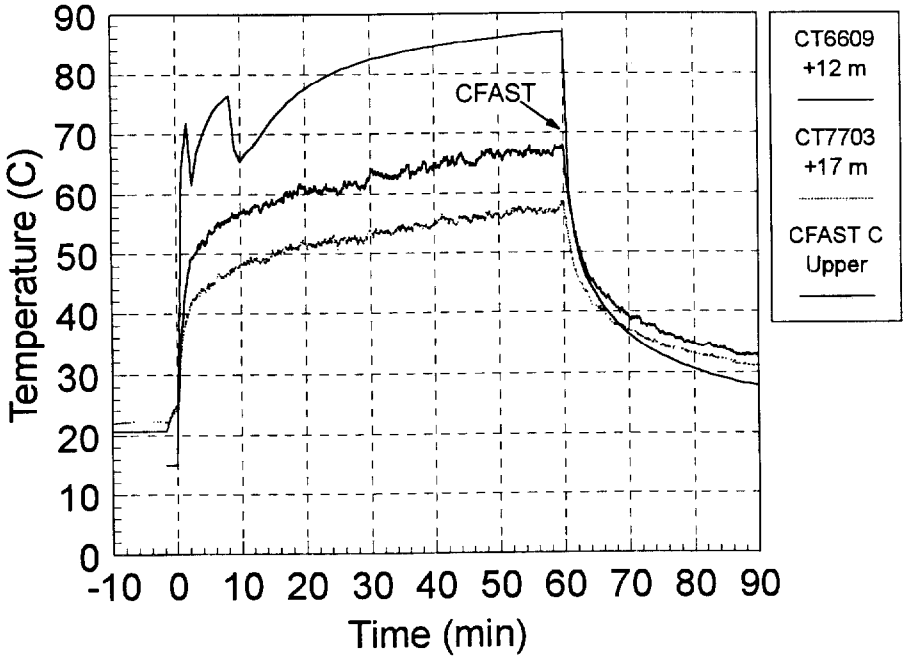


**Figure 3.27: T51.23 Main Staircase Hatch Temperature at Level 1.600**

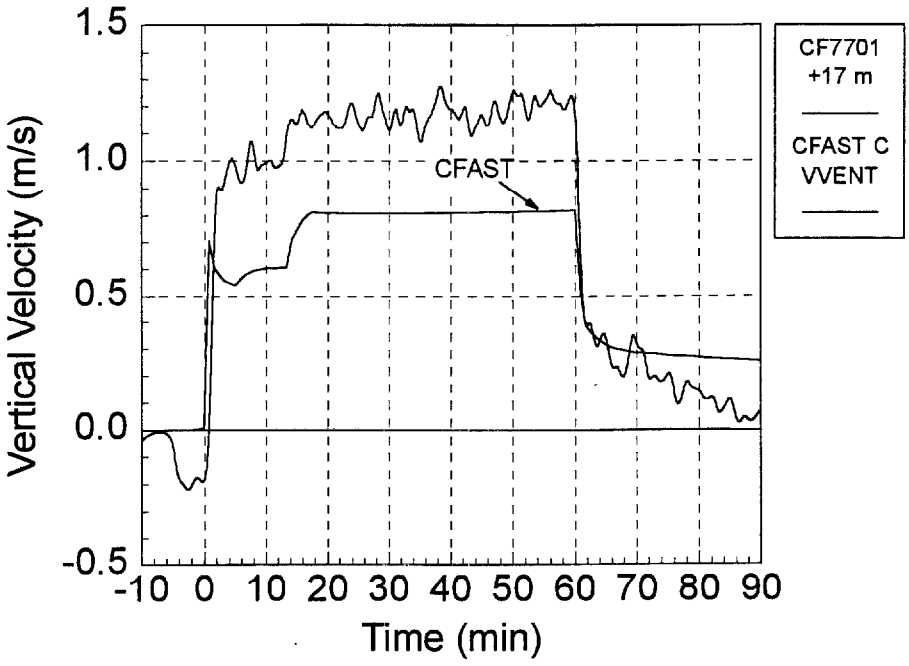


**Figure 3.28: T51.11 Main Staircase Hatch Velocity at Level 1.600**

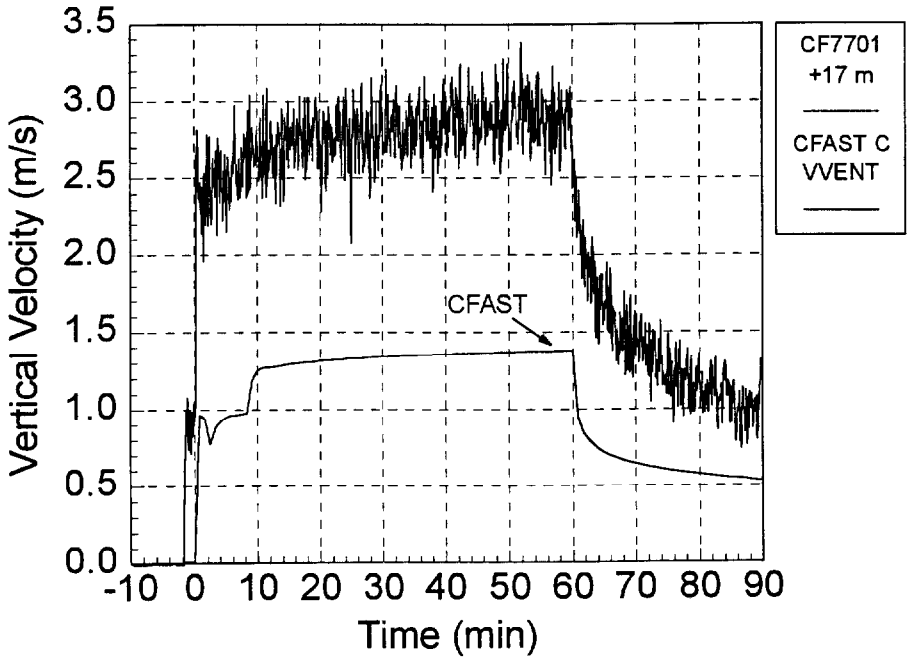


**Figure 3.29: T51.23 Main Staircase Hatch Velocity at Level 1.600**

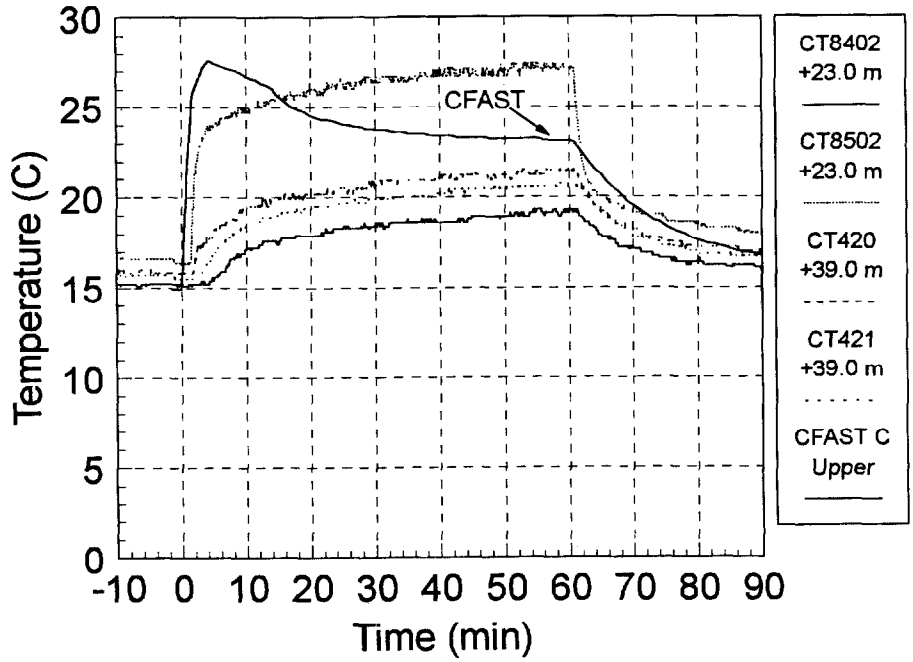


**Figure 3.30: T51.11 Level 1.700 - Dome Temperatures**

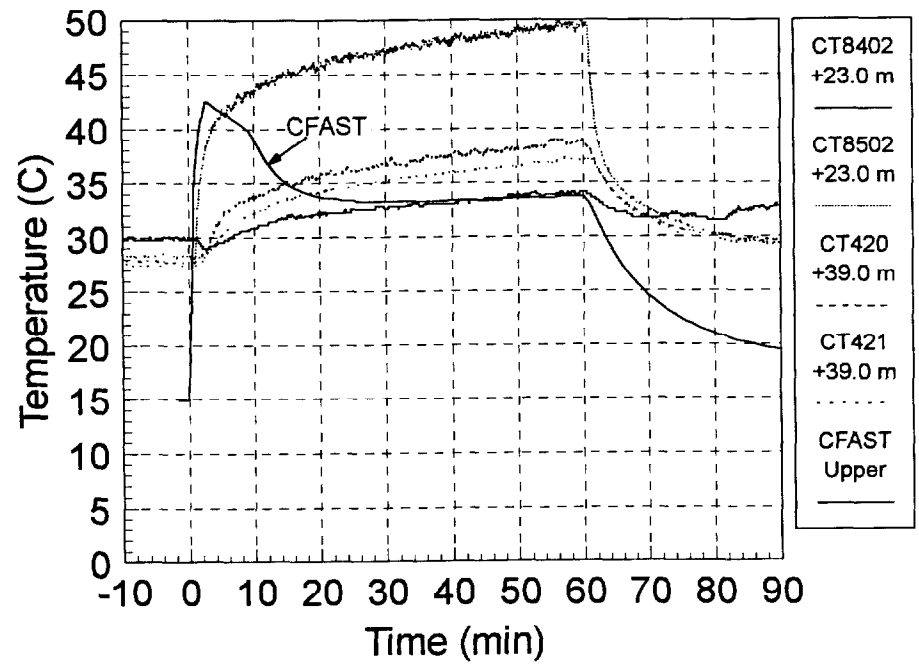


**Figure 3.31: T51.21 Level 1.700 - Dome Temperatures**

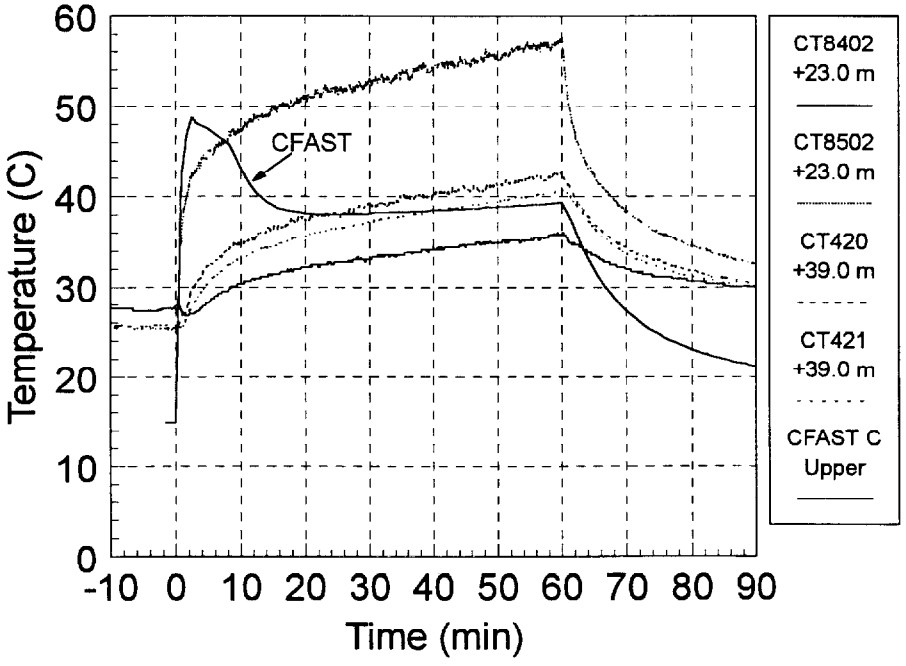


**Figure 3.32: T51.23 Level 1.700 - Dome Temperatures**

## 3.3 Time Dependent Ventilation (T51.25)

Test T51.25 was a repeat of test T51.23 with modified room ventilation using the additional ventilation duct connecting the fire room to Level 1.600. For the first 30 minutes of the fire the additional vent was 100% open. For the second 30 minutes of the fire the vent was fully closed; therefore, for the second half of the fire the ventilation parameters were the same as for test T51.23.

The figures on the next page, Figures 3.34 and 3.35, show the measured and predicted hot and cold layer temperatures in the fire room. With the addition of the extra fire room ventilation CFAST predicts very well the hot layer temperature throughout the fire test as opposed to the T51.23 model which overpredicted early fire room temperatures. However, as with T51.23, CFAST did a substantially underpredicts the lower layer temperatures. In addition to the greatly underpredicted temperatures, CFAST still predicts a jump at +10 minutes.

The CFAST predicted fire room layer height for is displayed for test T51.25 in Figure 3.33 along with the predicted layer height for T51.23. The additional vent results in oscillatory behavior early in the fire test with a more severe jump at +10 minutes. Furthermore, up until the +10 minute discontinuity, the layer height for T51.25 is on average predicted to be below that for T51.23. Since the additional vent acts to remove heat from the top of the fire room in addition to the doorway, it seems likely that the cold layer for T51.25 should be larger than for T51.23. This is shown in the temperature data for the fire room, Figure 3.35, which shows cooler temperatures in the lower layer of the fire room with the additional ventilation duct. It would appear that multiple fire room vents may create difficulties for CFAST.

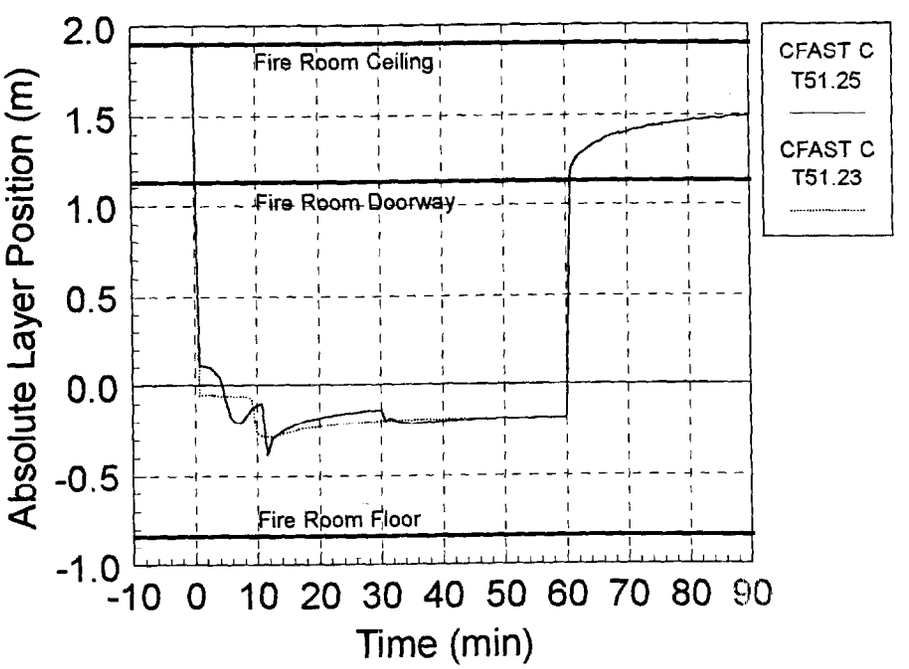


**Figure 3.33: T51.25 Fire Room Layer Height**

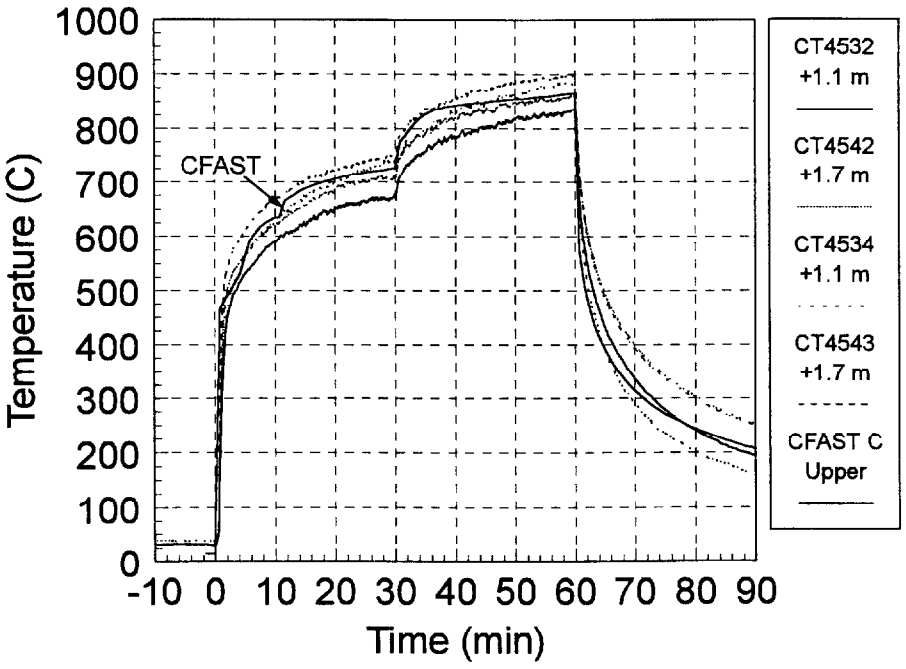


**Figure 3.34: T51.25 Fire Room Upper Layer Temperature**

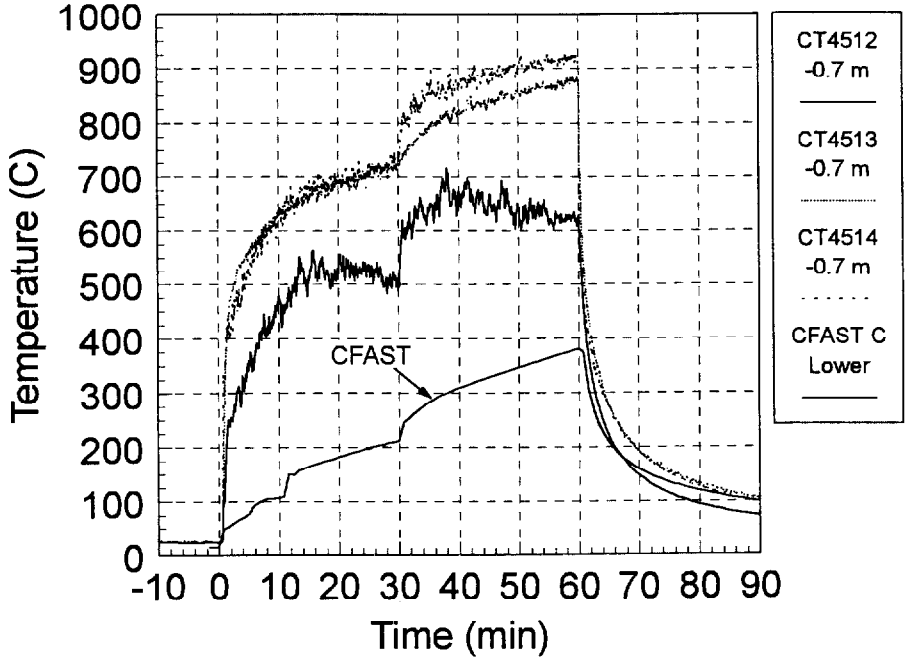


**Figure 3.35: T51.25 Fire Room Lower Layer Temperature**

Figures 3.36 and 3.37 on the next page show the upper layer concentrations of oxygen and carbon dioxide. During the first half of the fire test, the open ventilation duct results in higher $O_2$ and lower $CO_2$ concentrations than for test T51.23. The levels quickly shift towards the T51.23 values once the duct is closed. During the vent open phase of the test, CFAST performs very well in predicting both the $CO_2$ and the $O_2$ concentrations. However, once the vent closes, CFAST does not predict the correct magnitude of change in the gas concentrations.

The next two figures, Figures 3.38 and 3.39 on page 3-27, show the measured vs. predicted velocities in the fire room doorway. The overall effect of the vent is to reduce the flow velocity through the fire room doorway. In the upper layer, Figure 3.38, this results from gasses venting through the duct rather than the doorway, and in the lower layer, Figure 3.39, this results from a larger cold flow area which acts to reduce the velocity field. CFAST performs well in calculating the lower layer flow which experiences little impact from the vent changes. In the upper layer, CFAST does not perform as well. The doorway flow calculated in the early portion of the test is very unstable, whereas the data shows a stable flow developing almost immediately. There is also some instability in the predicted results when the vent changes position which is not reflected in the data. CFAST does not succeed in predicting flows which are dependent upon multiple ventilation parameters.

Figures 3.40 and 3.41 on page 3-28 show the measured vs. predicted temperatures in the hatch between Level 1.400 and Level 1.500 and for the levels above Level 1.600. CFAST accurately predicts both the trend and the magnitude for the temperatures in the hatch at the entrance to Level 1.500. The prediction lies between the measured data taken above and below the hatch, and the magnitude of the temperature shift resulting from the vent closing is reproduced well be CFAST. In the dome, CFAST does not perform as well. The data indicates that early in the test, regions of the upper level see temperature changes of over 20° C due to the plume rising from the ventilation duct up the spiral staircase hatches. CFAST calculates a temperature increase in the first ten minutes of the fire test which is not seen on the data, and that temperature increase is not sustained. The early temperature increase decays to a temperature lower than the temperature predicted for test T51.23, even though there is more energy transfer from the fire room to the upper levels at this stage in the test. After the vent closes, CFAST predictions begin to match the measured data.

The final two figures in this section on page 3-29 show the measured temperature and velocity inside the ventilation duct. CFAST performs well in predicting the velocity inside the duct, Figure 3.42, though it does overshoot the measured velocity and calculates a near instantaneous stable flow whereas the data never reaches stable flow before the vent closes. CFAST does not perform as well in predicting the temperature inside the duct, Figure 3.43. However, since the duct was insulated for the experiment and CFAST would only run when modelling the pipe with concrete walls, this is most likely due to the heat transfer of the duct as modeled in CFAST versus the actual duct. Most likely, heat losses to the duct is a major factor in CFAST's failure to capture the increased upper level temperatures. Improvements in the code's stability in this case would improve its predictive capabilities by eliminating the need to have these unneeded heat transfer surfaces.

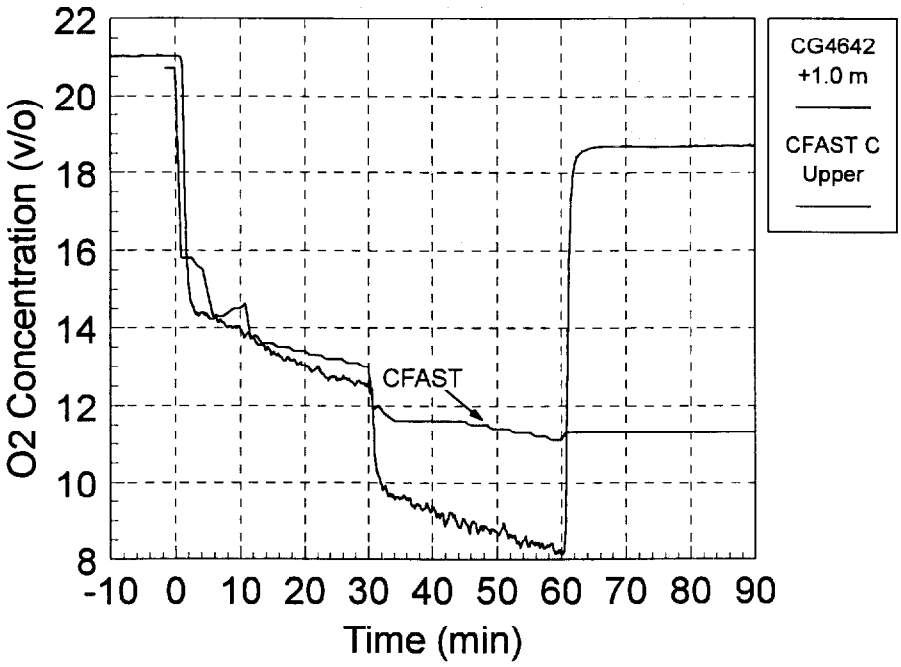


**Figure 3.36: T51.25 Fire Room Upper Layer $O_2$ Concentration**

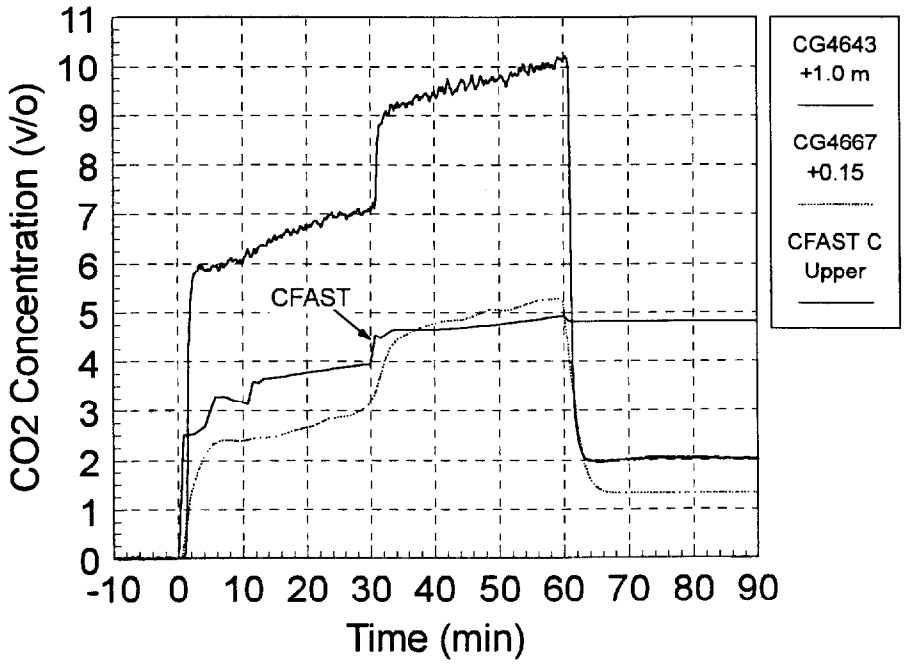


**Figure 3.37: T51.25 Fire Room Upper Layer $CO_2$ Concentration**

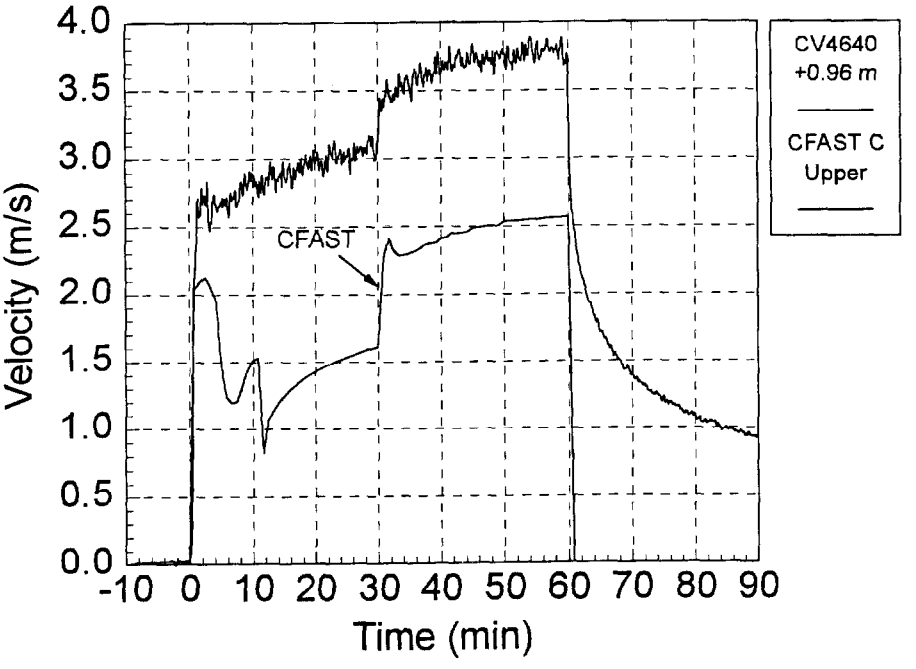


**Figure 3.38: T51.25 Fire Room Upper Layer Velocity**

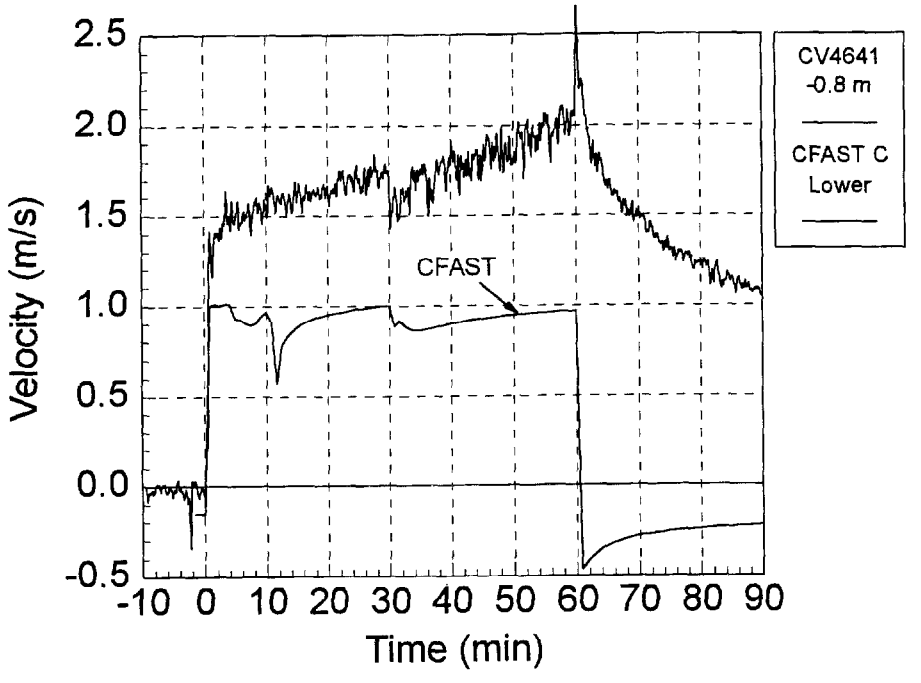


**Figure 3.39: T51.25 Fire Room Lower Layer Velocity**

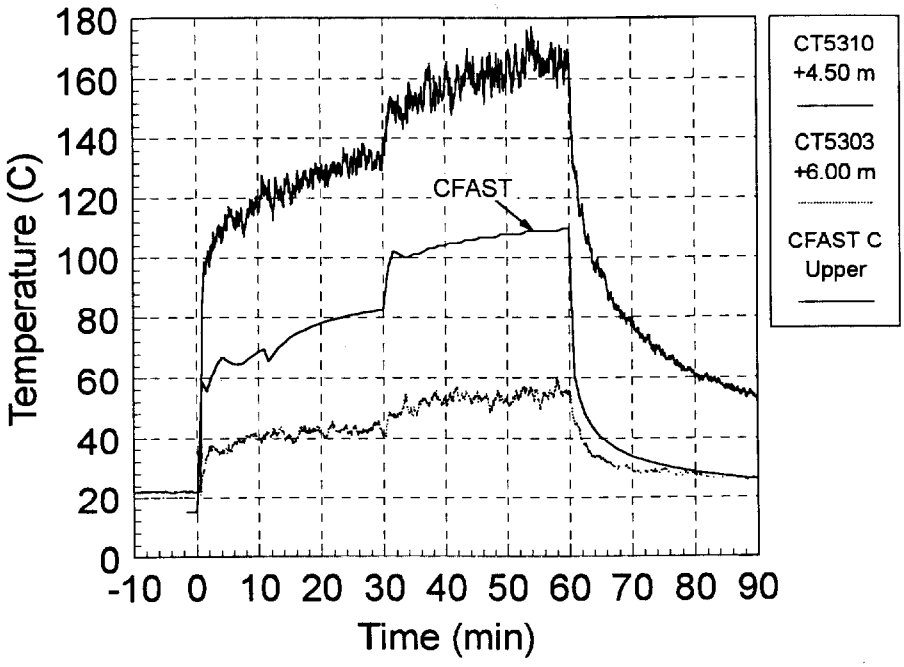


**Figure 3.40: T51.25 Main Staircase Hatch Temp. at Levels 1.400+1.500**

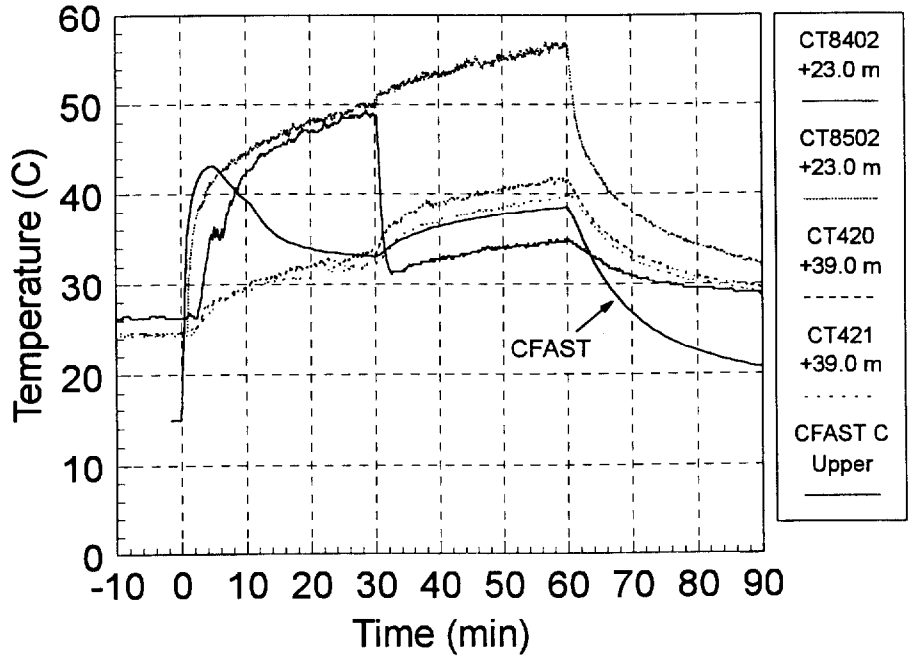


**Figure 3.41: T51.25 Level 1.700 - Dome Temperatures**

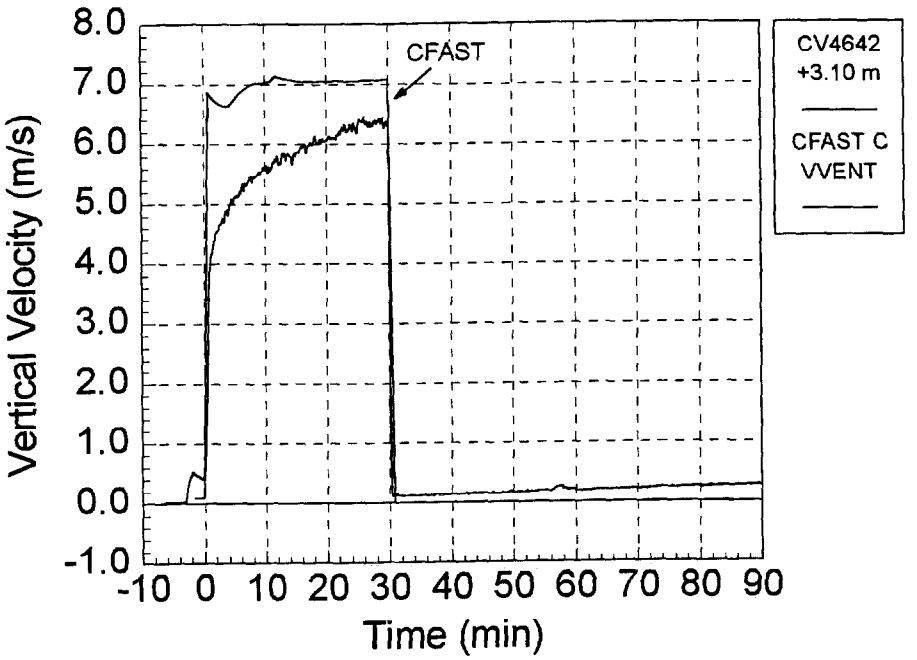


**Figure 3.42: T51.25 Additional Duct Velocity**

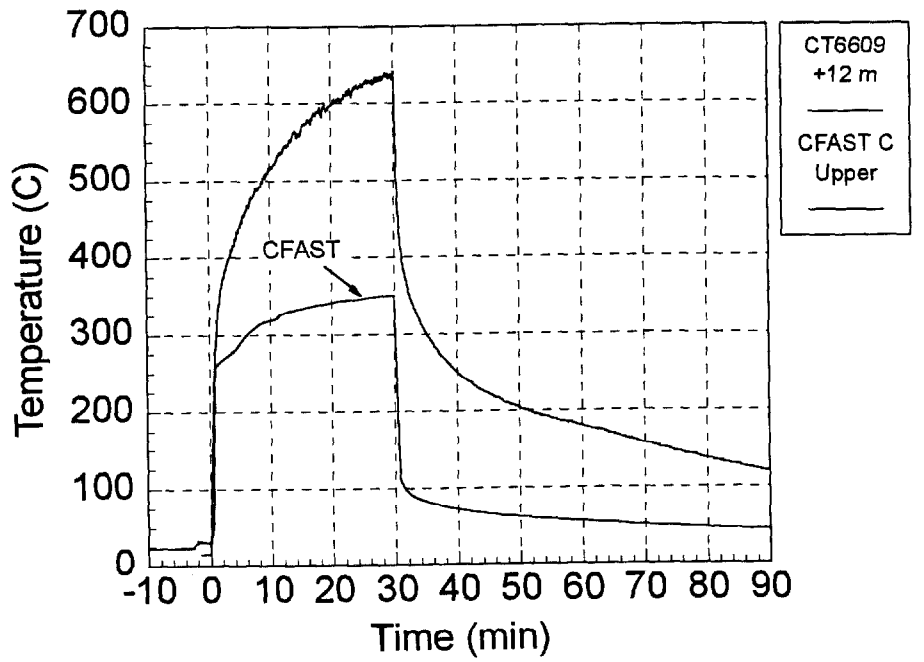


**Figure 3.43: T51.25 Additional Duct Temperature**

## 3.4 Sensitivity (T51.11)

A series of eight permutations were made to the reference T51.11 C model to test CFAST's sensitivity of results to changes in input parameters. The eight permutations were grouped into pairs of changes for four different input parameters likely to have had experimental error in their determination. The four pairs of permutations were:

1. Fire power: The actual fire power may have varied due to errors in measuring gas flow rate.
   - Increasing the fire power by 10%
   - Decreasing the fire power by 10%
2. Radiant heat fraction: No data was given for this parameter so the user must supply a value which leads to the question of how much does the user's choice effect the end results.
   - Decreasing the radiant heat fraction by 50%, i.e. changing it from 10% to 5%.
   - Increasing the radiant heat fraction by 50%, i.e. changing it from 10% to 15%.
3. Vent opening beneath curtain: The curtain hung around the maintenance hatch is the most likely spot for an error in geometric measurement as it is not a fixed surface.
   - Increasing the gap beneath the maintenance hatch curtain by 10 cm.
   - Decreasing the gap beneath the maintenance hatch curtain by 10 cm.
4. Gas burner fresh air supply: The actual air supplied to the gas burners is also a likely source of error. This would change the combustion products of the fire, especially the $CO_2$ and CO yields. Modifications to the air supply included the changes in combustion products as per the data in reference [4].
   - Decreasing the gas burner air supply by 0.2 required air to 0.9 required air.
   - Increasing the gas burner air supply by 0.2 required air to 1.2 required air.

The remainder of the subsection will discuss CFAST's sensitivity in terms of some of the more significant output parameters. While the permutations were run for the same time history as the previously discussed models, the output is only displayed for the time from 0 minutes to 25 minutes. This was done to eliminate the uninteresting regions for comparison, namely the steady state conditions before the fire ends and the near equilibrium flow conditions reached near 30 minutes test time. In this approach the focus is placed on the initial transient period of the fire where the permutation's effects are most notable.

The first figure, Figure 3.44, shows the predicted temperatures for the upper layer of the fire room. As expected, changes in the pyrolisys rate result directly in shifts in the temperature in the direction of the pyrolisys change. Changing the radiant heat fraction of the fire has a small effect on the layer temperature in the opposite direction of the change. The small magnitude of the temperature shift indicates that CFAST is not very sensitive to this parameter in determining temperatures. Changing the height of the curtain has an interesting effect on the results. For the first 15 minutes of the fire the larger curtain gap has higher temperatures, and for the second 15 minutes of the fire the smaller curtain gap has higher temperatures. As the slightly increased gap should aid in the early ventilation of the fire room, it is puzzling that the code would predict higher temperatures early in the fire. Changing the burner air supply also has an interesting effect on the layer prediction. The changes made in the input were such that the fire power was not affected and both cases had the same heat output to the fire room. Therefore, since CFAST uses

a constant specific heat and the heat release rates were identical for the two cases, there should be no discernible difference between the two cases in terms of temperatures except for those caused by air flow out of the room. Because the increased air supply case has a larger air flow into the fire room, it should result in a higher mass flow rate out of the fire room and thus lower upper layer temperatures. This is not the case; however, as the changes in air supply resulted in temperature changes larger than any other permutation except modifying the fire power.

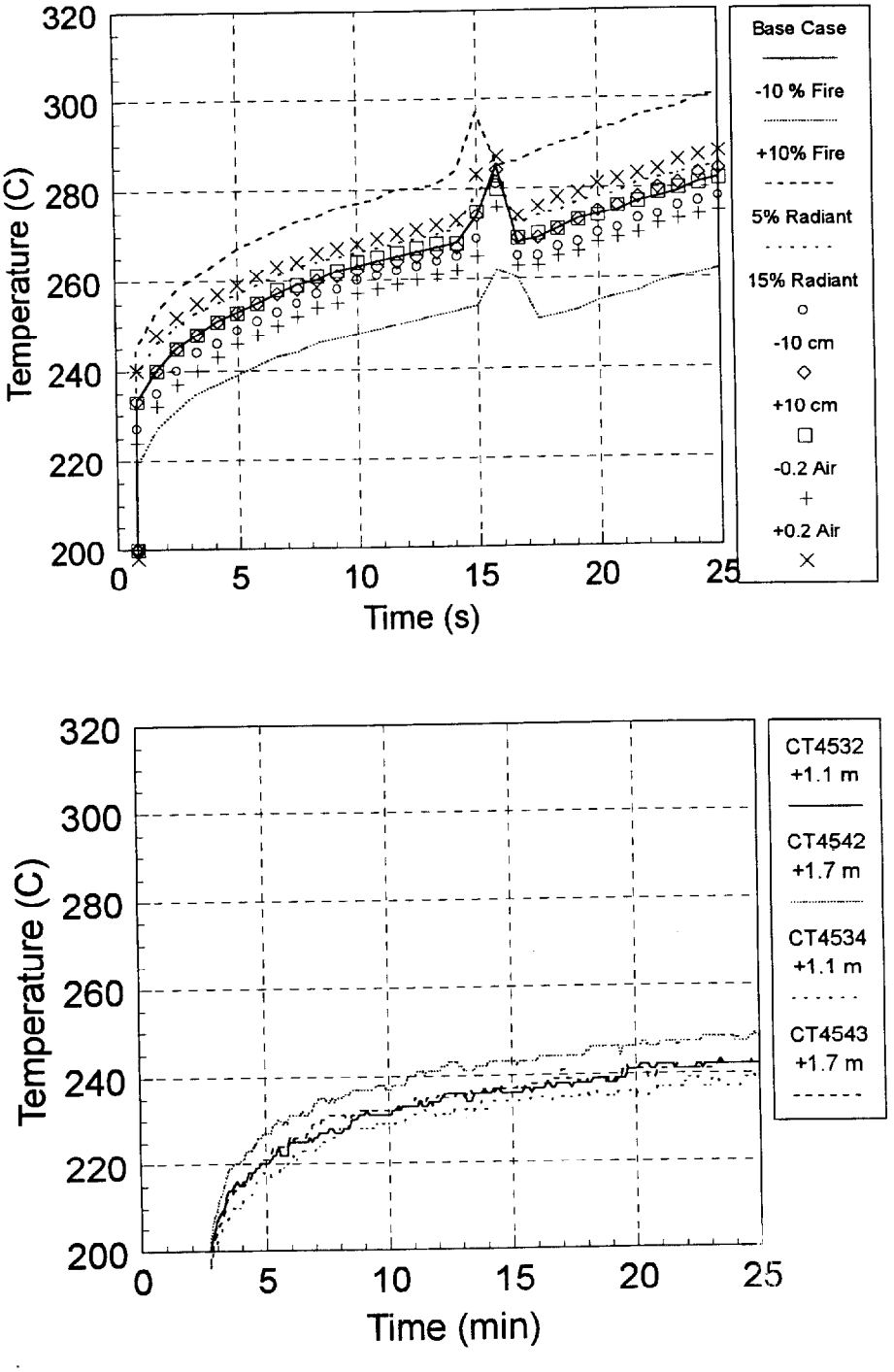


**Figure 3.44: T51.11 Sensitivity Study Fire Room Upper Layer Temperature**

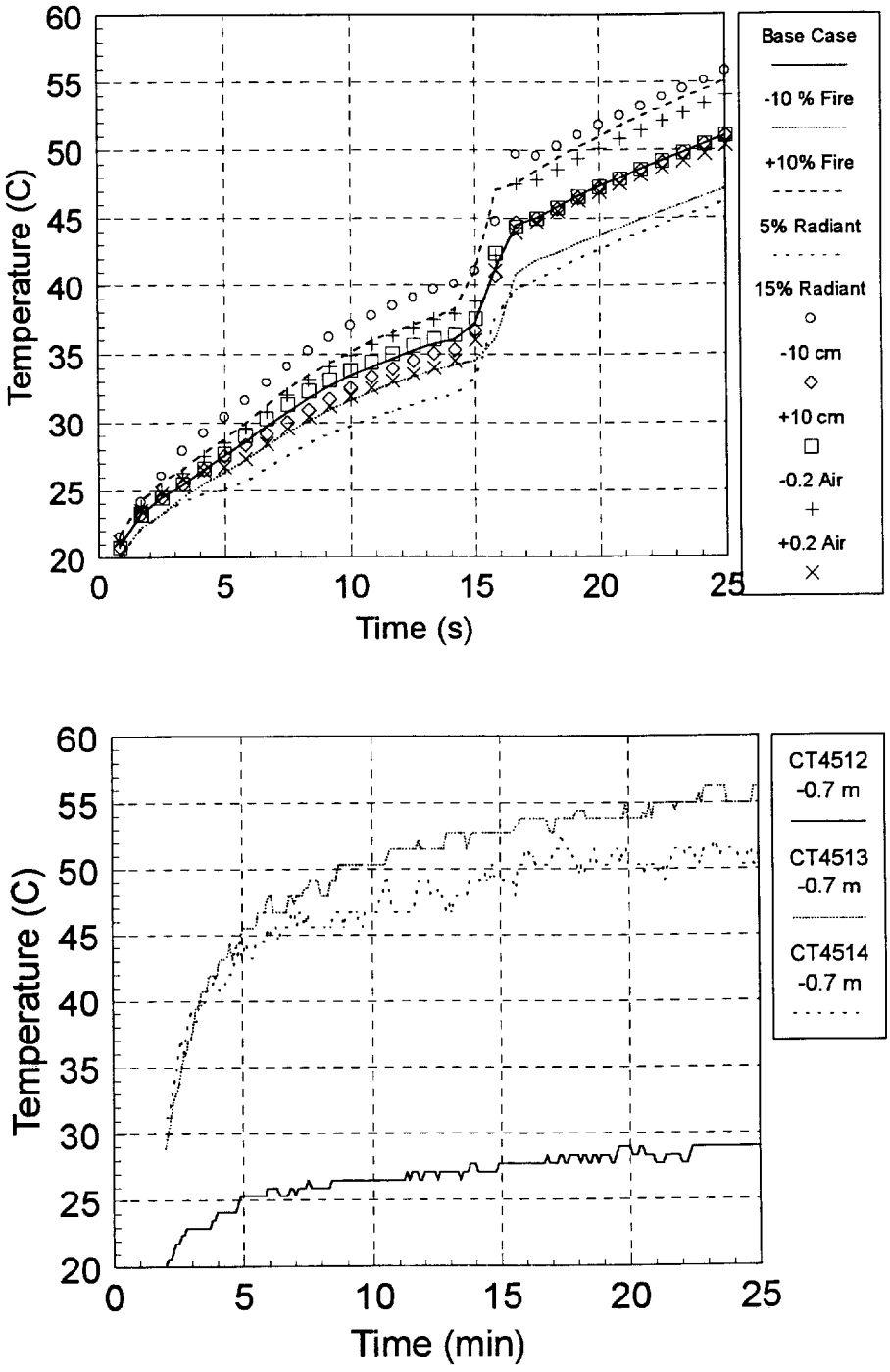


**Figure 3.45 T51.11 Sensitivity Study Fire Room Lower Layer Temperature**

Examining the predictions for the fire room's lower layer temperature, Figure 3.45, yields similar results to those of the upper layer. Changing the pyrolisys rate has the expected effects on temperature. The radiant heat fraction change has a large effect on the lower layer; however, since the lower layer temperatures are low to begin with any small changes in heat input should be expected to yield noticeable results. There is again the interesting and unexpected result that

increasing the vent space below the curtain results in higher fire temperatures in the first fifteen minutes of the fire. In the lower layer, the changing of the burner air supply has a small effect on the room temperature. Unlike the upper layer, however, this change is in the expected direction. That is the reduced air supply with its expected reduced mass flow out of the fire room has a higher temperature, and the increased air supply has a lower temperature

Figure 3.46 shows the fire room layer height as predicted by each of the sensitivity cases. A small change in layer height can be seen for the modified fire power cases which is expected. The remaining cases with the exception of the increased burner air supply case result in nearly indiscernible changes in the layer height. The increased burner air supply case predicts a noticeably lower layer height than the base case. This is somewhat contradictory to the higher upper layer temperature that was predicted as an increased volume of the upper layer should results in a lower temperature.

The next two figures, Figures 3.47 and 3.48, depict the predicted upper and lower layer velocities for the fire room doorway. Once again, changes in the fire power yield the expected results that a larger fire has a greater mass efflux in the doorway. Changes to the radiant heat output had little observable effect on the velocities at the doorway. Changing the size of the gap below the curtain had no effect on the velocities for the first fifteen minutes of the fire, but for the latter portion of the fire the larger gap had larger flow rates. As with other parameters, changing the air supply had unexpected results on the flow rates. Both the decreased and the increased air supply cases resulted in decreased flow rates for the upper layer and increased flow rates for the lower layer. One would not expect that both modifications would result in code predictions being shifted in the same direction. Lastly, all the permutations contain a sudden decrease in velocity at +15 minutes which is not depicted by the data.

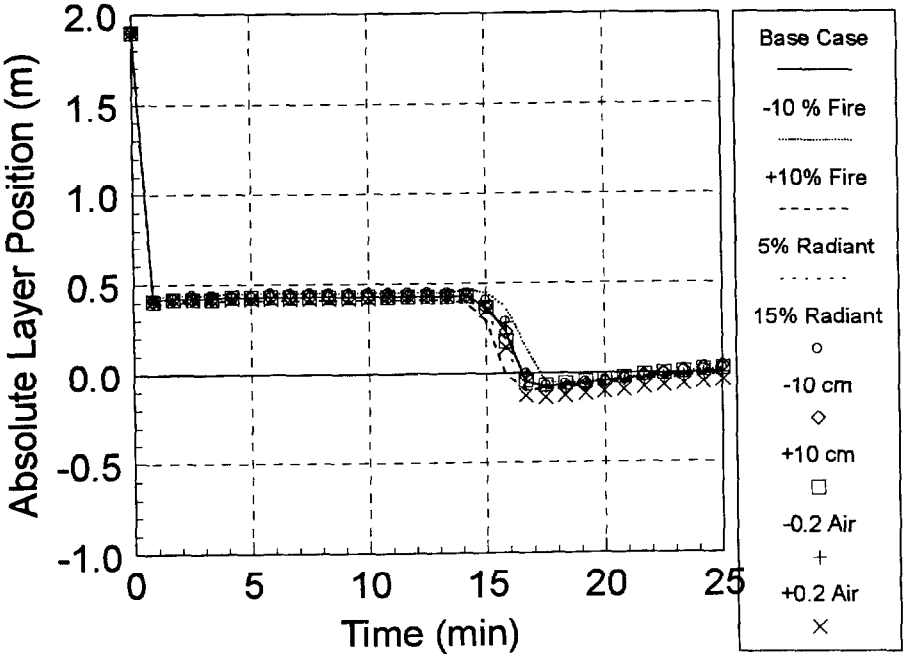


**Figure 3.46 T51.11 Sensitivity Study Fire Room Layer Height**

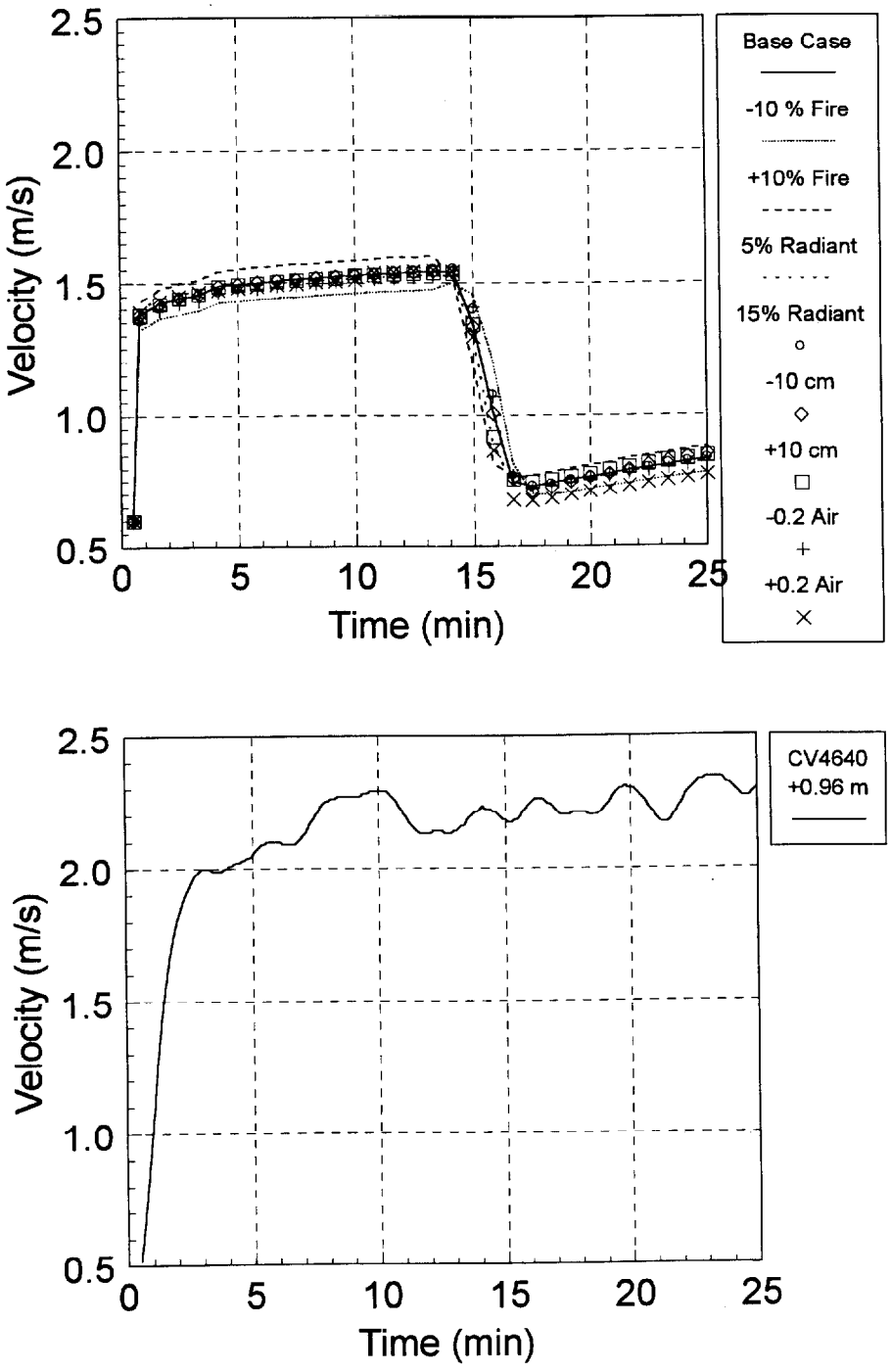


**Figure 3.47 T51.11 Sensitivity Study Fire Room Upper Layer Velocity**

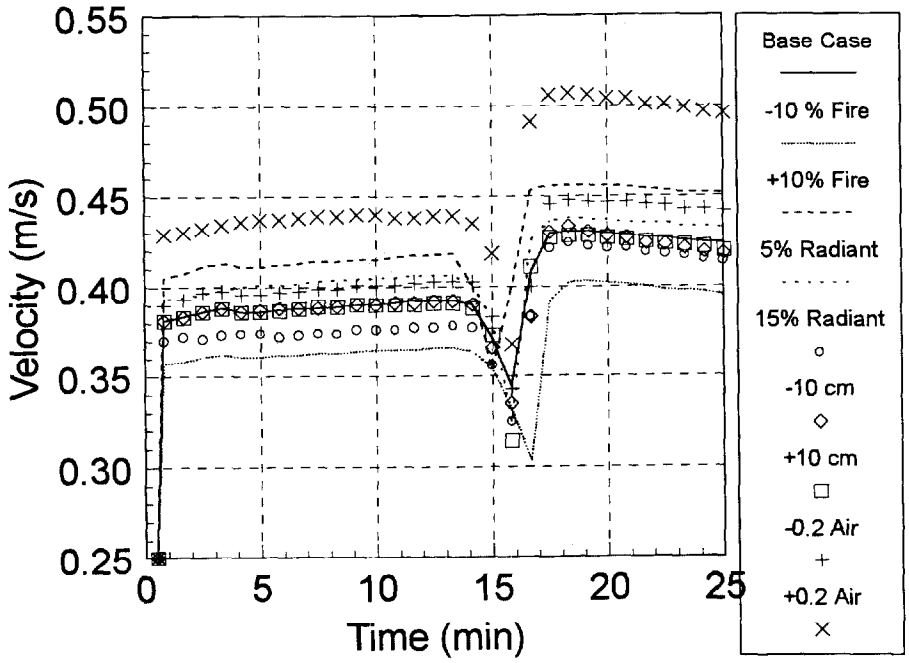


**Figure 3.48 T51.11 Sensitivity Study Fire Room Lower Layer Velocity**

The final figure of this subsection, Figure 3.49, shows the upper layer temperature beneath the maintenance hatch on the 1.400 Level. As can be seen each of the permutations has a large effect on the hatch temperature in the first few minutes of the fire. As the flow develops, however, this result changes. The fire power changes has its usual expected differences of a higher temperature for a higher fire power. The radiant heat changes also has the anticipated effect for this parameter, which is a lower radiant heat fraction results in more heat transfer to the combustion products leaving the fire room which should result in higher upper layer temperatures outside the fire room. The curtain modifications also have expected results. The smaller curtain gap, which acts to reduce mixing with colder air in this compartment results in higher temperatures, while the opposite is true for the larger curtain gap. Lastly, the changes to the gas burner air supply yields output changes that would seem to indicate that a higher heat output is released by the fire, which is not the case.

Overall it can be concluded that CFAST results are very sensitive to input changes that directly effect the fire, i.e. changes in the pyrolisys rate or the combustion products. Changes to the radiant heat fraction have little effect on the end results of a calculation for this experiment. CFAST results are not very sensitive to this parameter and it would appear that little emphasis should be placed on determining the appropriate input values for this parameter given the current models. Vent opening changes at rooms not immediately coupled to the fire room also have small effects on the end results calculated. This would indicate that modeling efforts in terms of room size accuracy should be focused on the fire room and adjacent compartments.

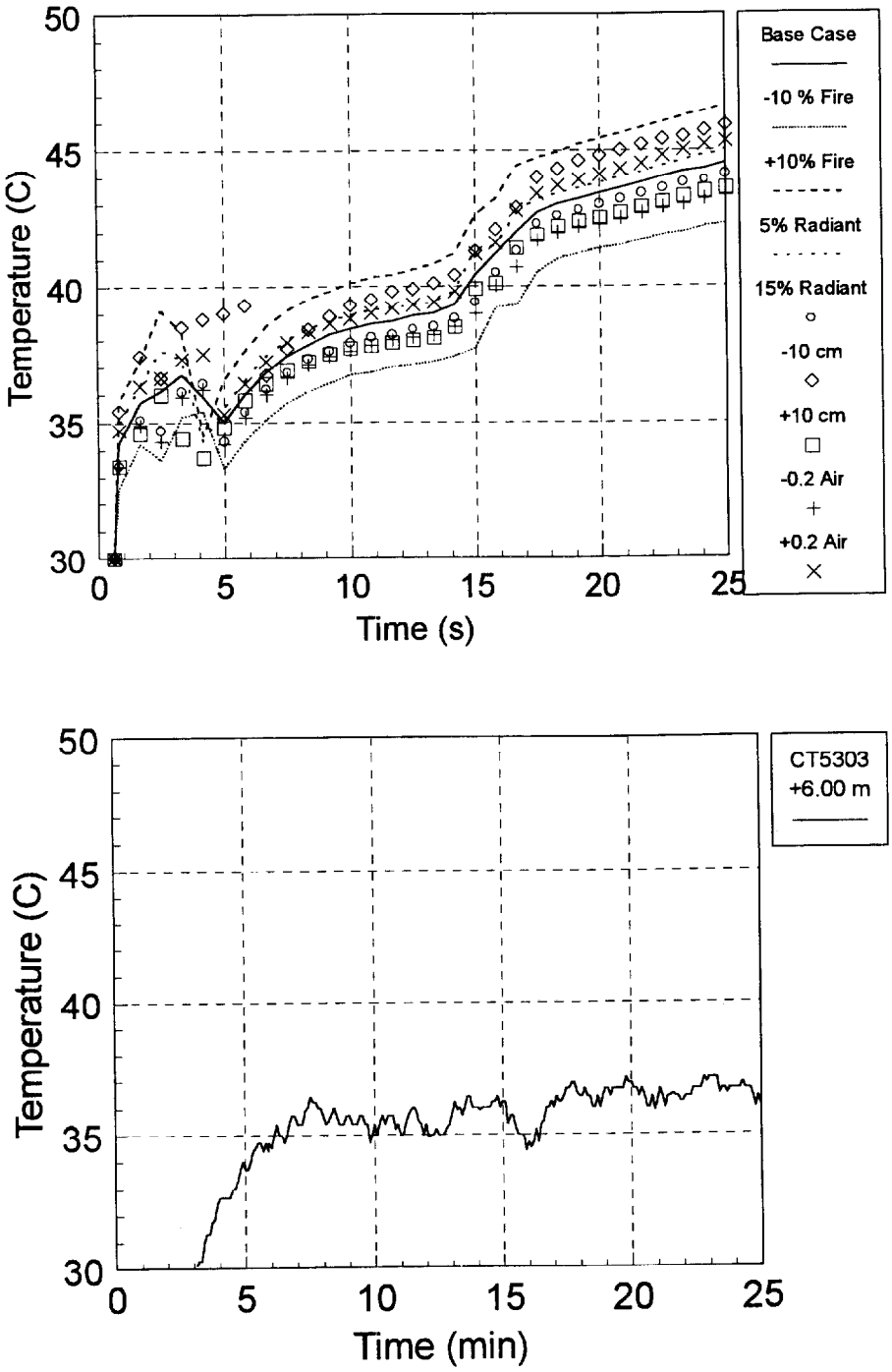


**Figure 3.49 T51.11 Sensitivity Study Curtained Area Upper Layer Temperature**

# 4 OBSERVATIONS AND COMMENTS

This section documents the general usability impressions the authors had while using CFAST for simulating the HDR T51 gas fire experiments. The first part addresses the accomplishments by and with CFAST over the spectrum of experiments covered during this validation effort. The second part covers differences and deviations in comparison with the data, behavior during code execution, performance of the implemented models, comments about the documentation, and comments about the capabilities and limitations of pre- and post-processors. The comments are made with respect to performance based trends as they impose requirements in terms of quality. The chapter closes with suggestions for continued validation.

## 4.1 Accomplishments with CFAST

The following accomplishments were achieved with CFAST during the validation efforts using the gas fire tests T51.11, T51.21, T51.23, and T51.25. The accomplishments listed in the following refer to the predictions made by the C model which was determined to be the best overall of the three models used in terms of performance:

- Even though CFAST was developed to handle open structures, i.e. structures with large leakage rates to the outside, and fixed state ventilation systems, the current input options were sufficient to reasonably model a closed building with a time dependent ventilation system.
- Fire room layer temperatures were reasonably well predicted though there was a tendency to overpredict the upper layer and underpredict the lower layer. Upper layer predictions were especially good for the higher power tests though flashover conditions for these tests resulted in poor lower layer temperature calculations.
- Velocity predictions through the fire room and the hallway were qualitatively comparable to measured velocities.
- Gas concentrations are well predicted during the course of the fire.
- Basic trends for temperature, velocity, and gas concentration were captured by CFAST when modeling the ventilation change test, T51.25.
- The velocity prediction in the additional ventilation duct was excellent, Figure 3.42.
- CFAST responds as expected to changes in the inputted fire power.
- CFAST is relatively insensitive to small changes in input parameters indicating an overall stability within the code's models and algorithms, although the authors' note that using a higher powered fire test for a comparative sensitivity study may yield a different conclusion.

## 4.2 User Observations

This subsection documents various aspects of code usage, applications, and executions that were observed by the authors during this project.

### 4.2.1 Model Building

For simple building structures, the model development is a simple task. The user can directly translate rectangular rooms with rectangular doorways to equivalent CFAST compartments. The

HDR and many other buildings, however, are complex structures. The HDR has multiple levels, compartments have multiple, irregularly shaped vent connections in all directions to other compartments, and the compartments themselves are rarely rectangular parallelepipeds. These particular features do not readily translate to the compartment geometry used by CFAST. The User's Guide gives no guidance to the model builder for dealing with these difficulties. The user must guess at appropriate simplifications for modeling complex structures and hope that those assumptions will function properly. As the results for the three models developed for this report show, reasonable assumptions may lead to unreasonable results as demonstrated in the B model with its unphysical flow through the main staircase maintenance hatches as discussed in Section 3.1.

In addition to general difficulties in creating input models without guidance, creating a model capable of being executed can also be a challenge. When modeling multiple level structures, CFAST's treatment of layer heights in compartments connecting levels can lead to unstable conditions and either cause the code to abort execution, or reduce the time step to near zero. Under these condition, which were experienced in the C model, discussed in Section 2.4.3, and the additional ventilation models, Section 2.4.4, the problematic compartment must be modified until the code runs. This must be accomplished without any guidance from the user's manual in resolving such difficulties. In the cases of both the C and the additional ventilation models, these manipulations resulted in a compartment that preserved some, but not all of the desired geometric features, thereby leading to possible distortions.

### 4.2.2 Observations During Code Execution

There are a number of issues related to CFAST's runtime stability that occur when running the code. The following summarizes a few observations:

- If a simple, one room, constant power fire, vent to the outside model is created, it will run without any problems. Attempting to restart this model results in the code's time step being reduced from seconds to microseconds. The time required to execute a model with microsecond time steps is considerable; therefore, the restart feature appears to be of little use for practical purposes. However, since the restart capabilities are poorly documented in the user's, the aforementioned outcome could primarily result from user error.
- As discussed in Sections 2.4.3 and Sections 2.4.4, very small changes in input parameters can mean the difference between a case that executes and a case that essentially does not. This is indicative of a generic instability induced by the discretized equations.
- A case can be executing successfully with large time steps and with well-behaved room temperatures and layers, and suddenly have time step sizes drop down to nanoseconds where they remain with no apparent reason for these difficulties. This occurred during attempts to generate a working C model and additional ventilation model.

### 4.2.3 Physical Models

The following are some observed deficiencies in the CFAST physical models:

- Use of the SHAFT keyword results in significantly different layer heights in neighboring compartments for simple models. As a results of this observation none of the HDR compartments were modeled using the SHAFT keyword, even though compartments such as the staircase could be considered shafts.
- CFAST is not able to compute fires in a completely sealed structure. Granted most structures have large leakages; however, there do exist specialized industrial facilities that are essentially sealed.
- The vertical flow correlations can result in large nonphysical flows as seen in the B model, see Figure 3.12 and Appendix B. It is important to note that these nonphysical flows cannot truly be attributed to a stack effect. The stack effect requires a temperature difference or a wind speed at the top of the stack. In the case of the B model there was neither.
- Gas mixing between hot and cold layers can vary greatly with small model changes. It is possible for CFAST to not calculate any mixing between layers. This was seen in the $CO_2$ concentrations in the lower layer of the A and B models, see Figure 3.8.
- Post fire mass flow rates drop very quickly, when in fact, after a sustained fire, buoyancy effects and radiant heat from structures should cause flow fields to decay more slowly as shown by all the cooldown phases of the HDR-experiments documented in [1] and Section 3.
- Gas concentrations at the end of a fire do not gradually return to ambient levels, but rather recover slightly and level off at a plateau. This is a secondary effect of the lack of a proper cooldown prediction.
- Another secondary effect of the lack of a cooldown period is that the upper layer collapses nearly instantaneously at the end of the fire causing lower layer temperatures to spike up. Though this spike is accurate given the collapse of the upper layer, it obscures information about conditions at the floor level in a compartment.
- CFAST has difficulties with post-flashover fires as seen in the results for test T51.23 in Figure 3.16 where CFAST greatly underpredicts the cold layer temperatures in the fire room. Since a zone model requires a cold layer, it seems unlikely that this issue can be completely resolved without changes to the basic CFAST assumptions, or incorporation of a special model covering this aspect.
- The ventilation change test, T51.25, shows a series of oscillations in the fire room parameters that result from the code bifurcating between the two flowpaths out of the fire room before settling into some steady flow rate out of both.
- The fire room hot layer temperatures for test T51.11 contains a spike discontinuity at +10 minutes, Figure 3.13, which is not seen in any other parameters or in other fire tests.
- For all of the C model predictions there is a sharp, significant shift in predicted values at +10 minutes.

## 4.3 User Comments

The following documents general issues related to current documentation and pre- and post-processing options.

### 4.3.1 Documentation

The documentation readily available to CFAST users consists of the technical description of the code [3] and a user's guide [2]. Both of these documents are written for older versions of the

code than the current release. The documentation gives a good review of the physical models used in the code and some of the assumptions that went into them; however, since they are for older versions of the code the extent to which these descriptions are still valid for the current release is not easily determined. The documentation also has a well written summary of all the input variables for the code version it was written for as well as the actual variables used internal to the code. There are a few improvements that could be added to the current documentation.

- Updated documentation of the new variables available in the current CFAST version.
- The documentation gives little advice on how to model structures with complex floor shapes, complex ventilation systems, or multiple levels. Without guidelines for modeling complex, real structures, the reliability of any computation can not be judged. The unfortunate result of this is that CFAST has a very high user effect which will limit its usefulness for performance based applications.
- The documentation poorly describes how to use the runtime plotting features of CFAST.
- The CFAST input files used for verification purposes are not provided as an appendix or with the code distribution disk.
- The restart capabilities of the code, including its limitations and guidance on how to use it, are not documented.

### 4.3.2 Pre -Processing

CFAST users have two options for pre-processing. Users can either create the ASCII input file by hand with a text editor or use a GUI input processor. Using a text editor to create an input file is fairly straight forward; however, this route lacks syntax checking and other logic to verify the validity of an input file. Thus, use of the GUI input processor has clear advantages. Unfortunately, this route is lacking in a number of aspects, which are summarized below:

- When beginning a new case the user is forced to chose among a very limited set of predefined fire scenarios. If the desired fire does not exist among this group, the user is forced to choose an unwanted distribution, then delete it time point by time point, and then redefine the fire.
- When creating a ceiling/floor vent, the syntax checking logic will sometimes declare two rooms being unconnectable, when in fact they do meet the requirements for having a ceiling/floor vent between them.
- The input file generated by the preprocessor is not very readable. That is, the spacing and numerical format used for writing the various input cards results in a file that is difficult to read.
- If one is editing a time based parameter and wishes to delete or insert a time point, there is no easy way to do this. The only method available is to delete from that point forward and reenter the numbers.
- When reading in a previously created input file, the preprocessor performs error checking on that file. If the error checking discovers a problem with a vent, it deletes the entire vent. This of course removes all information about that vent from the file. It would be more useful to flag those portions of a vent description that are invalid as bad and allow the user to change them without having to recreate the entire vent.

- When editing room data and room connection data only the currently selected compartment can be modified. To change another compartment the user must close the edit menu, select another room, and then reopen the edit menu. The ability to stay in the edit menu and cycle through compartments would be desirable.
- The preprocessor is a DOS based program. Considering that CFAST appears to be predominately executed on x86 compatible platforms and that almost all of these are running some version of Windows, remaining in the DOS environment only restricts the ease of use of the processor and complicates its upgrading

#### 4.3.3 Post-Processing

There are two post-processing utilities, REPORT and CPLOT. REPORT generates an ASCII output file containing user specified sets of data. CPLOT extracts individual parameters from the CFAST binary history file and plots them; it is also capable of saving the parameters in ASCII format.

With CFAST v3.0 the biggest difficulty the authors had with post-processing was that no simple way existed to take the binary history file and extract data in a format suitable for use with a spreadsheet. REPORT's output, while in ASCII format and capable of accessing all parameters, was in a row based format that could not be used easily in a spreadsheet. CPLOT was capable of outputting parameters in a columnar time vs. parameter format; however, it did not access all parameters; for example, horizontal openings, and it could only write six parameters at a time to a file. CFAST v3.1 can now post-process files into a spreadsheet format, which is a large step in the right direction. The second difficulty arose in attempting to compare the results of two different CFAST cases using CPLOT. One can read and plot with CPLOT data from multiple CFAST executions, which is very useful for performing quick sensitivity checks. However, ventilation mass flow rates cannot be read in from multiple files. The internal data set verification does not recognize vent flows from two different input files as being independent data sets. A final problem with post processing occurred when attempting to write ASCII data files from within CPLOT. When CPLOT requests a file name to be used for saving from the code user, it does not set any previous filename to a null string rather it just overwrites the previous filename used. Therefore, if some data are saved to a file named data1.txt and then tried to save to d.txt, CPLOT will try to save a file called d.txt.txt which will of course yield an error message as it is not a valid DOS filename.

### 4.4 Suggestions for Further Validation

While the gas fire tests contain a large number of phenomena of interest to performance based codes, there are some deficiencies in this test series for a complete validation of a computation tool like CFAST. This test series contains data regarding flashover, ventilation system changes during a fire, and large vertical shafts. Since the gas fires were premixed with air, this test series does not examine underventilated fires. Also, since the fire was low in the containment building, the large dome region saw a minimal impact from the fire. Therefore additional validation for large atrium spaces is suggested. Lastly, the work performed for this report indicates that further study is needed to resolve how to appropriately model structures with multiple, vertical shafts. Some of these issues will be addressed during the continuation of

research work during the FY 1998 on the basis of validation efforts regarding the wood crib fires, T51.16-18, as well as the high-positioned hydrocarbon fire test series, T52, which specifically addressed entrainment, large plume behavior, and high-ceilinged compartments. Furthermore, it is suggested to perform an additional sensitivity study of the type presented in Section 3.4 for an experiment with higher fire power, i.e. T51.21 or T51.23..

# 5 REFERENCES


1. Floyd, J. and Wolf. , L. *Evaluation of the HDR Fire Test Data and Accompanying Computational Activities with Conclusions from Present Code Capabilities, **Volume 1**: Test Series Description Report for T51 Gas Fire Test Series.* Dept. Materials and Nuclear Engineering, University of Maryland. College Park, Maryland. Report NUMAFIRE:04-97. 1997.

2. Portier, R. , et al. *A User's Guide for CFAST Version 1.6.* Building and Fire Research Laboratory, NIST. Gaithersburg, Maryland. NISTIR 4985. Dec. 1992.

3. Peacock, R., et al. *CFAST, the Consolidated Model of Fire Growth and Smoke Transport.* Building and Fire Research Laboratory, NIST. Gaithersburg, Maryland. NIST Technical Note 1299. Feb. 1993.

4. Beyler, C., "Major Species Production by Diffusion Flames in a Two-layer Environment." *Fire Safety Journal.* Volume 10. pp. 47-56. 1986.

5. Schall, M. and Valencia, L. *Data Compilation of the HDR Containment Fire for Input Data Processing for Pre-Test Calculations* (English Translation of PHDR Working Report 3.143179). Project HDR Nuclear Center. Karlsruhe, Germany. PHDR Working Report 3.279/82. Jan. 1982.

6. Müller, K. and Dobbernack, R. *Evaluation of Fire Behavior in Compartment Networks in a Closed Containment, Design Report, Test Group BRA-E, Exploratory Experiments T51.1* (In German). Project HDR Nuclear Center. Karsruhe, Germany. PHDR Working Report 5.025/84. Dec. 1984.

7. Tenhumberg. *Evaluation of Fire Behavior in Compartment Networks in a Closed Containment, Data Report, Test Group BRA-E, Experiments T51.11-T51.15, Test Period 01/24 - 02/01/1985* (In German). Project HDR Nuclear Center. Karlsruhe, Germany. PHDR Working Report 5.43/85. Feb. 1985.

8. *Supplemental Data Report, Test Group BRA-E, Experiments T51.11-T51.15* (In German). Project HDR Nuclear Center. Karlsruhe, Germany. PHDR Working Report 5.038/85. April 1985.

9. Müller, K., Wegener, H. and Dobbernack, R. *Evaluation of Fire Behavior in a Compartment Network in a Closed Containment, Supplemental Design Report, Test Group BRA, Experiments T51.2.* Project HDR Nuclear Center. Karlsruhe, Germany. PHDR Working Report 5.069/86. June 1986.

10. Grimm. *Evaluation of Fire Behavior in a Compartment Network in a Closed Containment, Supplemental Design Report, Test Group BRA, Test Group T51.21-T51.24* (In German). Project HDR Nuclear Center. Karlsruhe, Germany. PHDR Working Report 5.078/86. May 1986.

11. *Evaluation of Fire Behavior in a Compartment Network in a Closed Containment, Quick Look Report, Test Group BRA, Experiments T51.11-T51.19* (In German). Project HDR Nuclear Center. Karlsruhe, Germany. PHDR Working Report 61-85. June 1986.

12. Rautenberg, J., Dobbernack, R., Müller, K., and Volk, R. *Evaluation of Fire Behavior in a Compartment Network in a Closed Containment, Final Evaluation Report, Test Group BRA, Experiments T51.1; T51.2* (In German). Project HDR Nuclear Center. Karlsruhe, Germany. PHDR Working Report 82-91. March 1991.

13. Nowlen, S. *A Summary of the Fire Testing Program at the German HDR Test Facility.* Sandia National Laboratories. NUREG/CR-6173. Nov, 1995.

14. Max, Müller, K., et al. *Behavior of Oil Fires in a Closed Subsystem With Ventilation Connected and Variable Door Opening, Quick Look Report, Experiments E41.5-10* (In German). Project HDR Nuclear Center. Karlsruhe, Germany. PHDR Technical Report 122-93.

15. Rockett, J. *HDR Reactor Containment Fire Modeling with BR12.* Fire Technology Laboratory. Technical Research Centre of Finland (VTT). VTT Publication 113. 1992.

16. Green, J. Notebook for Development of E11.4 CONTAIN Model for the HDR Hydrogen Mixing Test. Dept. of Materials and Nuclear Engineering. University of Maryland. College Park, MD. 1992.

17. Holzbauer, H. *Blind Post-Test Predictions of HDR-$H_2$-Distribution Experiements E11.2 and E11.4 Using FATHOMS* (In German).Batelle Institute e.v. Frankfurt/Main, FRG. Final Report BIEV R67238-1. Dec. 1990.

18. Holzbauer, H. *Parametric Open Post-Test Predictions and Analysis of the HDR-$H_2$-Distribution Experiment E11.2 and E11.4 with the Computer Code GOTHIC* (In German). Batelle Institute e.v. Frankfurt/Main, FRG. Final Report BIEV R67706-1. August 1990.

19. Wiles, L., et al. *GOTHIC Containment Analysis Package, V3.4e.* Electric Research Power Institute.

## APPENDIX A: INPUT FILES

This appendix gives the complete CFAST input file for all computations documented in this report. The filename nomenclature isT51XX-YZ.INP where XX indicates the test number in the T51 test series, Y indicates the CFAST model variant (A, B, or C), and Z indicates a model permutation as used in the parametric studies documented in Section 3.4.

**T5111-C.INP**:CFAST input file for Test T51.11 (229 kW) using the C model with no additional ventilation.

```
VERSN    3T51-11: 9 Room+Dome+Level 1.4 Connect
TIMES   5500    100     50      0      0
DUMPR T5111-c.HIS
STPMAX  1.00000
TAMB  288.000  101300. 0.000000
EAMB  288.000  101300. 0.000000
HI/F   0.250  0.000  0.000  0.000  0.000 11.100 11.100 11.100 11.100 16.150  0.300
WIDTH  2.950  4.950  4.300  4.330  1.800  7.920  4.300  4.330  9.670 14.370  3.000
DEPTH  3.650  1.800  2.750  2.720  6.350  7.920  2.750  2.720  9.670 14.370  3.000
HEIGH  2.750  2.485 11.100 11.100  3.500  4.600  5.050  5.050  5.050 34.950 13.200
CEILI FIRECEIL YTONG100 CONCR050 CONCR050 CONCR050 CONCR050 CONCR050 CONCR050 CONCR050 CONCR050 CONCR050
WALLS YTONG250 YTONG100 CONCR050 CONCR050 CONCR050 CONCR050 CONCR050 CONCR050 CONCR050 CONCR050 CONCR050
FLOOR FIRE_FLR CONCR100 CONCR050 CONCR050 CONCR050 CONCR050 CONCR050 CONCR050 CONCR050 CONCR050 CONCR050
HVENT  1  2  1  1.010  1.975  0.000
CVENT  1  2  1  1.000  1.000  1.000  1.000  1.000  1.000
HVENT  2  3  1  1.800  2.485  0.000
CVENT  2  3  1  1.000  1.000  1.000  1.000  1.000  1.000
HVENT  3  4  1  4.300  0.500  0.000
CVENT  3  4  1  1.000  1.000  1.000  1.000  1.000  1.000
HVENT  3  5  1  2.000  0.500  0.000
CVENT  3  5  1  1.000  1.000  1.000  1.000  1.000  1.000
HVENT  4  5  1  2.700  3.100  1.100
CVENT  4  5  1  1.000  1.000  1.000  1.000  1.000  1.000
HVENT  5 11  1  1.800  3.500  0.300
CVENT  5 11  1  1.000  1.000  1.000  1.000  1.000  1.000
HVENT  6  7  1  3.000  4.250  0.000
CVENT  6  7  1  1.000  1.000  1.000  1.000  1.000  1.000
HVENT  6  8  1  3.000  4.250  0.000
CVENT  6  8  1  1.000  1.000  1.000  1.000  1.000  1.000
HVENT  6  9  1  3.000  4.250  0.000
CVENT  6  9  1  1.000  1.000  1.000  1.000  1.000  1.000
HVENT  7  8  1  3.000  4.250  0.000
CVENT  7  8  1  1.000  1.000  1.000  1.000  1.000  1.000
HVENT 11 12  1  0.050  9.800  3.300
CVENT 11 12  1  1.000  1.000  1.000  1.000  1.000  1.000
HVENT  6 11  1  3.000  2.400  0.000
CVENT  6 11  1  1.000  1.000  1.000  1.000  1.000  1.000
VVENT  7  3  4.54000  2
VVENT  8  4  5.75000  2
VVENT 10  7  4.54000  2
VVENT 10  8  6.97000  2
VVENT 10  9  5.28000  2
MVDCT  1  2   1.000  0.300  1.00E-004  0.000  1.000  0.000  1.000  0  0
MVDCT  3  4  18.000  0.300  1.00E-004  0.000  1.000  0.000  1.000  0  0
MVFAN  3  2   0.000 900.00  0.0073     0.000  0.000  0.000  0.000  0  0
MVOPN  1  1 H  0.375  0.143  0  0  0  0
MVOPN  9  4 V  0.500  0.070  0  0  0  0
INELV  2  0.625  0  0
INELV  3  0.625  0  0
CHEMI  44.000  0.000  0.000  4.650E+007  300.000  388.000  0.100
LFBO 1
LFBT 2
CJET OFF
FPOS   1.47500   3.65000   0.00000
FTIME   100.00    101.00   3700.00   3701.00   5500.00
FHIGH  0.00000   0.00000   0.37500   0.37500   0.00000   0.00000
FAREA  0.00000   0.00000   0.14300   0.14300   0.00000   0.00000
FMASS  0.00000   0.00000   0.00484   0.00484   0.00000   0.00000
FQDOT  0.00000   0.00000   225000.   225000.   0.00000   0.00000
HCR    0.00000   0.00000   0.22200   0.22200   0.22200   0.22200
```

```
OD      0.00000    0.00000    0.02200    0.02200    0.02200    0.02200
CO      0.00000    0.00000    0.04200    0.04200    0.04200    0.04200
#GRAPHICS ON
DEVICE 1
WINDOW    0.     0.     0. 1279. 1023. 4095.
```

**T5111-C1.INP**: CFAST input file for Test T51.11 (229 kW) using the C model with no additional ventilation and -10% fire power.

Original Input File:

```
VERSN    3T51-11: 9 Room+Dome+Level 1.4 Connect
DUMPR T5111-c.HIS
FMASS  0.00000    0.00000    0.00484    0.00484    0.00000    0.00000
FQDOT  0.00000    0.00000    225000.    225000.    0.00000    0.00000
```

Modifications:

```
VERSN    3T51-11: 9 Room+Dome+Level 1.4 Connect - 10% Fire
DUMPR T5111-c1.HIS
FMASS  0.00000    0.00000    0.00436    0.00436    0.00000    0.00000
FQDOT  0.00000    0.00000    202600.    202600.    0.00000    0.00000
```

**T5111-C2.INP**: CFAST input file for Test T51.11 (229 kW) using the C model with no additional ventilation and +10% fire power.

Original Input File:

```
VERSN    3T51-11: 9 Room+Dome+Level 1.4 Connect
DUMPR T5111-c.HIS
FMASS  0.00000    0.00000    0.00484    0.00484    0.00000    0.00000
FQDOT  0.00000    0.00000    225000.    225000.    0.00000    0.00000
```

Modifications:

```
VERSN    3T51-11: 9 Room+Dome+Level 1.4 Connect + 10% Fire
DUMPR T5111-c2.HIS
FMASS  0.00000    0.00000    0.00532    0.00532    0.00000    0.00000
FQDOT  0.00000    0.00000    247600.    247600.    0.00000    0.00000
```

**T5111-C3.INP**: CFAST input file for Test T51.11 (229 kW) using the C model with no additional ventilation and 5% radiant heat.

Original Input File:

```
VERSN    3T51-11: 9 Room+Dome+Level 1.4 Connect
DUMPR T5111-c.HIS
CHEMI  44.000  0.000  0.000  4.650E+007  300.000  388.000  0.100
```

Modifications:

```
VERSN    3T51-11: 9 Room+Dome+Level 1.4 Connect + 5% Radiant Heat
DUMPR T5111-c3.HIS
CHEMI  44.000  0.000  0.000  4.650E+007  300.000  388.000  0.050
```

**T5111-C4.INP**: CFAST input file for Test T51.11 (229 kW) using the C model with no additional ventilation and 15% radiant heat.

Original Input File:

```
VERSN    3T51-11: 9 Room+Dome+Level 1.4 Connect
DUMPR T5111-c.HIS
CHEMI  44.000  0.000  0.000  4.650E+007  300.000  388.000  0.100
```

Modifications:

```
VERSN    3T51-11: 9 Room+Dome+Level 1.4 Connect + 5% Radiant Heat
DUMPR T5111-c4.HIS
CHEMI  44.000  0.000  0.000  4.650E+007  300.000  388.000  0.150
```

**T5111-C5.INP**: CFAST input file for Test T51.11 (229 kW) using the C model with no additional ventilation and -10 cm curtain gap.

Original Input File:

```
VERSN    3T51-11: 9 Room+Dome+Level 1.4 Connect
DUMPR T5111-c.HIS
CVENT  2  3  1  1.000  1.000  1.000  1.000  1.000  1.000
HVENT  3  4  1  4.300  0.500  0.000
CVENT  3  4  1  1.000  1.000  1.000  1.000  1.000  1.000
HVENT  3  5  1  2.000  0.500  0.000
```

Modifications:

```
VERSN    3T51-11: 9 Room+Dome+Level 1.4 Connect - 10 cm Curtain Gap
DUMPR T5111-c5.HIS
CVENT  2  3  1  1.000  1.000  1.000  1.000  1.000  1.000
HVENT  3  4  1  4.300  0.400  0.000
CVENT  3  4  1  1.000  1.000  1.000  1.000  1.000  1.000
HVENT  3  5  1  2.000  0.400  0.000
```

**T5111-C6.INP**: CFAST input file for Test T51.11 (229 kW) using the C model with no additional ventilation and +10 cm curtain gap.

Original Input File:

```
VERSN    3T51-11: 9 Room+Dome+Level 1.4 Connect
DUMPR T5111-c.HIS
CVENT  2  3  1  1.000  1.000  1.000  1.000  1.000  1.000
HVENT  3  4  1  4.300  0.500  0.000
CVENT  3  4  1  1.000  1.000  1.000  1.000  1.000  1.000
HVENT  3  5  1  2.000  0.500  0.000
```

Modifications:

```
VERSN    3T51-11: 9 Room+Dome+Level 1.4 Connect + 10 cm Curtain Gap
DUMPR T5111-c5.HIS
CVENT  2  3  1  1.000  1.000  1.000  1.000  1.000  1.000
HVENT  3  4  1  4.300  0.600  0.000
CVENT  3  4  1  1.000  1.000  1.000  1.000  1.000  1.000
HVENT  3  5  1  2.000  0.600  0.000
```

**T5111-CA.INP**: CFAST input file for Test T51.11 (229 kW) using the C model with no additional ventilation and -0.2 air supply ratio.

Original Input File:

```
VERSN    3T51-11: 9 Room+Dome+Level 1.4 Connect
DUMPR T5111-c.HIS
MVFAN  3  2   0.000 900.00  0.0073     0.000  0.000  0.000  0.000  0  0
CHEMI  44.000  0.000  0.000  4.650E+007  300.000  388.000  0.100
OD     0.00000   0.00000   0.02200   0.02200   0.02200   0.02200
CO     0.00000   0.00000   0.04200   0.04200   0.04200   0.04200
```

Modifications:

```
VERSN    3T51-11: 9 Room+Dome+Level 1.4 Connect + 0.9 Excess Air Ratio
DUMPR T5111-ca.HIS
CHEMI  44.000  0.000 10.000  4.650E+007  300.000  388.000  0.100
MVFAN  3  2   0.000 900.00  0.0597     0.000  0.000  0.000  0.000  0  0
OD     0.00000   0.00000   0.04800   0.04800   0.04800   0.04800
CO     0.00000   0.00000   0.08500   0.08500   0.08500   0.08500
```

**T5111-CB.INP**: CFAST input file for Test T51.11 (229 kW) using the C model with no additional ventilation and +0.2 air supply ratio.

Original Input File:

```
VERSN    3T51-11: 9 Room+Dome+Level 1.4 Connect
DUMPR T5111-c.HIS
MVFAN  3  2   0.000 900.00  0.0073     0.000  0.000  0.000  0.000  0  0
OD     0.00000   0.00000   0.02200   0.02200   0.02200   0.02200
CO     0.00000   0.00000   0.04200   0.04200   0.04200   0.04200
```

Modifications:

```
VERSN    3T51-11: 9 Room+Dome+Level 1.4 Connect + 1.3 Excess Air Ratio
DUMPR T5111-cb.HIS
OD     0.00000   0.00000   0.01100   0.01100   0.01100   0.01100
CO     0.00000   0.00000   0.02100   0.02100   0.02100   0.02100
```

**T5121-A.INP**:CFAST input file for Test T51.21 (716 kW) using the A model with no additional ventilation.

```
VERSN    3T51-21: Level 1.4
TIMES  5500    100    50     0     0
DUMPR T5121-A.HIS
STPMAX  1.000
TAMB  288.000  101300. 0.000
EAMB  288.000  101300. 0.000
HI/F   0.250  0.000  0.000  0.000  0.000
WIDTH  2.950  4.950  4.300  4.330  1.800
DEPTH  3.650  1.800  2.750  2.720  6.350
HEIGH  2.750  2.485  4.600  4.600  3.500
CEILI FIRECEIL YTONG100 CONCR050 CONCR050 CONCR050
WALLS YTONG250 YTONG100 CONCR050 CONCR050 CONCR050
FLOOR FIRE_FLR CONCR100 CONCR050 CONCR050 CONCR050
HVENT  1  2  1  1.010  1.975  0.000
CVENT  1  2  1  1.000  1.000  1.000  1.000  1.000  1.000
HVENT  2  3  1  1.800  2.485  0.000
CVENT  2  3  1  1.000  1.000  1.000  1.000  1.000  1.000
HVENT  3  4  1  4.300  0.500  0.000
CVENT  3  4  1  1.000  1.000  1.000  1.000  1.000  1.000
HVENT  3  5  1  2.000  0.500  0.000
CVENT  3  5  1  1.000  1.000  1.000  1.000  1.000  1.000
HVENT  4  5  1  2.700  3.100  0.000
CVENT  4  5  1  1.000  1.000  1.000  1.000  1.000  1.000
HVENT  5  6  1  0.800  1.500  0.000
CVENT  5  6  1  1.000  1.000  1.000  1.000  1.000  1.000
VVENT  6  3  4.54000  2
VVENT  6  4  5.75000  2
MVDCT  1  2   1.000  0.300  1.00E-004  0.000  1.000  0.000  1.000  0  0
MVDCT  3  4  18.000  0.300  1.00E-004  0.000  1.000  0.000  1.000  0  0
MVFAN  3  2   0.000 900.00  0.2300     0.000  0.000  0.000  0.000  0  0
MVOPN  1  1 H  0.375  0.280  0  0  0  0
MVOPN  6  4 V 11.600  0.070  0  0  0  0
INELV  2  0.625  0  0
INELV  3  0.625  0  0
CHEMI  44.000  0.000  0.000  4.650E+007  300.000  388.000  0.100
LFBO 1
LFBT 2
CJET OFF
FPOS   1.47500   3.65000   0.00000
FTIME   100.00    101.00   3700.00   3701.00   5500.00
FHIGH  0.00000   0.00000   0.37500   0.37500   0.00000   0.00000
FAREA  0.00000   0.00000   0.28000   0.28000   0.00000   0.00000
FMASS  0.00000   0.00000   0.01540   0.01540   0.00000   0.00000
FQDOT  0.00000   0.00000   716000.   716000.   0.00000   0.00000
HCR    0.00000   0.00000   0.22200   0.22200   0.22200   0.22200
OD     0.00000   0.00000   0.02200   0.02200   0.02200   0.02200
CO     0.00000   0.00000   0.04200   0.04200   0.04200   0.04200
#GRAPHICS ON
DEVICE 1
WINDOW    0.    0.    0. 1279. 1023. 4095.
```

**T5121-B.INP**:CFAST input file for Test T51.21 (716 kW) using the B model with no additional ventilation.

```
VERSN    3T51-21: 9 Room Case
TIMES   5500    100     50      0      0
DUMPR T5121-B.HIS
STPMAX  1.00000
TAMB  288.000  101300. 0.000000
EAMB  288.000  101300. 0.000000
HI/F   0.250  0.000  0.000  0.000  0.000 11.100 11.100 11.100 11.100
WIDTH  2.950  4.950  4.300  4.330  1.800  7.920  4.300  4.330  9.760
DEPTH  3.650  1.800  2.750  2.720  6.350  7.920  2.750  2.720  9.760
HEIGH  2.750  2.485 11.100 11.100  3.500  4.600  5.050  5.050  5.050
CEILI FIRECEIL FIRECEIL YTONG100 CONCR050 CONCR050 CONCR050 CONCR050 CONCR050 CONCR050 CONCR050
WALLS YTONG250 YTONG250 YTONG100 CONCR050 CONCR050 CONCR050 CONCR050 CONCR050 CONCR050 CONCR050
FLOOR FIRE_FLR FIRE_FLR CONCR100 CONCR050 CONCR050 CONCR050 CONCR050 CONCR050 CONCR050 CONCR050
HVENT  1  2  1  1.010  1.975  0.000
CVENT  1  2  1  1.000  1.000  1.000  1.000  1.000  1.000
HVENT  2  3  1  1.800  2.485  0.000
CVENT  2  3  1  1.000  1.000  1.000  1.000  1.000  1.000
HVENT  3  4  1  4.300  0.500  0.000
CVENT  3  4  1  1.000  1.000  1.000  1.000  1.000  1.000
HVENT  3  5  1  2.000  0.500  0.000
CVENT  3  5  1  1.000  1.000  1.000  1.000  1.000  1.000
HVENT  4  5  1  2.700  3.100  1.100
CVENT  4  5  1  1.000  1.000  1.000  1.000  1.000  1.000
HVENT  5 10  1  0.800  3.500  0.000
CVENT  5 10  1  1.000  1.000  1.000  1.000  1.000  1.000
HVENT  6  7  1  3.000  4.250  0.000
CVENT  6  7  1  1.000  1.000  1.000  1.000  1.000  1.000
HVENT  6  8  1  3.000  4.250  0.000
CVENT  6  8  1  1.000  1.000  1.000  1.000  1.000  1.000
HVENT  6  9  1  3.000  4.250  0.000
CVENT  6  9  1  1.000  1.000  1.000  1.000  1.000  1.000
HVENT  7  8  1  3.000  4.250  0.000
CVENT  7  8  1  1.000  1.000  1.000  1.000  1.000  1.000
VVENT  7  3  4.54000  2
VVENT  8  4  5.75000  2
VVENT 10  7  4.54000  2
VVENT 10  8  6.97000  2
VVENT 10  9  5.28000  2
MVDCT  1  2   1.000  0.300  1.00E-004  0.000  1.000  0.000  1.000  0  0
MVDCT  3  4  18.000  0.300  1.00E-004  0.000  1.000  0.000  1.000  0  0
MVFAN  3  2   0.000 900.00  0.230      0.000  0.000  0.000  0.000  0  0
MVOPN  1  1 H  0.375  0.280  0  0  0  0
MVOPN  9  4 V  0.500  0.070  0  0  0  0
INELV  2  0.625  0  0
INELV  3  0.625  0  0
CHEMI  44.000  0.000  0.000  4.650E+007  300.000  388.000  0.100
LFBO 1
LFBT 2
CJET OFF
FPOS   1.47500   3.65000   0.00000
FTIME   100.00    101.00   3700.00   3701.00   5500.00
FHIGH  0.00000   0.00000   0.37500   0.37500   0.00000   0.00000
FAREA  0.00000   0.00000   0.28000   0.28000   0.00000   0.00000
FMASS  0.00000   0.00000   0.01540   0.01540   0.00000   0.00000
FQDOT  0.00000   0.00000   716000.   716000.   0.00000   0.00000
HCR    0.00000   0.00000   0.22200   0.22200   0.22200   0.22200
OD     0.00000   0.00000   0.02200   0.02200   0.02200   0.02200
CO     0.00000   0.00000   0.04200   0.04200   0.04200   0.04200
#GRAPHICS ON
DEVICE 1
WINDOW    0.    0.    0. 1279. 1023. 4095.
```

**T5121-C.INP**:CFAST input file for Test T51.21 (716 kW) using the C model with no additional ventilation.

```
VERSN    3T51-21: 9 Room+Dome+Level 1.4 Connect
TIMES   5500    100     50      0      0
DUMPR T5121-c.HIS
STPMAX  1.00000
TAMB  288.000  101300. 0.000000
EAMB  288.000  101300. 0.000000
HI/F   0.250  0.000  0.000  0.000  0.000 11.100 11.100 11.100 11.100 16.150  0.300
WIDTH  2.950  4.950  4.300  4.330  1.800  7.920  4.300  4.330  9.670 14.370  3.000
DEPTH  3.650  1.800  2.750  2.720  6.350  7.920  2.750  2.720  9.670 14.370  3.000
HEIGH  2.750  2.485 11.100 11.100  3.500  4.600  5.050  5.050  5.050 34.950 13.200
CEILI FIRECEIL YTONG100 CONCR050 CONCR050 CONCR050 CONCR050 CONCR050 CONCR050 CONCR050 CONCR050 CONCR050
WALLS YTONG250 YTONG100 CONCR050 CONCR050 CONCR050 CONCR050 CONCR050 CONCR050 CONCR050 CONCR050 CONCR050
FLOOR FIRE_FLR CONCR100 CONCR050 CONCR050 CONCR050 CONCR050 CONCR050 CONCR050 CONCR050 CONCR050 CONCR050
HVENT  1  2  1  1.010  1.975  0.000
CVENT  1  2  1  1.000  1.000  1.000  1.000  1.000  1.000
HVENT  2  3  1  1.800  2.485  0.000
CVENT  2  3  1  1.000  1.000  1.000  1.000  1.000  1.000
HVENT  3  4  1  4.300  0.500  0.000
CVENT  3  4  1  1.000  1.000  1.000  1.000  1.000  1.000
HVENT  3  5  1  2.000  0.500  0.000
CVENT  3  5  1  1.000  1.000  1.000  1.000  1.000  1.000
HVENT  4  5  1  2.700  3.100  1.100
CVENT  4  5  1  1.000  1.000  1.000  1.000  1.000  1.000
HVENT  5 11  1  1.800  3.500  0.300
CVENT  5 11  1  1.000  1.000  1.000  1.000  1.000  1.000
HVENT  6  7  1  3.000  4.250  0.000
CVENT  6  7  1  1.000  1.000  1.000  1.000  1.000  1.000
HVENT  6  8  1  3.000  4.250  0.000
CVENT  6  8  1  1.000  1.000  1.000  1.000  1.000  1.000
HVENT  6  9  1  3.000  4.250  0.000
CVENT  6  9  1  1.000  1.000  1.000  1.000  1.000  1.000
HVENT  7  8  1  3.000  4.250  0.000
CVENT  7  8  1  1.000  1.000  1.000  1.000  1.000  1.000
HVENT 11 12  1  0.050  9.800  3.300
CVENT 11 12  1  1.000  1.000  1.000  1.000  1.000  1.000
HVENT  6 11  1  3.000  2.400  0.000
CVENT  6 11  1  1.000  1.000  1.000  1.000  1.000  1.000
VVENT  7  3  4.54000  2
VVENT  8  4  5.75000  2
VVENT 10  7  4.54000  2
VVENT 10  8  6.97000  2
VVENT 10  9  5.28000  2
MVDCT  1  2   1.000  0.300  1.00E-004  0.000  1.000  0.000  1.000  0  0
MVDCT  3  4  18.000  0.300  1.00E-004  0.000  1.000  0.000  1.000  0  0
MVFAN  3  2   0.000 900.00  0.230      0.000  0.000  0.000  0.000  0  0
MVOPN  1  1 H  0.375  0.280  0  0  0  0
MVOPN  9  4 V  0.500  0.070  0  0  0  0
INELV  2  0.625  0  0
INELV  3  0.625  0  0
CHEMI  44.000  0.000  0.000  4.650E+007  300.000  388.000  0.100
LFBO 1
LFBT 2
CJET OFF
FPOS   1.47500   3.65000   0.00000
FTIME   100.00    101.00   3700.00   3701.00   5500.00
FHIGH  0.00000   0.00000   0.37500   0.37500   0.00000   0.00000
FAREA  0.00000   0.00000   0.28000   0.28000   0.00000   0.00000
FMASS  0.00000   0.00000   0.01540   0.01540   0.00000   0.00000
FQDOT  0.00000   0.00000   716000.   716000.   0.00000   0.00000
HCR    0.00000   0.00000   0.22200   0.22200   0.22200   0.22200
OD     0.00000   0.00000   0.02200   0.02200   0.02200   0.02200
CO     0.00000   0.00000   0.04200   0.04200   0.04200   0.04200
#GRAPHICS ON
DEVICE 1
WINDOW    0.    0.    0. 1279. 1023. 4095.
```

**T5123-C.INP**:CFAST input file for Test T51.23 (1011 kW) using the C model with no additional ventilation.

```
VERSN    3T51-23: 9 Room+Dome+Level 1.4 Connect
TIMES   5500    100     50      0      0
DUMPR T5123-c.HIS
STPMAX  1.00000
TAMB  288.000  101300. 0.000000
EAMB  288.000  101300. 0.000000
HI/F   0.250  0.000  0.000  0.000  0.000 11.100 11.100 11.100 11.100 16.150  0.300
WIDTH  2.950  4.950  4.300  4.330  1.800  7.920  4.300  4.330  9.670 14.370  3.000
DEPTH  3.650  1.800  2.750  2.720  6.350  7.920  2.750  2.720  9.670 14.370  3.000
HEIGH  2.750  2.485 11.100 11.100  3.500  4.600  5.050  5.050  5.050 34.950 13.200
CEILI FIRECEIL YTONG100 CONCR050 CONCR050 CONCR050 CONCR050 CONCR050 CONCR050 CONCR050 CONCR050 CONCR050
WALLS YTONG250 YTONG100 CONCR050 CONCR050 CONCR050 CONCR050 CONCR050 CONCR050 CONCR050 CONCR050 CONCR050
FLOOR FIRE_FLR CONCR100 CONCR050 CONCR050 CONCR050 CONCR050 CONCR050 CONCR050 CONCR050 CONCR050 CONCR050
HVENT  1  2  1  1.010  1.975  0.000
CVENT  1  2  1  1.000  1.000  1.000  1.000  1.000  1.000
HVENT  2  3  1  1.800  2.485  0.000
CVENT  2  3  1  1.000  1.000  1.000  1.000  1.000  1.000
HVENT  3  4  1  4.300  0.500  0.000
CVENT  3  4  1  1.000  1.000  1.000  1.000  1.000  1.000
HVENT  3  5  1  2.000  0.500  0.000
CVENT  3  5  1  1.000  1.000  1.000  1.000  1.000  1.000
HVENT  4  5  1  2.700  3.100  1.100
CVENT  4  5  1  1.000  1.000  1.000  1.000  1.000  1.000
HVENT  5 11  1  1.800  3.500  0.300
CVENT  5 11  1  1.000  1.000  1.000  1.000  1.000  1.000
HVENT  6  7  1  3.000  4.250  0.000
CVENT  6  7  1  1.000  1.000  1.000  1.000  1.000  1.000
HVENT  6  8  1  3.000  4.250  0.000
CVENT  6  8  1  1.000  1.000  1.000  1.000  1.000  1.000
HVENT  6  9  1  3.000  4.250  0.000
CVENT  6  9  1  1.000  1.000  1.000  1.000  1.000  1.000
HVENT  7  8  1  3.000  4.250  0.000
CVENT  7  8  1  1.000  1.000  1.000  1.000  1.000  1.000
HVENT 11 12  1  0.050  9.800  3.300
CVENT 11 12  1  1.000  1.000  1.000  1.000  1.000  1.000
HVENT  6 11  1  3.000  2.400  0.000
CVENT  6 11  1  1.000  1.000  1.000  1.000  1.000  1.000
VVENT  7  3  4.54000  2
VVENT  8  4  5.75000  2
VVENT 10  7  4.54000  2
VVENT 10  8  6.97000  2
VVENT 10  9  5.28000  2
MVDCT  1  2   1.000  0.300  1.00E-004  0.000  1.000  0.000  1.000  0  0
MVDCT  3  4  18.000  0.300  1.00E-004  0.000  1.000  0.000  1.000  0  0
MVFAN  3  2   0.000 900.00  0.330      0.000  0.000  0.000  0.000  0  0
MVOPN  1  1 H  0.375  0.350  0  0  0  0
MVOPN  9  4 V  0.500  0.070  0  0  0  0
INELV  2  0.625  0  0
INELV  3  0.625  0  0
CHEMI  44.000  0.000  0.000  4.650E+007  300.000  388.000  0.100
LFBO 1
LFBT 2
CJET OFF
FPOS   1.47500   3.65000   0.00000
FTIME   100.00    101.00   3700.00   3701.00   5500.00
FHIGH  0.00000   0.00000   0.37500   0.37500   0.00000   0.00000
FAREA  0.00000   0.00000   0.35000   0.35000   0.00000   0.00000
FMASS  0.00000   0.00000   0.02170   0.02170   0.00000   0.00000
FQDOT  0.00000   0.00000  1011000.  1011000.   0.00000   0.00000
HCR    0.00000   0.00000   0.22200   0.22200   0.22200   0.22200
OD     0.00000   0.00000   0.02200   0.02200   0.02200   0.02200
CO     0.00000   0.00000   0.04200   0.04200   0.04200   0.04200
#GRAPHICS ON
DEVICE 1
WINDOW    0.    0.    0. 1279. 1023. 4095.
```

## **T5125-C.INP**:CFAST input file for Test T51.25 (1011 kW) using the C model with additional ventilation

```
VERSN    3T51-25: 9 Room Case+Dome+Connect 1.4
TIMES   5500    100     50      0      0
DUMPR T5125-C.HIS
STPMAX  1.00000
TAMB  288.000        101300. 0.000000
EAMB  288.000        101300. 0.000000
HI/F   0.250  0.000  0.000  0.000  0.000 11.100 11.100 11.100 11.100 16.150  0.300  2.650
WIDTH  2.950  4.950  4.300  4.330  1.800  7.920  4.300  4.330  9.670 14.370  3.000  0.700
DEPTH  3.650  1.800  2.750  2.720  6.350  7.920  2.750  2.720  9.670 14.370  3.000  0.700
HEIGH  2.750  2.485 11.100 11.100  3.500  4.600  5.050  5.050  5.050 34.950 13.200 13.500
CEILI FIRECEIL YTONG100 CONCR050 CONCR050 CONCR050 CONCR050 CONCR050 CONCR050 CONCR050 CONCR050 CONCR050 CONCR05C
WALLS YTONG250 YTONG100 CONCR050 CONCR050 CONCR050 CONCR050 CONCR050 CONCR050 CONCR050 CONCR050 CONCR050 CONCR05C
FLOOR FIRE_FLR CONCR100 CONCR050 CONCR050 CONCR050 CONCR050 CONCR050 CONCR050 CONCR050 CONCR050 CONCR050 CONCR05C
HVENT  1  2  1  1.010  1.975  0.000
CVENT  1  2  1  1.000  1.000  1.000  1.000  1.000  1.000  1.000  1.000
HVENT  1 12  1  0.700  2.750  2.570
CVENT  1 12  1  1.000  1.000  1.000  1.000  0.000  0.000  0.000  0.000
HVENT  9 12  1  0.350  5.050  4.700
CVENT  9 12  1  1.000  1.000  1.000  1.000  1.000  1.000  1.000  1.000
HVENT  2  3  1  1.800  2.485  0.000
CVENT  2  3  1  1.000  1.000  1.000  1.000  1.000  1.000  1.000  1.000
HVENT  3  4  1  4.300  0.500  0.000
CVENT  3  4  1  1.000  1.000  1.000  1.000  1.000  1.000  1.000  1.000
HVENT  3  5  1  2.000  0.500  0.000
CVENT  3  5  1  1.000  1.000  1.000  1.000  1.000  1.000  1.000  1.000
HVENT  4  5  1  2.700  3.100  1.100
CVENT  4  5  1  1.000  1.000  1.000  1.000  1.000  1.000  1.000  1.000
HVENT  5 11  1  1.800  3.500  0.300
CVENT  5 11  1  1.000  1.000  1.000  1.000  1.000  1.000  1.000  1.000
HVENT  6  7  1  3.000  4.250  0.000
CVENT  6  7  1  1.000  1.000  1.000  1.000  1.000  1.000  1.000  1.000
HVENT  6  8  1  3.000  4.250  0.000
CVENT  6  8  1  1.000  1.000  1.000  1.000  1.000  1.000  1.000  1.000
HVENT  6  9  1  3.000  4.250  0.000
CVENT  6  9  1  1.000  1.000  1.000  1.000  1.000  1.000  1.000  1.000
HVENT  7  8  1  3.000  4.250  0.000
CVENT  7  8  1  1.000  1.000  1.000  1.000  1.000  1.000  1.000  1.000
HVENT 11 13  1  0.060  9.700  3.400
CVENT 11 13  1  1.000  1.000  1.000  1.000  1.000  1.000  1.000  1.000
HVENT  6 11  1  3.000  2.400  0.000
CVENT  6 11  1  1.000  1.000  1.000  1.000  1.000  1.000  1.000  1.000
VVENT  7  3  4.54000  2
VVENT  8  4  5.75000  2
VVENT 10  7  4.54000  2
VVENT 10  8  6.97000  2
VVENT 10  9  5.28000  2
MVDCT  1  2   1.000  0.300  1.00E-004  0.000  1.000  0.000  1.000  0  0
MVDCT  3  4  18.000  0.300  1.00E-004  0.000  1.000  0.000  1.000  0  0
MVFAN  3  2   0.000 900.00  0.330      0.000  0.000  0.000  0.000  0  0
MVOPN  1  1 H  0.375  0.350  0  0  0  0
MVOPN  9  4 V  0.500  0.070  0  0  0  0
INELV  2  0.625  0  0
INELV  3  0.625  0  0
CHEMI  44.000  0.000  0.000  4.650E+007  300.000  388.000  0.100
LFBO 1
LFBT 2
CJET OFF
FPOS   1.47500   3.65000   0.00000
FTIME   100.00    101.00   1900.00   1911.00   3700.00   3701.00   5500.00
FHIGH  0.00000   0.00000   0.37500   0.37500   0.37500   0.37500   0.00000   0.00000
FAREA  0.00000   0.00000   0.35000   0.35000   0.35000   0.35000   0.00000   0.00000
FMASS  0.00000   0.00000   0.02170   0.02170   0.02170   0.02170   0.00000   0.00000
FQDOT  0.00000   0.00000  1011000.  1011000.  1011000.  1011000.   0.00000   0.00000
HCR    0.00000   0.00000   0.22200   0.22200   0.22200   0.22200   0.22200   0.22200
OD     0.00000   0.00000   0.02200   0.02200   0.02200   0.02200   0.02200   0.02200
CO     0.00000   0.00000   0.04200   0.04200   0.04200   0.04200   0.04200   0.04200
#GRAPHICS ON
DEVICE 1
WINDOW    0.    0.    0. 1279. 1023. 4095.
```

## APPENDIX B: UNPHYSICAL VERTICAL FLOW

This appendix will further examine the unphysical vertical flow that was documented in Section 3.1, Figure 3.12. For the B model, CFAST generated a large, artificial flow before the start of the fire. This particular compartment arrangement, a small compartment connected vertically to a very large compartment (the outside), is not a trivial one for a lumped-parameter type code. The author's decided that further investigation of this flow was warranted to determine if it is a generic problem for lumped-parameter codes or an instability within the CFAST vertical flow algorithm. To do this a simplified model was created and computations were performed with both CFAST and with GOTHIC v3.4e [19], a nuclear safety code.

The CFAST model, shown below, consisted of two 3 m x 3 m compartments with horizontal connections to the outside environment and stacked one on top of the other with vertical flow connection between them and the outside environment. When this model was executed, immediately a 17.7 kg/s flow exited the ceiling vent between the upper compartment and the environment. With neither an outside vs. inside temperature or pressure difference (i.e. no stack effect) nor a ventilation driven flow present, this large vertical flow must be considered as completely unphysical.

```
VERSN    3Vertical Vent Case #3
TIMES    100     10     10      0      0
DUMPR VVENT3.HIS
STPMAX  1.00000
TAMB  288.000        101300. 0.000000
EAMB  288.000        101300. 0.000000
HI/F  0.000000  3.00000
WIDTH  3.00000  3.00000
DEPTH  3.00000  3.00000
HEIGH  3.00000  3.00000
CEILI OFF OFF
WALLS OFF OFF
FLOOR OFF OFF
HVENT  1  3  1  1.00000  2.00000 0.000000 0.000000
CVENT  1  3  1       1.00000       1.00000       1.00000       1.00000
HVENT  2  3  1  1.00000  2.00000 0.000000 0.000000
CVENT  2  3  1       1.00000       1.00000       1.00000       1.00000
VVENT  2  1  4.00000  2
VVENT  3  2  4.00000  2
CHEMI  44.0000 0.000000 0.000000 5.00000E+007  300.000  388.000 0.1000000
LFBO 1
LFBT 2
CJET OFF
FPOS  1.50000  1.50000 0.000000
FTIME       30.0000        31.000      100.000
FAREA      0.000000      0.000000      0.500000      0.500000
FMASS      0.000000      0.000000      0.010000      0.010000
FQDOT      0.000000      0.000000       500000.       500000.
HCR        0.000000      0.000000      0.000000      0.200000
OD         0.000000      0.000000      0.000000      0.020000
CO         0.000000      0.000000      0.000000      0.040000
#GRAPHICS ON
DEVICE 1
WINDOW    0.    0.    0. 1279. 1023. 4095.
```

When an equivalent model was created with GOTHIC 3.4e, input file shown below, the results were very different. GOTHIC also calculated a flow between compartments; however, both the direction and magnitude were different than for the CFAST model. GOTHIC computed a 0.3 kg/s flow into the upper compartment from the outside.

```
Two room stack plus outside
1 40 0 .0001 /
0 0 /
1     1     3     0     1/  group 1 - initial conditions
1.0 1.0 0.1 1.0 0 0 0 /
101.325 15 0 0 0 0 0 0 0 /
1 'Air' 28.97 3.617 97 1 3
1.023 -0.000178421 1 2.26607e-07 2 -1.52443e-11 3 /s. h. coeffs. and exps.
1  /
1 2 101.328 15 0 0 0 0 /
1  /
2 2 101.327 15 0 0 0 0 /
1  /
3 2 101.325 15 0 0 0 0 /
1  /
2 3/  group 2 - channel parameters
1 9 6.13999 0.0 0.0 0 0 1.0 9 /
2 9 6.13999 0.0 0.0 0 3 1.0 9 /
3 100000 1121 0.0 0.0 0 0 1.0 100000 /
3 0 4 1/  group 3 - connector parameters
1 1 2 0 2 3 2 0 2/
2 6.00015 1.5 1.5 179.91 1 0 0 0/
 0 0 0 0 0/
0 0 0 0 0 0 0 0 0 0 1 1/
2 1 2 2.9998 0.0001 2 2 3 0.0001/
4 8 1.5 1.5 6 1 0 0 0/
 0 0 0 0 0/
0 0 0 0 0 0 0 0 0 0 1 1/
3 2 2 5.9998 0.0001 3 2 6 0.0001/
4 8 1.5 1.5 0.5 1 0 0 0/
 0 0 0 0 0/
0 0 0 0 0 0 0 0 0 0 1 1/
4 2 2 3 2 3 2 3 2/
2 6.0015 1.5 1.5 179.91 1 0 0 0/
 0 0 0 0 0/
0 0 0 0 0 0 0 0 0 0 1 1/
4 3 1 0/  group 4 - section data
1 1 1 3 1 /
1 1 0 0 0 0 0 1/
2 1 1 3 1 /
2 2 0 0 0 0 0 2/
3 1 1 10 1 /
3 3 0 0 0 0 0 3/
3
5     0 /  group 5 - variation tables
6 0 /  group 6 - variation assignments
12     0 / group 12 - shear stress data
13     6     0     0     0     0 0 0 0     0/  group 13 - boundary conds.
1 1 3/
1 2 3/
2 1 3/
2 2 3/
3 1 3/
```

```
3 2 3/
14/ group 14 - output control
0/ end of group data
0.001 1 50 1 600 /
50 1 0 1000000.0 0.0 /
0.001 1 10000 1 2000 /
5000 100 0 1000000.0 0.0 /
-1.0 0.0 0.0 0.0 0.0 /
0.0 0.0 0.0 0.0 /
```

Since both models computed a flow when in fact none should exist, this particular geometry is generically difficult for lumped-parameter codes. However, the numerical flow induced in GOTHIC is quite small, resulting in an average velocity of 0.07 m/s, whereas the CFAST induced flow is quite large, resulting in an average velocity of 3.96 m/s. Thus, while this geometry is a challenge for lumped-parameter codes, it is clear that CFAST's performance warrants improvement.

NIST-114
(REV. 6-93)
ADMAN 4.09

U.S. DEPARTMENT OF COMMERCE
NATIONAL INSTITUTE OF STANDARDS AND TECHNOLOGY

# MANUSCRIPT REVIEW AND APPROVAL

(ERB USE ONLY)
ERB CONTROL NUMBER | DIVISION
PUBLICATION REPORT NUMBER: NIST-GCR-97-731 | CATEGORY CODE
PUBLICATION DATE: November 1997 | NUMBER PRINTED PAGES

INSTRUCTIONS: ATTACH ORIGINAL OF THIS FORM TO ONE (1) COPY OF MANUSCRIPT AND SEND TO THE SECRETARY, APPROPRIATE EDITORIAL REVIEW BOARD

TITLE AND SUBTITLE (CITE IN FULL)

Evaluation of the HDR Fire Test Data and Accompanying Computational Activities with Conclusions from Present Code Capabilities Volume 2: CFAST Validation for T51 Gas Fire Test Series

CONTRACT OR GRANT NUMBER
NIST Contract 60NANB6D0127

TYPE OF REPORT AND/OR PERIOD COVERED

AUTHOR(S) (LAST NAME, FIRST INITIAL, SECOND INITIAL)
Jason Floyd, Lothar Wolf, and John Krawiec
Dept. of Materials and Nuclear Engineering
University of Maryland
College Park, MD 20742

PERFORMING ORGANIZATION (CHECK (X) ONE BOX)
[X] NIST/GAITHERSBURG
[ ] NIST/BOULDER
[ ] JILA/BOULDER

LABORATORY AND DIVISION NAMES (FIRST NIST AUTHOR ONLY)

SPONSORING ORGANIZATION NAME AND COMPLETE ADDRESS (STREET, CITY, STATE, ZIP)
U.S. Department of Commerce
National Institute of Standards and Technology
Gaithersburg, MD 20899

PROPOSED FOR NIST PUBLICATION

| | | |
|---|---|---|
| [ ] JOURNAL OF RESEARCH (NIST JRES) | [ ] MONOGRAPH (NIST MN) | [ ] LETTER CIRCULAR |
| [ ] J. PHYS. & CHEM. REF. DATA (JPCRD) | [ ] NATL. STD. REF. DATA SERIES (NIST NSRDS) | [ ] BUILDING SCIENCE SERIES |
| [ ] HANDBOOK (NIST HB) | [ ] FEDERAL INF. PROCESS. STDS. (NIST FIPS) | [ ] PRODUCT STANDARDS |
| [ ] SPECIAL PUBLICATION (NIST SP) | [ ] LIST OF PUBLICATIONS (NIST LP) | [X] OTHER NIST-GCR |
| [ ] TECHNICAL NOTE (NIST TN) | [ ] NIST INTERAGENCY/INTERNAL REPORT (NISTIR) | |

PROPOSED FOR NON-NIST PUBLICATION (CITE FULLY) [ ] U.S. [ ] FOREIGN

PUBLISHING MEDIUM
[ ] PAPER [ ] CD-ROM
[ ] DISKETTE (SPECIFY)
[ ] OTHER (SPECIFY)

SUPPLEMENTARY NOTES

ABSTRACT (A 2000-CHARACTER OR LESS FACTUAL SUMMARY OF MOST SIGNIFICANT INFORMATION. IF DOCUMENT INCLUDES A SIGNIFICANT BIBLIOGRAPHY OR LITERATURE SURVEY, CITE IT HERE. SPELL OUT ACRONYMS ON FIRST REFERENCE.) (CONTINUE ON SEPARATE PAGE, IF NECESSARY.)

Between 1984 and 1992 four major fire test series were performed in the HDR containment encompassing various fuels and three different axial positions in the high-rise, multi-level, multi-compartment facility. At that time each HDR fire test series was accompanied by extensive efforts to evaluate the predictive capabilities of a variety of fire models and codes developed in different countries by both blind pre-test and open post-test computations. A quite large number of open issues remained in the area of fire computer code predictive qualities upon completion of the HDR program. Volume 1: Test Series Description for T51 Gas Fire Test Series, NIST-GCR-97-727.

KEY WORDS (MAXIMUM OF 9; 28 CHARACTERS AND SPACES EACH; SEPARATE WITH SEMICOLONS; ALPHABETIC ORDER; CAPITALIZE ONLY PROPER NAMES)
combustion products; compartment fires; doors; fire models; large scale fire tests; temperature; validation; vents

AVAILABILITY
[X] UNLIMITED [ ] FOR OFFICIAL DISTRIBUTION - DO NOT RELEASE TO NTIS
[ ] ORDER FROM SUPERINTENDENT OF DOCUMENTS, U.S. GPO, WASHINGTON, DC 20402
[X] ORDER FROM NTIS, SPRINGFIELD, VA 22161

NOTE TO AUTHOR(S): IF YOU DO NOT WISH THIS MANUSCRIPT ANNOUNCED BEFORE PUBLICATION, PLEASE CHECK HERE. [ ]

WORDPERFECT